F. W. Klaiber, K. F. Dunker, S. M. Planck, W. W. Sanders, Jr.

Strengthening of an Existing Continuous-Span, Steel-Beam, Concrete-Deck Bridge by Post-Tensioning

Iowa Department of Transportation

report

College of Engineering Iowa State University

F. W. Klaiber, K. F. Dunker, S. M. Planck, W. W. Sanders, Jr.

Strengthening of an Existing Continuous-Span, Steel-Beam, Concrete-Deck Bridge by Post-Tensioning

**engineering
research institute**

iowa state university

The opinions, findings, and conclusions expressed in this publication are those of the authors and not necessarily those of the Highway Division of the Iowa Department of Transportation.

ABSTRACT

The need to upgrade a large number of understrength and obsolete bridges in the United States has been well documented in the literature. Through several Iowa DOT projects, the concept of strengthening simple-span bridges by post-tensioning has been developed. The purpose of the project described in this report was to investigate the use of post-tensioning for strengthening continuous composite bridges. In a previous, successfully completed investigation, the feasibility of strengthening continuous, composite bridges by post-tensioning was demonstrated on a laboratory 1/3-scale-model bridge (3 spans: 41 ft 11 in. × 8 ft 8 in.). This project can thus be considered the implementation phase.

The bridge selected for strengthening was in Pocahontas County near Fonda, Iowa, on County Road N28. With finite element analysis, a post-tensioning system was developed that required post-tensioning of the positive moment regions of both the interior and exterior beams. During the summer of 1988, the strengthening system was installed along with instrumentation to determine the bridge's response and behavior. Before and after post-tensioning, the bridge was subjected to truck loading (one or two trucks at various predetermined critical locations) to determine the effectiveness of the strengthening system. The bridge, with the strengthening system in place, was inspected approximately every three months to determine any changes in its appearance or behavior.

In 1989, approximately one year after the initial strengthening, the bridge was retested to identify any changes in its behavior. Post-tensioning forces were removed to reveal any losses over the one-year period. Post-tensioning was reapplied to the bridge, and the bridge was tested using the same loading program used in 1988. Except for at a few locations, stresses were reduced in the bridge the desired amount. At a few locations flexural stresses in the steel beams are still above 18 ksi, the allowable inventory stress for A7 steel. Although maximum stresses are above the inventory stress by about 2 ksi, they are about 5 ksi below the allowable operating stress; therefore, the bridge no longer needs to be load-posted. Although considerably more involved than the post-tension strengthening of single-span bridges, post-tensioning of continuous-span bridges is a feasible practical strengthening technique.

TABLE OF CONTENTS

LIST OF FIGURES

LIST OF TABLES

1. INTRODUCTION

1.1. General Background

Nearly half of the approximately 600,000 highway bridges in the United States were built before 1940. A majority of those bridges were designed for lower traffic volumes, smaller vehicles, slower speeds, and lighter loads than they experience today. The problem has been compounded by inadequate maintenance of many of these older bridges. According to the Federal Highway Administration, almost 40% of the nation's bridges are classified as deficient and thus in need of rehabilitation or replacement. A large number of these bridges are deficient in their ability to carry current legal live loads. Strengthening, rather than posting for reduced loads or replacement, has been found to be a cost-effective alternative in many cases.

Many different methods exist for increasing the live-load carrying capacity of the various types of bridges in use today. Through Iowa Department of Transportation (Iowa DOT) Projects HR-214 [1] and HR-238 [2,3,4], the concept of strengthening simple-span, composite steel-beam and concrete-deck bridges by post-tensioning was developed. These projects developed the concept from the feasibility phase through the implementation and design methodology phase. In the feasibility phase [1], the response of a 1/2-scale simple-span bridge model (26 ft long × 15 ft 8 in. wide) to various configurations of post-tensioning was determined. On the basis of the success of the laboratory testing, the implementation phase [2,4] was undertaken. In this phase, two simple-span bridges were strengthened by post-tensioning during the summer of 1982 and retested during the summer of 1984. One of the bridges (prototype of the laboratory model: 51 ft 3 in. long × 31 ft 10 1/2 in. wide) is 2.2 miles north of Terril on County Road N14. The other bridge (45° skew: 71 ft 3 in. long × 31 ft 10 1/2 in. wide) is just south of the Greene-Webster County line on State Road I-144. Results of these tests verified that

strengthening of simple-span bridges by post-tensioning is a viable, economical strengthening technique. The design methodology developed by Dunker et al. [3] provided a procedure by which the required post-tensioning force could be determined relatively easily. Since its development, this design methodology has been used by the Iowa DOT and various other agencies in the design of post-tension strengthening systems for numerous bridges.

As a result of the success in strengthening simple-span bridges by post-tensioning, a study was undertaken to extend the method to continuous-span bridges. Because Iowa began designing and constructing continuous, composite steel-beam and concrete-deck bridges earlier than most states, Iowa has a considerable inventory of those bridges in need of rehabilitation and/or strengthening, or possible replacement. The investigation of strengthening continuous-span bridges parallels the work completed for simple-span bridges in that a feasibility study has recently been completed HR-287 [5], while this study, HR-308, is the implementation phase.

In the feasibility study [5], a 1/3-scale, three-span continuous model bridge (41 ft 11 in. long × 8 ft 8 in. wide) was fabricated and tested when subjected to various post-tensioning schemes. In addition to the testing of the model, a full-size mockup of the negative moment region at an interior support was constructed. The full-size mockup made it possible to investigate various tendon arrangements--straight threadbars, harped cables, and the like--that were not possible to test on the three-span bridge model because of its small size. On the basis of the results of the feasibility study, it was determined that it is possible to strengthen continuous, composite bridges by post-tensioning.

1.2. Objectives and Scope

On the basis of experience from the feasibility investigation on strengthening continuous-span bridges by post-tensioning (HR-287) and that

from previous Iowa DOT simple-span strengthening projects (HR-214 and HR-238) it appeared that post-tensioning could be used to strengthen continuous bridges. The primary goals of this study were to design and install a post-tension strengthening system on a continuous-span, steel-beam, concrete-deck bridge; instrument the bridge for measurement of deflections and strains; and document the bridge's behavior for a one-year period after the installation of the post-tension strengthening system. The bridge selected for strengthening was identified by an advisory committee consisting of the Office of Bridge Design of the Iowa DOT, county engineers, and the research team. More details on the bridge selection procedure as well as the bridge are presented in Chapter 2. In line with the primary goals previously noted, more specific objectives were

- to determine the overstress magnitudes and locations in the bridge selected for strengthening.
- to determine the location and magnitude of post-tensioning forces required to strengthen the bridge.
- to determine the distribution of post-tensioning longitudinally and transversely for the post-tension strengthening system designed.
- to determine if end restraint exists in the bridge selected for strengthening.

These as well as several other secondary objectives were pursued by the research team through undertaking the various tasks outlined in the following section.

1.3. Research Program

The research program consisted of numerous distinct tasks, which will be briefly outlined in the following paragraphs; however, the main emphasis was the field testing. The research team has made several comprehensive

literature reviews on post-tension strengthening of bridges and bridge strengthening in general:

- post-tensioning of simple-span bridges [1,2,3,4]
- post-tensioning of continuous-span bridges [5]
- strengthening of highway bridges [6]

Reference [6] is the final report of a National Cooperative Highway Research Program Project that reviewed essentially all techniques of bridge strengthening. This reference has a bibliography that lists over 375 articles on bridge strengthening and closely related areas. Of these articles, approximately 95 are written in a foreign language, and additional articles are from English-speaking foreign countries.

Because the literature reviews previously cited are readily available to the majority of engineers, to avoid duplication the literature review undertaken as part of this study (see Section 1.4) reviews only post-tension strengthening articles that have been published since the last literature review was completed in July 1987 (Ref. [5]). This literature review should thus be considered supplemental to the previous literature reviews.

As has been previously stated, the main objective of this investigation was to design and install a post-tension strengthening system on a continuous-span, steel-beam, concrete-deck bridge and to monitor its behavior over a one-year period. With the assistance of the Office of Bridge Design at the Iowa DOT, numerous bridges were reviewed for possible strengthening. The bridge selected for strengthening was a three-span bridge from the V12 (1957) series of composite bridges; additional details on this bridge are presented in Chapter 2. After a specific bridge had been selected for strengthening (henceforth simply referred to as the bridge), it was possible to analyze it to determine where and by how much it was overstressed when subjected to Iowa legal loads. With finite element programs previously developed, a strengthening system was selected and designed.

In the summer of 1988, the post-tensioning system was installed on the bridge. Instrumentation was also installed on the bridge for measurement of strains at critical locations, for detecting the presence of end restraint, for measurement of midspan vertical displacements, and for detecting longitudinal movements. Additional instrumentation was added to the bridge for determination of the bridge temperature during testing.

The bridge was subjected to the following four loading conditions to determine its response, strains, and longitudinal and vertical displacements:

1. An overloaded truck at various predetermined locations on the bridge.

2. Various stages of the post-tensioning sequence. Because all 12 beams of the bridge required post-tensioning (2 tendons per beam), and there were only 4 hydraulic cylinders available, it was necessary to post-tension the bridge in 6 stages.

3. The same overloaded truck at the same locations after post-tensioning of the bridge was completed to determine the effectiveness of the strengthening system.

4. Two overloaded trucks at various predetermined locations on the bridge, to maximize the moments at various locations, in order to determine the behavior of the strengthening system when subjected to overload.

The bridge was inspected approximately every three months after it was strengthened during the summer of 1988. In the summer of 1989, the strengthened bridge was retested.

A review of the data obtained in 1988 revealed the need for additional instrumentation to better our understanding of the bridge's behavior. Thus, in 1989 additional strain gages and direct-current displacement transducers (DCDT's) for strain and displacement measurements, respectively, were

installed. The testing program employed in 1989 was essentially the same as that in 1988 with the following additions:

- The strengthened bridge was subjected to an overloaded truck at the locations used in 1988.
- Post-tensioning force on the bridge was removed in six stages, thus making it possible to determine if any post-tensioning force was lost during the one-year period.

After these two loading events, the bridge was subjected to the four loading events employed during 1988—overloaded truck at various predetermined locations on the unstrengthened bridge, various stages of the post-tensioning sequence, and so forth. The results from the various parts of this investigation are summarized in this report. The supplemental literature review is presented in Section 1.4. Chapter 2 describes the bridge, which was strengthened and tested, as well as the strengthening system that was employed. The instrumentation and the testing procedure used in each of the two years are presented in Chapter 3. The results from the field testing and the finite element analysis employed are summarized in Chapter 4. Following the results are the summary and conclusions in Chapter 5.

1.4. Literature Review

In addition to the previous literature reviews cited, the articles summarized below relate to the concept of post-tensioning as a strengthening method. Several analysis techniques have been developed and tested experimentally; furthermore, design criteria have been established as well as implemented. Although the emphasis of the articles reviewed is on prestressed composite girders, additional methods and applications are included to provide a comparison of techniques.

Simple-span composite girders were examined analytically and experimentally to compare the concepts of pre-tensioning and post-tensioning; the concepts differed in timing of stress application relative to placement of the concrete slab [7]. Straight, short and straight, and bent-up strand configurations were analyzed, with the emphasis placed on stress distribution due to prestressing and increase in initial tendon force due to application of external loads. An incremental increase as high as 25% of the initial tendon force was measured in the case of the short, straight tendon.

By investigating parameters such as cable position and curvature, intensity of prestress and accompanying incremental increase, geometry of the steel section, and live loading patterns, a procedure to optimize the design of prestressed steel girders was established [8]. For the simple-span case an asymmetrical "I" section was chosen to alleviate understress conditions in the bottom flange following application of prestress, and a cable located below the bottom flange with constant eccentricity provided the optimal arrangement. Further comparative analysis of six cable configurations indicated that a draped, segmental cable arrangement was most effective for a girder of two equal spans where negative dead-load moment governed the design.

The aforementioned six cable configurations were evaluated experimentally to verify the analytical results [9]. Deemed the most likely possible configurations, the six examined consisted of parabolic, trapezoidal, trapezoidal-triangular, draped-segmental, segmental, and double-segmental arrangements. Testing was performed on a scaled plexiglass model of a two-span continuous bridge prestressed with high-strength piano wires; strains were monitored by load cells connected to the prestressing wires. Although test results showed close agreement to the analytical results, conclusions were not formulated to select the most appropriate configuration. Effectiveness of configuration was provided as the ratio of prestressing moments to the associated cable length, saddle, and anchorage costs.

Troitsky et al. [10] introduced an analysis method for continuous prestressed steel beams that was based on flexibility and virtual work methods. A numerical example of a three-span case located in the appendix demonstrated that prestressing the girders can reduce the negative bending moment by as much as 20%. The authors concluded that a greater reduction in negative bending moment will be realized in longer spans as well as an accompanying increase in incremental prestressing force.

An analysis procedure based on the simplex method was provided for prestressed steel cable trusses [11]. Both symmetric constant loading and variable and moving loading conditions were considered in using this approach. Examination of a few existing cable truss bridges illustrated the advantages of material savings and effective structural stiffness through use of the prestressing technique.

Whereas earlier analytical methods concentrated on behavior of prestressed composite steel girders in the elastic range, an analytical model based on the incremental deformation technique was introduced to predict behavior in the inelastic range [12]. Ten prestressed composite girders tested to their ultimate capacity provided experimental agreement with the analytical values. Included in the experimental program were aspects such as tendon type and profile, epoxy coating on tendons, slab type, bond between the concrete and the tendons, geometric characteristics of the girder, and construction sequence.

In a pair of companion papers, Saadatmanesh [13] examined two prestressed composite beams experimentally as well as analytically. One beam, which was prestressed before the concrete slab was cast, was subjected to positive bending moment, while the other was prestressed after the slab was cast and then subjected to negative bending moment. Equations based on equilibrium of internal forces and compatibility of deformations adequately predicted structural behavior throughout the full range of loading to failure.

The two beams tested experimentally were selected for further analytical study [14]. Both elastic and inelastic behavior were considered through nonlinear analysis, while the stiffness method was applied to model elastic behavior alone. To demonstrate the advantages of prestressed over conventionally fabricated composite beams, the methods developed were applied to three cases: a conventional composite beam, a composite beam with a non-prestressed tendon, and a composite beam with a prestressed tendon. Results indicated that the addition of a tendon increased ultimate capacity, whereas the prestressed tendon increased yield capacity.

In terms of application, a change in lane configuration and subsequent assessment to current code requirements affected the structural adequacy of the six-span continuous M62 Rakewood Viaduct over Longden End Valley in England [14]. Post-tensioning was the chosen method of strengthening. Three pairs of prestressing bars of overlapping lengths were attached beneath the bottom flange of each steel beam in the positive moment region in each span. Consequently, service load stresses in the bottom flanges over the piers were reduced to acceptable limits through deck continuity. Strain gages were installed on 20 bars; readings at regular intervals are planned to monitor the post-tensioning effect.

Increased permit loadings established by the state of California necessitated strengthening of many steel and concrete bridges on the highway system. Two methods, consisting of post-tensioning existing girders and deck rehabilitation, have proven to be cost-effective strengthening techniques and have performed adequately to increase live-load capacity [16]. Generally, straight tendon configurations were used to strengthen both steel and concrete girders; however, the tendon path was dropped below the bottom flange in a few steel girder examples, while the tendons were draped along the sides of concrete girders in a few instances. Deck rehabilitation was categorized by the three techniques used to increase the resisting section. The first method

involved making the old deck slab composite with the girders; the second consisted of deck replacement to achieve composite action while the old deck was used as form work; the third technique involved placement of a new slab on top of the old and usually required additional strengthening by post-tensioning.

The deck overlay concept, in conjunction with epoxy ejection of flexural cracks and a comparison of post-tensioning with the addition of a bottom soffit panel, was further investigated at the University of California, San Diego [17]. The test section, consisting of two main girders, two intermediate bents, and the associated deck slab, was cut from the Gepford Overhead scheduled for demolition on California State Highway 42. After the placement of a full-depth reinforced overlay over the entire test section, flexural cracks extending through the concrete girders were injected with epoxy adhesive. Preliminary testing indicated an increase in transverse stiffness attributed to the overlay, a surprising increase in stiffness attributed to the epoxy injection of flexural cracks, and virtually no stiffness change due to external post-tensioning. (Testing was not complete on the additional thin, high-strength, prestressed concrete bottom panel at date of publication.)

Strengthening methods for both composite and noncomposite steel girders, as well as design and analysis recommendations, were presented to designers by the California Department of Transportation [18]. Of several methods listed relating to noncomposite steel girders, two involved post-tensioning: straight paths were suggested to relieve small overstresses, while harped tendon paths with inverted king posts were recommended to reduce large overstresses. Post-tensioning was deemed the preferred method for strengthening composite bridges. Designers were cautioned with respect to design of strand length, anchorage, secondary stresses, and incremental prestress forces.

An experimental research program at the University of Arizona, Tucson, proposed to investigate the concept of fiber-composite plates epoxy-bonded to the tension flange of concrete girders [19]. Four rectangular beams were constructed with consideration of two design variables: reinforcement ratio and initial camber. After being externally prestressed with fiber-composite plates bonded along their full lengths, the beams will be tested to failure and the accompanying load-deflection behavior will be analyzed. (At the time of publication the beams had yet to be tested.) The corrosion-resistant fiber-composite plates lend improved serviceability to the external prestressing technique.

The fatigue strength of prestressed composite beams for new construction was investigated at the University of Maryland, in conjunction with feasibility and behavioral studies of prestressing as a repair technique [20]. The authors ascertained that full prestressing of new and cracked beams makes them virtually fatigue proof for highway loading.

A review of the current literature reveals that prestressing concepts can be applied to post-tensioning composite girders; the difference lies in the time of application of the stressing force. The analysis procedures and applications cited above illustrate the capabilities of post-tensioning as a strengthening technique.

2. BRIDGE DESCRIPTION AND STRENGTHENING DESIGN

2.1. Bridge Description

For more than 40 years the Iowa DOT has followed a policy of preparing standard series of bridge plans for construction of bridges on primary and secondary road systems. For two of the standard series, V12 and similar V14 continuous bridges, between 1950 and 1975 about 90 bridges were constructed on the primary road system, and about 360 bridges were constructed on the secondary road system. Many of these bridges now require either load posting or strengthening in order to meet current Iowa legal load and bridge design standards [21].

A team consisting of members of the Iowa DOT Office of Bridge Design, Iowa county engineers, and the authors selected one of the V12 (1957) series of bridges for experimental strengthening and testing by using a post-tensioning system similar to that developed during Phase I of the investigation [22]. The bridge selected is in northwest Iowa, west of Fonda, Iowa, on Pocahontas County Road N28. The bridge is less than one mile south of the intersection of N28 and Iowa Highway 7 and is similar to the 125-ft length prototype for the model constructed in the ISU Structural Engineering Laboratory during Phase I of this research [5,22].

The framing plan and a section for the bridge are shown in Fig. 2.1, while photographs of the bridges are shown in Fig. 2.2. The bridge has a total length of 150 ft and consists of two end spans of 45 ft 9 in. and a center span of 58 ft 6 in. The four bridge beams are coverplated top and bottom near each of the two piers. The beams also are spliced at the nominal dead-load inflection points in the center span.

Steel channel diaphragms are located at the piers and abutments. There also are steel wide-flange diaphragms at the center of each end span and at the one-third points of the center span.

a. BRIDGE SECTION

b. BRIDGE FRAMING PLAN

Fig. 2.1. Framing plan of Fonda bridge.

a. SIDE VIEW
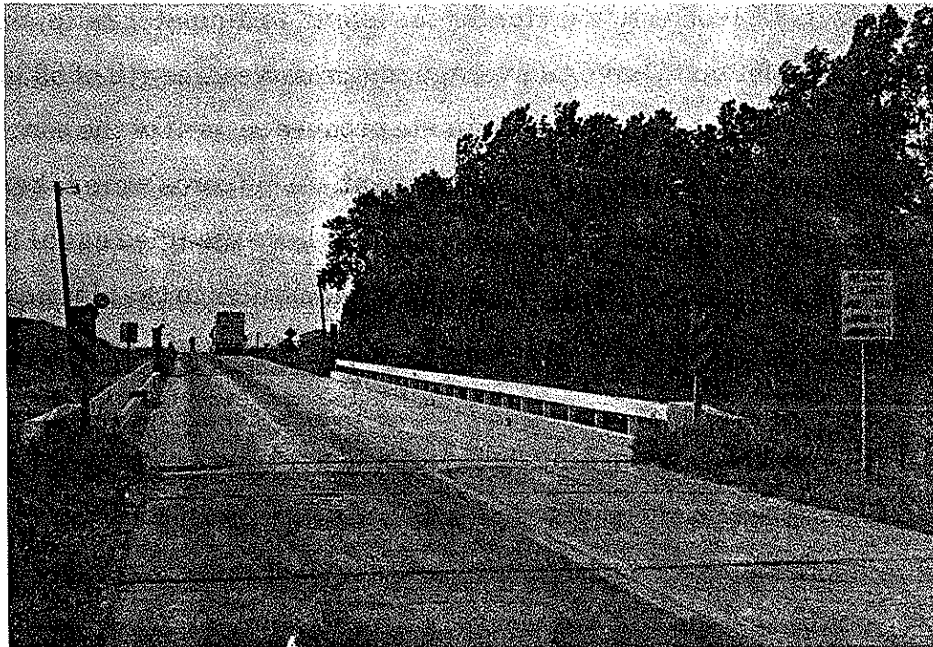
b. TOP VIEW

Fig. 2.2. Photographs of Fonda bridge.

The roadway width of the bridge is 24 ft, which allows for two 12-ft lanes but no shoulders. The deck varies in thickness from 6 and 7/16 in. over the beams to 6 and 3/4 in. between beams. For positive roadway drainage the bridge deck has a 3-in. crown, which is formed by interior beams that are 3 in. deeper than exterior beams and that bear at the same elevation as exterior beams. The bridge has shallow curbs integral with the deck and steel guard rails attached to the curbs.

The steel beams and cover plates were specified to be of A7 ($F_y = 33$ ksi) steel. The reinforcing bar strength is unknown, but it can be assumed to have a minimum yield strength of 40 ksi [23]. Because the bridge was built in 1965, it is unlikely that higher strength reinforcing was used in the deck and curbs.

Several of the concrete cores (4 in. in diameter by approximately 6 in. long) removed from the bridge deck for the addition of shear connectors were tested to determine an approximate value of the concrete strength. Using the ASTM C42-87 (6.7.2) correction factor for the length to diameter ratio, the deck concrete was found to have an average compressive strength of 5930 psi. This value should be considered approximate because several of the cores tested contained pieces of the deck reinforcement. As no cores were taken from the curbs, the strength of concrete in the curbs has been assumed equal to that in the deck. The strength of concrete in the deck is similar to that found in similar bridges; this strength has often been found to be 5000 psi and greater [4].

For convenience in describing behavior and analysis assumptions, a series of reference sections is given in Fig. 2.3. As illustrated in the figure, these reference sections are for an end span and half of the center span. Because of symmetry, the sections would be repeated, in reverse order, for the half of the bridge to the right of section L. In Table 2.1, the reference sections are described and located with respect to the left abutment.
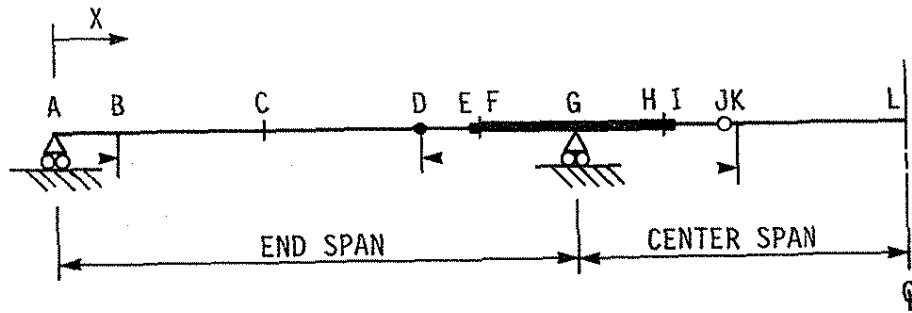
Table 2.1. Descriptions and locations of reference sections.

Section	Description	X, inches	
		Exterior Beam	Interior Beam
A	Abutment bearing	0	0
B	Tendon anchorage at Bracket A	66	66
C	Nominal maximum positive moment	219.6	219.6
D	Nominal dead-load inflection point and tendon anchorage at bracket A	387	387
E	Actual coverplate end	441	435
F	Theoretical coverplate end	456	451.5
G	Pier bearing	549	549
H	Theoretical coverplate end	642	646.5
I	Actual coverplate end	657	663
J	Splice and nominal dead-load inflection point	711	711
K	Tendon anchorage at bracket B	723	723
L	Nominal maximum positive moment and center of bridge	900	900

Fig. 2.3. Reference sections along half bridge length.

The table and figure show reference sections not only for items illustrated in Fig. 2.3 but also for items such as the post-tensioning brackets, which were added to the bridge. These additional items are discussed in subsequent sections of this report. Coverplate ends are located both with respect to the actual ends and the theoretical ends defined according to the AASHTO bridge design specifications [21].

For the original design of the Fonda bridge, the Iowa DOT presumably made the load-behavior assumptions given in Table 2.2. For ordinary dead load, only the steel frame was assumed to be effective. For curbs, rails, and future wearing surface, constructed after the deck, the deck was assumed to be composite with the steel beams within nominal dead-load positive moment regions. Under truck load, the curb and deck also were assumed to be composite with exterior beams within the same regions.

For flexural stress computations, the load-behavior assumptions used during design (and also used during subsequent ratings) neglect the curbs and deck within the nominal negative moment regions. The effect of the assumptions for live and impact load is to create bridge beams with large section properties in positive moment regions and coverplate regions. Between those regions are short regions, with relatively small section properties. Generally, the assumptions regarding and characteristics of the bridge lead to flexural overstresses at maximum positive moment sections of spans, in the short regions with small section properties, and at maximum negative moment sections at piers.

Excluding loads from a possible future wearing surface, flexural stress envelopes for top and bottom flanges of an exterior beam are given in Fig. 2.4. For A7 steel, the maximum allowable inventory stress, except for laterally unsupported regions with compression stress reductions, is 18 ksi. Figure 2.4a shows overstresses within the short regions, sections D-F and H-J, and near

Table 2.2. Iowa DOT bridge load-behavior assumptions.

Load	Length[1]	Assumed Effective Cross Section
Dead (steel frame and concrete deck)	A–F	wide flange beam
	F–H	coverplated wide-flange beam
	H–L	wide-flange beam
Long-Term Dead (curbs, rails, and future wearing surface)	A–D	composite deck and wide flange beam, n = 27
	D–F	wide flange beam
	F–H	coverplated wide flange beam
	H–J	wide flange beam
	J–L	composite deck and wide flange beam, n = 27
Live (Iowa legal trucks and impact)	A–D	composite deck (and curb for exterior beam) and wide-flange beam, n = 9
	D–F	wide-flange beam
	F–H	coverplated wide-flange beam
	H–J	wide-flange beam
	J–L	composite deck (and curb for exterior beam) and wide-flange beam, n = 9

[1]Lengths are defined by reference sections given in Figure 2.3 and Table 2.1. For stress checks, lengths (given in table) using theoretical coverplate end sections are used. For moment determination, however, actual coverplate end sections are used.

a. TOP FLANGE

b. BOTTOM FLANGE

Key
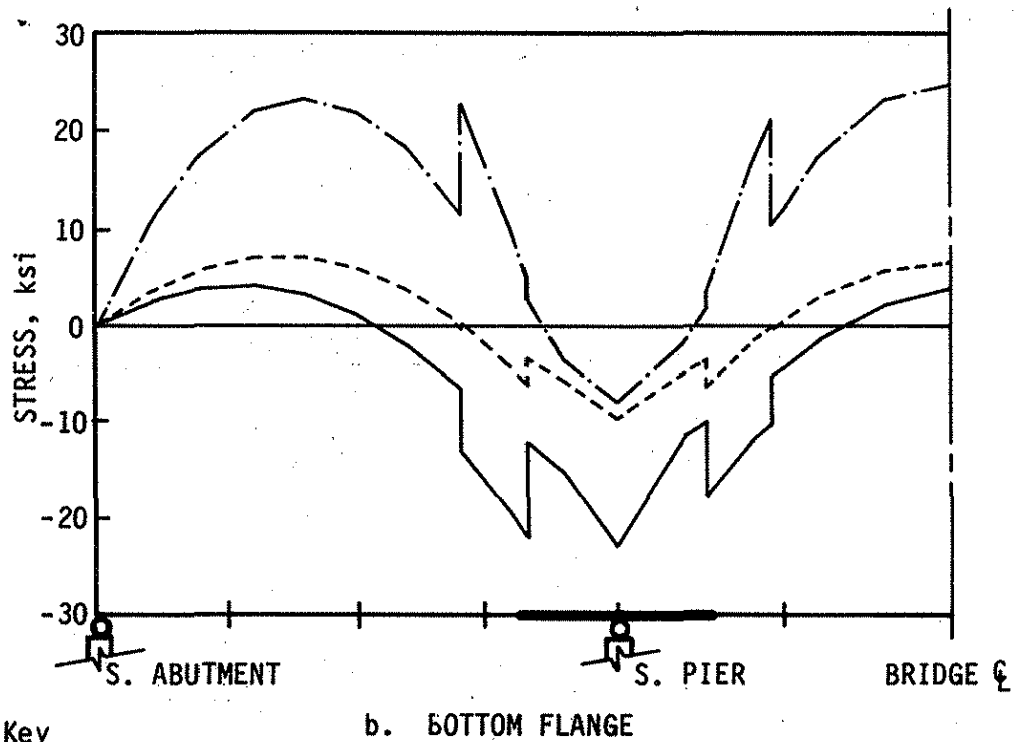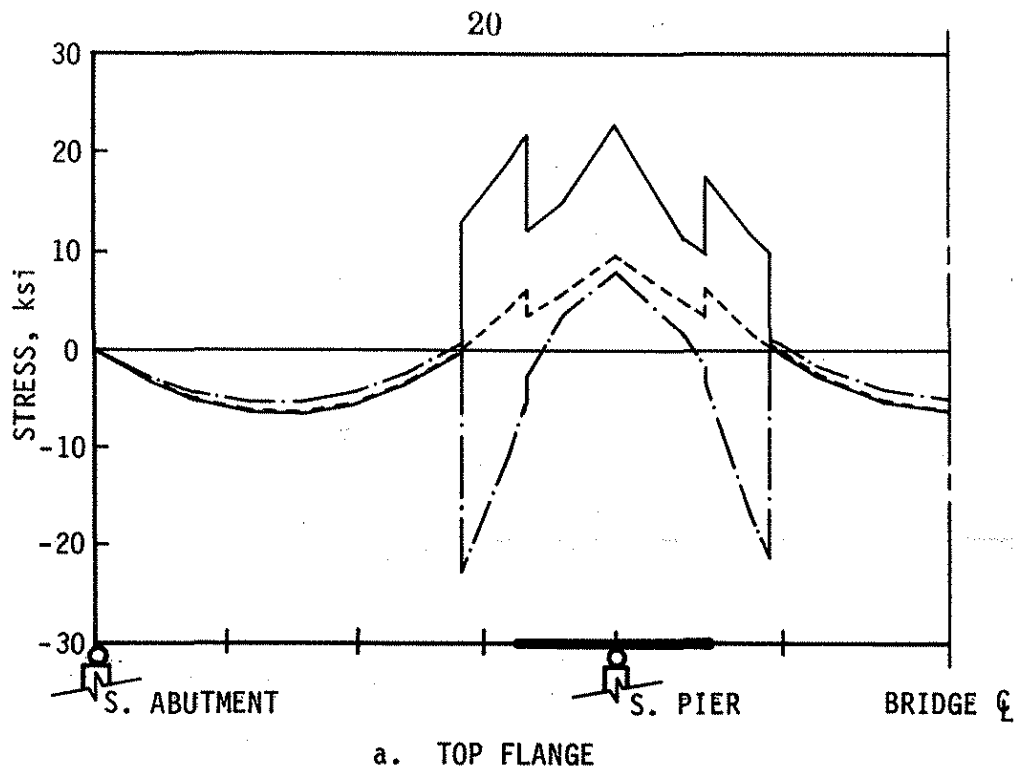
—·— Dead, long-term dead, and positive live-impact load envelope
---- Dead and long-term dead load
——— Dead, long-term dead, and negative live-impact load envelope

Fig. 2.4. Exterior beam stress envelopes for unstrengthened bridge.

the pier, section G. Overstresses for the bottom flange in Fig. 2.4b additionally occur at maximum positive moment (sections C and L).

Without the future wearing surface, the maximum allowable operating stress for A7 steel, 24.75 ksi, is exceeded only at section L, and that amount of overstress requires posting of the bridge. With the wearing surface, the operating stress would be exceeded at additional sections. Stress envelopes for an interior beam are similar but less critical than those for the exterior beam.

All bridge beams have shear connectors throughout their lengths. Under some typical truck-loading conditions, negative moment regions carry substantial positive moments, and the connections provide composite action under those conditions. This composite action may have been considered in the original bridge design.

Longitudinal deck bars were included only for distribution and nominal reinforcing requirements. Additional longitudinal bars were included in the deck over the piers for crack control. The total longitudinal deck reinforcing over the piers, however, does not meet current AASHTO standards for composite action in negative moment regions. During the original design, stresses in the deck reinforcing were not considered. The deck and curbs simply were neglected within the negative moment regions because they were not included in the flexural stress computations for negative bending moment.

2.2. Strengthening Design

As noted in the previous section, the Fonda bridge has flexural overstresses at both inventory and operating levels. The operating level overstresses require load posting. By current bridge design standards [21], the Fonda bridge also has an insufficient number of shear connectors. Thus, the bridge requires strengthening both to reduce flexural stresses and improve

shear connection for composite action. These two strengthening designs and additional design checks are discussed in the following sections.

2.2.1. Post-Tensioning Design

The post-tension strengthening for the Fonda bridge was more complex than the post-tension strengthening for single-span bridges [2,3,4]. In addition to the transverse distribution of post-tensioning, which occurs in single span bridges, the longitudinal distribution in continuous bridges needed to be taken into account. Because the designers of the Fonda bridge took advantage of continuity, the bridge was much more flexible and thus more sensitive to applied forces and moments than a single-span bridge. The existing deck of the Fonda bridge was moderately cracked, and the deck response to post-tensioning was an item of concern.

Initially, the post-tensioning design followed, as closely as possible, the usual Iowa DOT design and rating procedures for the V12 bridge series. This preliminary design is discussed in the next section (Section 2.2.1.1). After additional laboratory testing for another research project [5] and observation of the performance of the Fonda bridge for one year, the bridge was analyzed under different assumptions. This final analysis is then discussed in Section 2.2.1.2.

2.2.1.1. Preliminary Design

The usual Iowa DOT assumption, which neglects composite action in dead-load negative moment regions, creates a severe condition for design of a post-tension strengthening system. For an ideal longitudinal distribution of post-tensioning moments, the post-tensioning needs to be applied near the inflection points, the boundaries between dead-load positive and negative moment regions. The application of post-tensioning moments to the uncoverplated bridge beams, without assuming composite action, would give

stresses much higher than existing stresses. Therefore, for post-tension strengthening, the Iowa DOT composite action assumptions need to be modified within the limits of behavior of the bridge.

Figure 2.5 illustrates the typical moments, approximately to scale, for a bridge beam. Fig. 2.5a shows the dead-load moment diagram, which has inflection points at D and approximately at J, the center span beam splice. Inflection points for long-term dead load in Fig. 2.5b are shifted slightly because composite action is assumed in positive moment regions. With small, long-term dead moments (neglecting a future wearing surface), there is very little shift in inflection point locations for the total dead load.

For live and impact load there are no consistent locations of inflection points. As a truck passes over the bridge, it subjects different spans and portions of spans to positive or negative moment, depending on the position of the truck. Thus, inflection points constantly move and disappear under truck live load. Figure 2.5c shows the live and impact load moment envelope, which has no inflection points; therefore, no regions can be identified as positive or negative moment regions. Any section along a bridge beam, except the abutment bearing at A, will be subjected to both positive and negative truck load moments.

Figure 2.5d gives the approximate moment diagram for post-tensioning of positive moment regions in end and center spans. For the moments in the figure, post-tensioning brackets are located at the end-span dead-load inflection point, D, and at K, near the center span splice. The positive post-tensioning moments in Fig. 2.5d exceed the sum of (1) the long-term dead-load negative moment in Fig. 2.5b, and (2) the increase in live and impact load moment in Fig. 2.5c in the short regions between the dead-load moment inflection point and the theoretical start of coverplate. Thus, for purposes of the post-tensioning design, the assumption for the short regions, DF and HJ, was modified from noncomposite to composite. Those regions actually will be
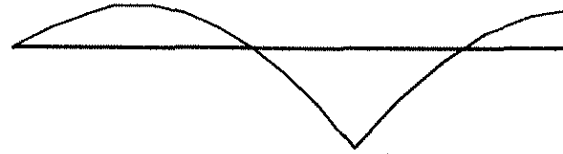
a. DEAD LOAD

b. LONG-TERM DEAD LOAD
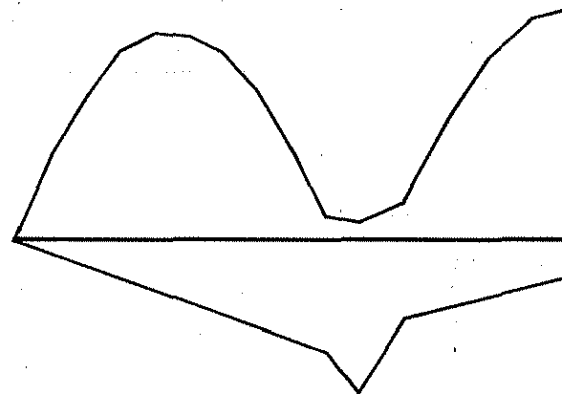
c. LIVE AND IMPACT LOAD ENVELOPE

d. POST-TENSIONING

A B   C   D EF G   HI JK   L
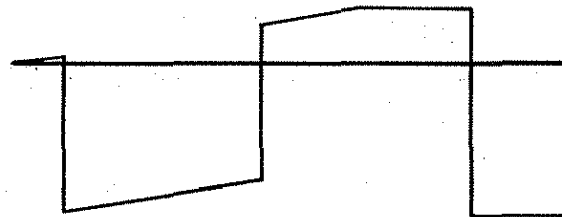
REFERENCE SECTIONS

Fig. 2.5. Bridge beam bending moments.

subjected to less negative moment in the post-tensioned bridge than in the existing bridge. Negative moments in the short regions will be comparable to those in the usually assumed composite action regions.

Previous analysis showed that the longitudinal distribution of post-tensioning moment could be controlled by location of post-tensioning brackets [5]. Brackets placed in dead-load positive moment regions distribute less moment to negative moment regions than brackets placed nearer the piers. Thus, the locations of post-tensioning brackets can be selected to distribute moment to compensate for the relative span and pier overstresses.

After consideration of the longitudinal distribution and the overstresses, it was decided to locate the post-tensioning brackets near the dead-load moment inflection points. In the end spans, the brackets were placed a short distance in from the abutments, at B, and near the nominal inflection point so that the tendon anchorage was at section D. In the center span, because of the splices at the nominal inflection points, brackets were located slightly toward the center of the bridge so that the tendon anchorage was at section K.

With the anchorages located, it was possible to use the SAP IV [24], quarter-symmetry finite element model developed under Phase I of this research [5] to determine the effects of post-tensioning. Because the Phase I laboratory post-tensioning tests correlated well with a finite element model that assumed complete composite action, the finite element model for the Fonda bridge also was developed with full composite action.

Preliminary results from the finite element model showed that it would be difficult to achieve a sufficiently large post-tensioning moment in the center span with a bracket located above the bottom flange of the beam. Therefore, the finite element model was modified for tendon anchorages below the beams in the center span.

The finite element model was run for four different load cases:

1. 100 kips tendon force in exterior beams, end span

2. 100 kips tendon force in exterior beams, center span

3. 100 kips tendon force in interior beams, end span

4. 100 kips tendon force in interior beams, center span

The exterior and interior beam bottom flange stresses at the one-tenth sections and at other critical locations were computed from the finite element analysis and separate dead-load, long-term dead-load, and live plus impact load analyses. The stresses were entered in a Lotus 1-2-3 [25] spreadsheet, along with multipliers for the four different post-tensioning cases. Table 2.3 gives the portion of the spreadsheet for the exterior beam, bottom flange.

The column headings across the top of the spreadsheet in Table 2.3 identify the location of the section (X with respect to Fig. 2.3) and various stresses and combinations of stresses. Stresses in the third column (f:LTD2) were for a future wearing surface, and they were not used in any of the stress combinations. The columns headed f:DLTDL+ and f:DLTDL- give the existing stress conditions under all dead-load plus live-load positive moment and negative moment envelopes, respectively. These stresses are the same as those graphed in Fig. 2.4, except for the short regions between dead-load inflection point and theoretical end of coverplate.

The last column, headed f:P1-4, gives the total post-tensioning stresses, and the three preceding columns give the stresses from which the envelopes in Fig. 2.6 were plotted. It was possible to alter the multipliers for the four post-tensioning load cases and observe the effect on the stresses in the last four columns. After considerable experimentation, the multipliers in Table 2.3 were found to reduce the maximum positive moment region stress and the maximum negative moment stresses for both exterior and interior beams to 18 ksi or less. Some local stresses at the post-tensioning brackets did, however, remain above 18 ksi. The overstresses were caused by point application of

Table 2.3. Preliminary exterior beam, bottom-flange stress spreadsheet.

X	f:DLTD1	f:LTD2	f:L+	f:L-	f:DLTDL+	f:DLTDL-	f:PO1	f:PO2	f:PO3	f:PO4	f:D+L14	f:D14	f:D-L14	f:P1-4
0.0	0.00	0.00	0.00	0.00	0.00	0.00	0.00	0.00	0.00	0.00	0.00	0.00	0.00	0.00
54.9	3.49	0.46	6.96	-0.96	10.45	2.53	1.58	0.26	-0.77	0.28	11.80	4.84	3.88	1.35
66.0	3.97	0.52	7.91	-1.15	11.88	2.82	2.30	0.33	-1.00	0.36	13.88	5.97	4.82	2.00
66.0	3.97	0.52	7.91	-1.15	11.88	2.82	-8.43	0.33	-1.00	0.36	3.15	-4.76	-5.91	-8.73
109.8	5.84	0.78	11.68	-1.92	17.52	3.92	-6.68	0.52	-1.59	0.57	10.34	-1.34	-3.26	-7.18
164.7	7.03	0.97	14.87	-2.87	21.90	4.16	-5.70	0.81	-2.17	0.88	15.71	0.84	-2.03	-6.19
219.6	7.08	1.02	16.22	-3.83	23.30	3.25	-5.26	1.05	-2.41	1.12	17.81	1.59	-2.24	-5.49
274.5	5.98	0.94	16.02	-4.79	22.00	1.19	-5.01	1.37	-2.43	1.40	17.33	1.31	-3.48	-4.67
329.4	3.73	0.72	14.71	-5.75	18.44	-2.02	-5.24	1.67	-2.09	1.59	14.36	-0.35	-6.10	-4.08
384.3	0.34	0.36	11.60	-6.70	11.94	-6.36	-6.57	2.05	-1.47	1.77	7.72	-3.88	-10.58	-4.22
387.0	0.12	0.34	11.38	-6.75	11.50	-6.63	-6.69	2.07	-1.42	1.78	7.23	-4.15	-10.90	-4.27
387.0	0.12	0.57	11.38	-6.75	11.50	-6.63	4.04	2.07	-1.42	1.78	17.96	6.58	-0.17	6.46
439.2	-4.24	-0.13	7.18	-7.66	2.94	-11.90	2.59	2.55	-0.79	1.99	9.28	2.10	-5.56	6.34
456.0	-6.04	-0.32	5.61	-7.95	-0.43	-13.99	2.41	2.78	-0.66	2.08	6.19	0.58	-7.37	6.62
456.0	-3.40	-0.29	6.26	-8.86	2.86	-12.26	1.48	1.68	-0.42	1.24	6.84	0.58	-8.28	3.98
494.1	-5.72	-0.70	2.52	-9.60	-3.20	-15.32	1.34	1.87	-0.14	1.33	1.20	-1.32	-10.92	4.40
549.0	-9.72	-1.42	1.70	-13.17	-8.02	-22.89	1.11	2.16	0.23	1.42	-3.10	-4.80	-17.97	4.92
619.2	-4.77	-0.48	3.22	-6.77	-1.55	-11.54	0.96	2.91	0.37	0.55	3.25	0.03	-6.74	4.80
642.0	-3.58	-0.01	5.49	-6.49	1.91	-10.07	0.91	3.14	0.40	0.27	6.63	1.14	-5.35	4.72
642.0	-6.41	-0.01	4.93	-5.83	-1.48	-12.24	1.50	5.18	0.67	0.51	6.39	1.46	-4.37	7.87
689.4	-1.68	0.26	9.17	-5.23	7.49	-6.91	1.30	6.83	0.75	-0.60	15.77	6.60	1.37	8.28
711.0	-0.25	0.72	10.75	-4.90	10.50	-5.15	1.23	8.56	0.81	-1.32	19.78	9.03	4.13	9.28
711.0	-0.25	0.43	10.75	-4.90	10.50	-5.15	1.23	8.56	0.81	-1.32	19.78	9.03	4.13	9.28
723.0	0.55	0.60	11.62	-4.77	12.17	-4.22	1.20	10.34	0.84	-1.74	22.81	11.19	6.42	10.64
723.0	0.55	0.60	11.62	-4.77	12.17	-4.22	1.20	-12.73	0.84	-1.74	-0.25	-11.87	-16.64	-12.42
759.6	2.98	0.81	14.29	-4.39	17.27	-1.41	1.15	-8.74	0.90	-2.59	7.99	-6.30	-10.69	-9.28
829.8	5.79	1.15	17.37	-3.54	23.16	2.25	1.09	-7.00	0.97	-3.65	14.56	-2.81	-6.35	-8.60
900.0	6.73	1.26	18.02	-2.70	24.75	4.03	1.07	-6.65	0.99	-4.01	16.15	-1.87	-4.57	-8.60
							1.00	1.30	1.00	1.50				

Key

|		
x	=	distance in inches from abutment bearing
f	=	stress in ksi
DLTD1	=	dead- plus long-term dead load
LTD2	=	additional long-term dead load from future wearing surface (not included in any totals)
L+	=	positive live load plus impact moment envelope
L-	=	negative live load plus impact moment envelope
DLTDL+	=	DLTD1 plus L+
DLTDL-	=	DLTD1 plus L-
PO1	=	force and moment for post-tensioning of exterior beams in end span
PO2	=	force and moment for post-tensioning of exterior beams in center span
PO3	=	force and moment for post-tensioning of interior beams in end spans
PO4	=	force and moment for post-tensioning of interior beams in center spans.
D + L14	=	DLTD1 plus L+ plus P1 - 4
D14	=	DLTD1 plus P1 - 4
D - L14	=	DLTD1 plus L- plus P1 - 4
P1 - 4	=	Sum of PO1, PO2, PO3, and PO4
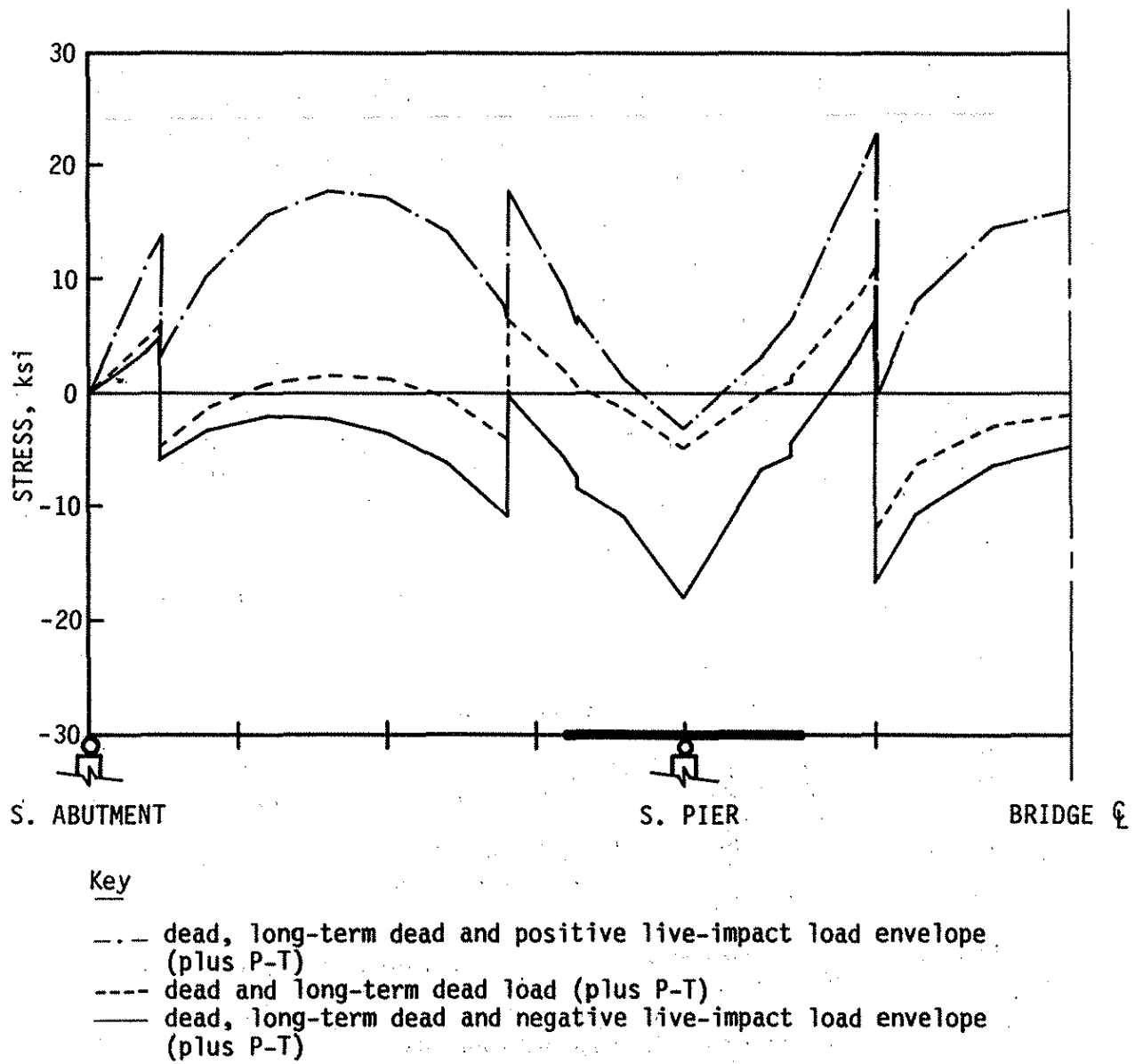
Fig. 2.6.   Preliminary exterior beam, bottom-flange stress
envelopes for post-tensioned bridge.

tendon forces, without consideration of the actual bracket lengths. In the following, Section 2.2.1.2. Final Analysis, the overstresses near brackets are discussed in more detail.

Comparison of Figs. 2.4 and 2.6 shows that the post-tensioning is successful in reducing the critical flexural stresses in the exterior beam. The post-tensioning drops the stress envelopes in positive moment regions and raises the envelopes in negative moment regions. Thus, there is less variation in the stress envelope along the length of the beam with post-tensioning. The stress graph for the post-tensioned interior beam is very similar to that for the exterior beam in Fig. 2.6.

The multipliers at the bottom of Table 2.3 indicate the need for tendon forces varying from 100 kips to 150 kips for the four post-tensioning load cases. These forces are desired after losses and thus must be increased at time of application. Losses for tendon relaxation were estimated as 3.7%, maximum, and losses for a potential temperature difference of 10° F were estimated as 2.1% [3]. (See Fig. A.1 of Appendix A of this report for measured temperatures, which support the 10° assumption.) These losses were taken as a total of 6%. Because there was insufficient information to estimate the tendon gains or losses for a truck at different locations on the bridge, these were not included in the tendon design forces. The gains occur on loaded or unloaded spans and the losses occur only on unloaded spans, thus neglecting the gains, and losses should be conservative. (Design tendon forces for the six different jacking stages are given later, in Fig. 3.10, with the discussion of experimental procedures.)

The final layout of the post-tensioning scheme, with brackets and tendons, is given in Fig. 2.7, while photographs of the system in place are presented in Fig. 2.8. For each span, a set of two 1 and 1/4-in. diameter threadbar tendons, at less than manufacturer's rated capacity, provide the required design force. Bracket A (see Fig. 2.8b) for end spans is similar to the
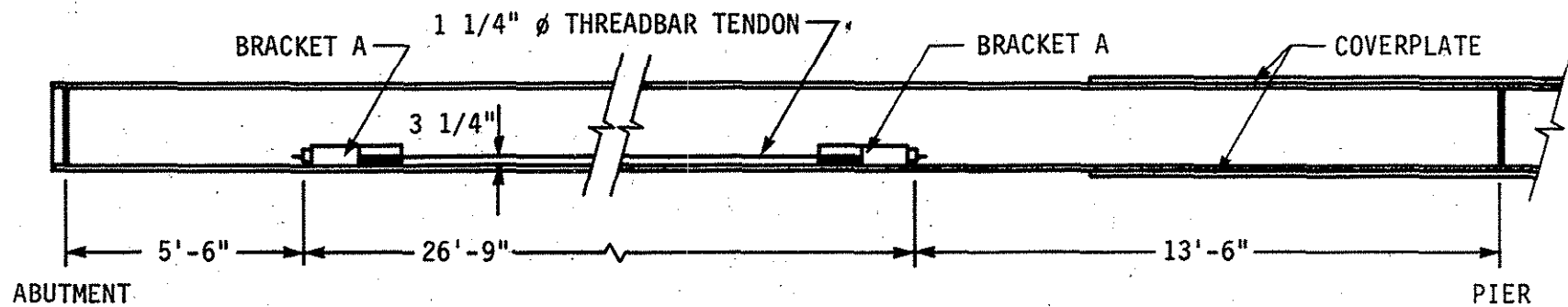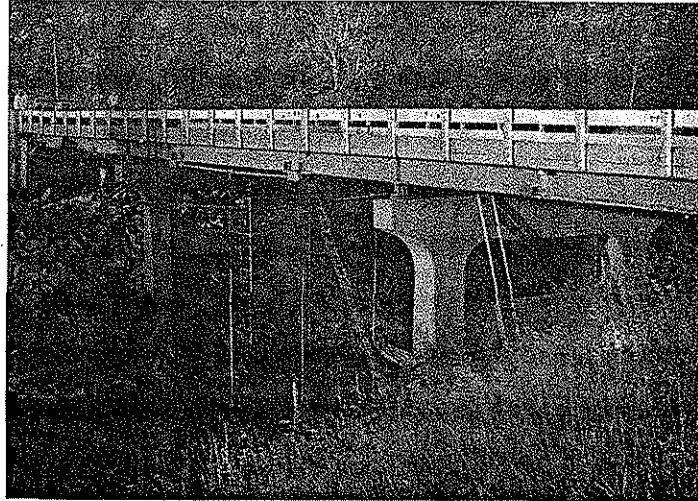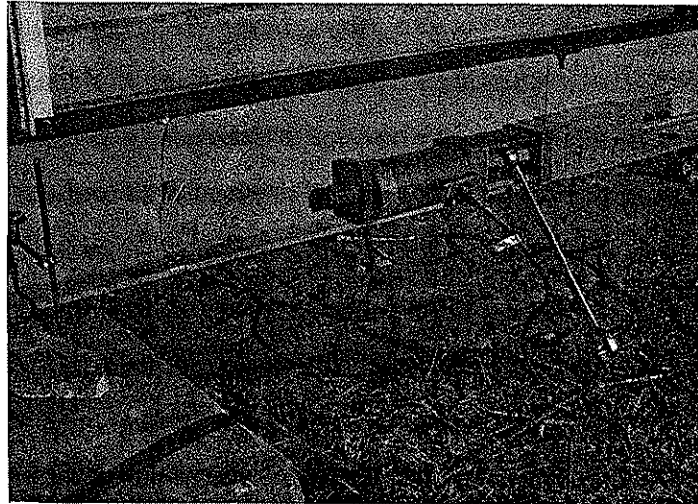
a. END SPAN
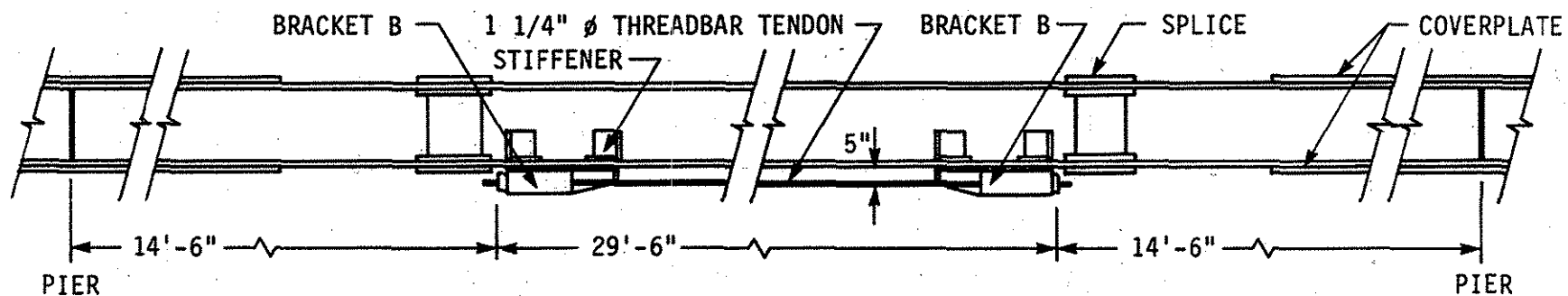
b. CENTER SPAN

Fig. 2.7. Post-tensioning layout.

a. OVERALL VIEW

b. BRACKET A IN PLACE

c. BRACKET B IN PLACE

Fig. 2.8. Post-tensioning system in place.

bracket used by the authors for post-tensioning of single span bridges [3,4]. Detailed drawings are given in Fig. B.1. of Appendix B.

Bracket B (see Fig. 2.8c) for the center span is of a new design for the Fonda bridge. Detailed drawings are given also in Fig. B.2 of Appendix B. Because bracket B is bolted only to the bottom flange of the beam, it could cause overstress in the beam web directly above the bracket. For that reason, the stiffeners detailed in Fig. B.3 were added to the beam web at each end of the bracket.

This preliminary design was completed in various stages under time constraints during preparation of the Fonda bridge for post-tensioning. Therefore there was little opportunity to explore options. Because the tendons and brackets generally are oversized, there is the possibility that future designs could use smaller tendons and refined bracket designs.

2.2.1.2. Final Analysis

After the initial post-tensioning was applied to the Fonda bridge in August 1988, the bridge was inspected several times before the post-tensioning was removed and re-applied in June 1989. It was apparent from the deck crack pattern in September 1988 that the deck had cracked since the post-tensioning was applied. (See Appendix C for deck crack patterns for the Fonda bridge and Appendix D for deck crack patterns in the single-span bridges previously strengthened [4,26].) The deck continued to crack and, in June 1989, the total estimated crack length was more than double the crack length in the bridge deck before post-tensioning. The cracks additionally were distributed throughout the deck rather than being concentrated over the piers and in the east lane of the center span.

Also, after the Fonda bridge was post-tensioned, as part of another research project, the authors continued to test and analyze a negative moment region mockup of a bridge beam similar to the beams in the Fonda bridge [5,26,27,28]. Testing after the mockup deck had been extensively cracked

indicated that the steel beam behaved essentially composite with the deck bars for negative moment and composite with the deck for positive moment.

The unexpected amount of deck cracking of the Fonda bridge and the behavior of the mockup suggested a somewhat different approach to the analysis of the Fonda bridge from the usual Iowa DOT assumptions. The revised load-behavior assumptions are listed in Table 2.4. For dead load, there are no changes because the dead load is applied only to the steel bridge frame. For long-term dead load, however, the assumptions are modified to make the steel beams composite with the deck bars in negative moment regions. For live and impact load and for post-tensioning, the behavior assumptions change depending on whether the positive or negative moment envelope stresses are required. For positive moment, at any section along the bridge the deck and curbs are assumed to act compositely with the steel beams. For negative moment, the deck and curb bars are assumed to act compositely with the steel beams.

Long-term dead load and live plus impact load beam analyses were re-run by the Office of Bridge Design of the Iowa DOT for the revised assumptions. The change in section property assumptions shifted moment from positive to negative moment regions.

Because of the rather extensive changes that would have been required in the SAP IV post-tensioning model to duplicate accurately the reinforcing bars composite with the beams, the SAP IV model was not re-run. Axial forces and moments were extrapolated from the composite steel beam and concrete-deck finite element model and then applied to composite sections composed of the steel beams and reinforcing bars.

The process of extrapolation is illustrated in Fig. 2.9. First the stresses, f_1 and f_2, were obtained for the SAP IV beam element at a section as indicated in Fig. 2.9b. These stresses then were converted to a combination of axial and bending stresses for the neutral axis of the composite section shown in Figs.

Table 2.4. Revised bridge load-behavior assumptions.

Load	Length[1,2]	Assumed Effective Cross Section
Dead (steel beam and concrete deck)	A–F F–H H–L	wide-flange beam coverplated wide-flange beam wide-flange beam
Long-Term Dead (curb and rail)	A–D D–F F–H H–J J–L	composite deck and wide-flange beam, n = 27 composite deck bars and wide-flange beam composite deck bars and coverplated wide-flange beam composite deck bars and wide-flange beam composite deck and wide-flange beam, n = 27
Long-Term Dead (tendons and brackets	A–D D–F F–H H–J J–L	composite deck (and curb for exterior beam) and wide-flange beam, n = 27 composite deck bars (and curb bars for exterior beam) and wide-flange beam composite deck bars (and curb bars for exterior beam) and coverplated wide-flange beam composite deck bars (and curb bars for exterior beam) and wide-flange beam composite deck (and curb for exterior beam) and wide-flange beam, n = 27
Live–positive moment envelope–(Iowa legal trucks and impact) and post-tensioning	A–F F–J J–L	composite deck (and curb for exterior beam) and wide-flange beam, n = 9 composite deck (and curb for exterior beam) and coverplated wide-flange beam, n = 9 composite deck (and curb for exterior beam) and wide-flange beam, n = 9
Live–negative moment envelope–(Iowa legal trucks and impact) and post-tensioning	A–F F–J J–L	composite deck bars (and curb bars for exterior beam) and wide-flange beam composite deck bars (and curb bars for exterior beam) and coverplated wide-flange beam composite deck bars (and curb bars for exterior beam) and wide-flange beam

[1] Lengths are defined by reference sections given in Figure 2.3 and Table 2.1. For stress checks, lengths (given in table) using theoretical coverplate end sections are used. For moment determination, however, actual coverplate end sections are used.

[2] All post-tensioning moments and axial forces were obtained from the same SAP IV analysis, which assumed a fully composite deck and curbs. For stress checks, however, the assumptions given in the table, which change from positive to negative moment envelopes, were used.

a. COMPOSITE BEAM

b. SAP IV BEAM
   ELEMENT
   STRESSES

c. COMPOSITE
   SECTION
   AXIAL
   STRESSES

d. COMPOSITE
   SECTION
   BENDING
   STRESSES

e. COMPOSITE
   SECTION
   AXIAL
   FORCE

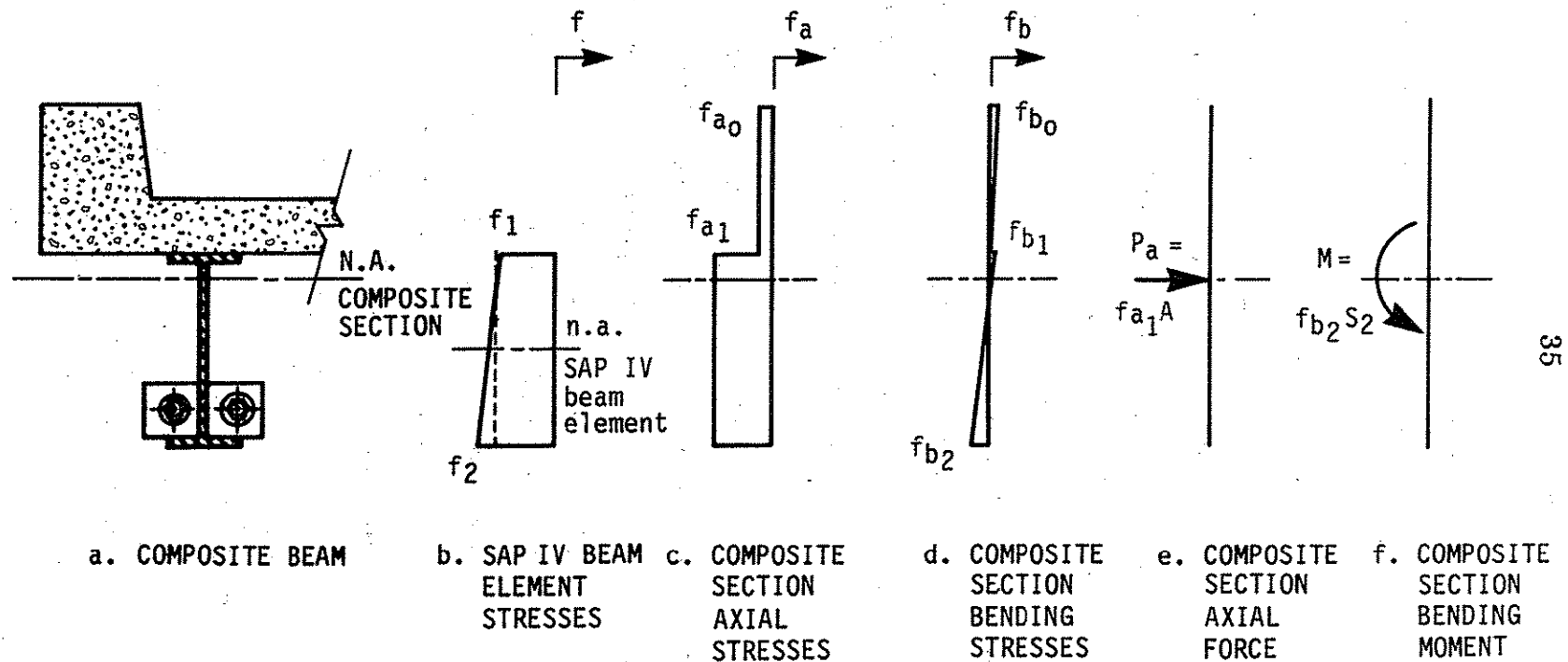f. COMPOSITE
   SECTION
   BENDING
   MOMENT

Fig. 2.9. Extrapolation of SAP IV beam element stresses to
composite section axial force and moment.

2.9c and 2.9d. Finally, the axial stresses and bending stresses were used to compute the axial force shown in Fig. 2.9e and the bending moment shown in Fig. 2.9f. This extrapolation process was used to estimate beam, deck and deck bar, and curb and curb bar stresses as required.

As noted in Section 2.2.1.1., the preliminary design stress spreadsheet showed that, although stresses were less than 18 ksi at the usual maximum stress sections, there were overstresses near the post-tensioning brackets. In the judgment of the authors, this overstress was at least partially caused by the severe bracket modeling in the SAP IV model. Each post-tensioning bracket was modeled as an arbitrarily stiff beam element from the tendon anchorage to the beam elements representing the steel bridge beam. This modeling applied the post-tensioning force to a point where, in reality, the bracket is two to three feet long and applies the post-tensioning to a finite length of the beam.

In order to estimate more accurately the post-tensioning stresses near the brackets, minor modifications were made to the SAP IV model, as shown in Fig. 2.10 for bracket B. The single, arbitrarily stiff beam element was changed to a series of triangular plate elements radiating from the tendon anchorage. Because there is some load spread within the bridge beam web, the length over which the plates are attached was made equal to the bracket length plus end distances. These distances each were approximately equal to the distance set by a vertical line beginning at the tendon anchorage and inclined at 40°. The plate element properties were made approximately equal to the properties of the vertical plates in bracket B.

The revised load-behavior assumptions, long-term dead and live load moments, and SAP IV model were used along with the actual 1989 post-tensioning forces (less 6% design losses) and extrapolated post-tensioning axial forces and moments to create a more extensive Lotus 1-2-3 spreadsheet than for the preliminary design. From this spreadsheet a series of stress envelope

SLAVE NODE LINKED TO DECK NODE
BEAM ELEMENT (CURB)
SHELL ELEMENT (DECK)

A

BOUNDARY ELEMENT WITH
NOMINAL STIFFNESS

100^k

BEAM ELEMENTS
(SHEAR CONNECTOR)

BEAM ELEMENT (BEAM)

FOUR PLATE
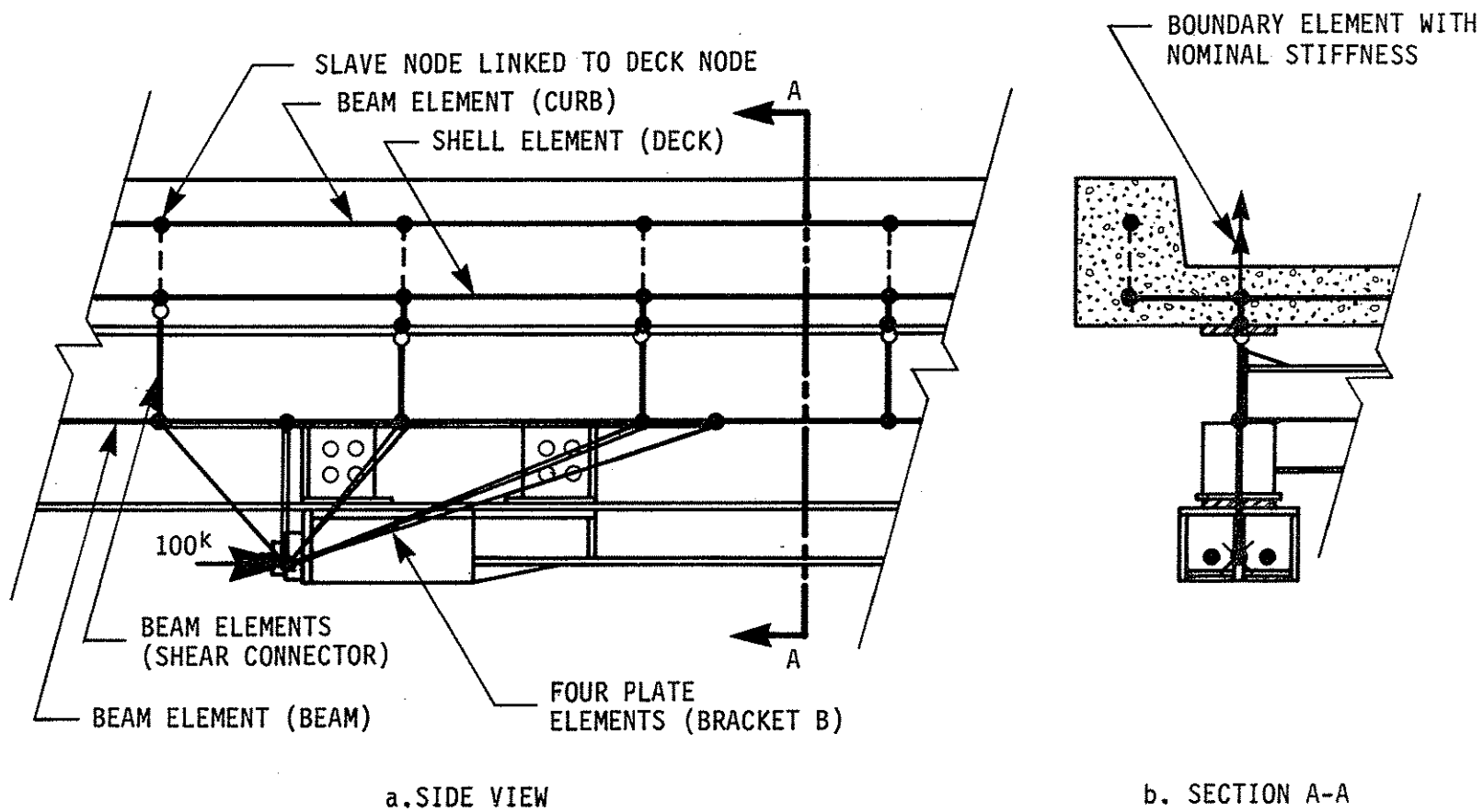ELEMENTS (BRACKET B)

A

37

a.SIDE VIEW

b. SECTION A-A

Fig. 2.10. Revised SAP IV bracket B modeling.

graphs were generated, and these graphs for the exterior bridge beam are given in Figs. 2.11 through 2.14.

In each figure, the envelope or envelopes are given for the existing bridge under the revised load-behavior assumptions, and then the envelope or envelopes are given for the post-tensioned bridge. Figures 2.11a and 2.12a, for example, give the envelopes for existing bottom and top flange stresses, respectively, and Figs. 2.11b and 2.12b give the post-tensioned bridge stress envelopes.

Figure 2.11 shows that post-tensioning reduces all of the bottom flange tension stresses to less than 18 ksi and reduces all of the compression stresses to less than 18 ksi except the stress at the pier and one stress either side of midspan. The pier stress is at approximately 19.5 ksi, which is an inventory load overstress but would not require load-posting of the bridge. Near the brackets are compression stresses that approach 18 ksi and that actually may be inventory load overstresses depending on evaluation of the lateral support of the flange.

Figure 2.12 shows only a slight reduction in maximum tension stresses. The tension stresses at the coverplate cutoffs are reduced to less than 18 ksi, but the stress at the pier only is reduced to approximately 19.2 ksi. This inventory load overstress, again, would not require posting of the bridge.

Assuming that the reinforcing in the Fonda bridge deck and curbs has a yield strength of 40 ksi, the allowable inventory load tension stress is 20 ksi, and the allowable operating stress is 28 ksi [23]. Assuming also that the concrete has a minimum strength of 5000 psi, the allowable inventory load compression stress is 2.0 ksi.

For Figs. 2.13 and 2.14, the stress envelopes are given in two parts. The upper part gives the tension stress envelope in the most highly stressed reinforcing bar, assuming that all loads after the deck and curbs are placed are applied to a composite section consisting of steel beams and reinforcing bars.
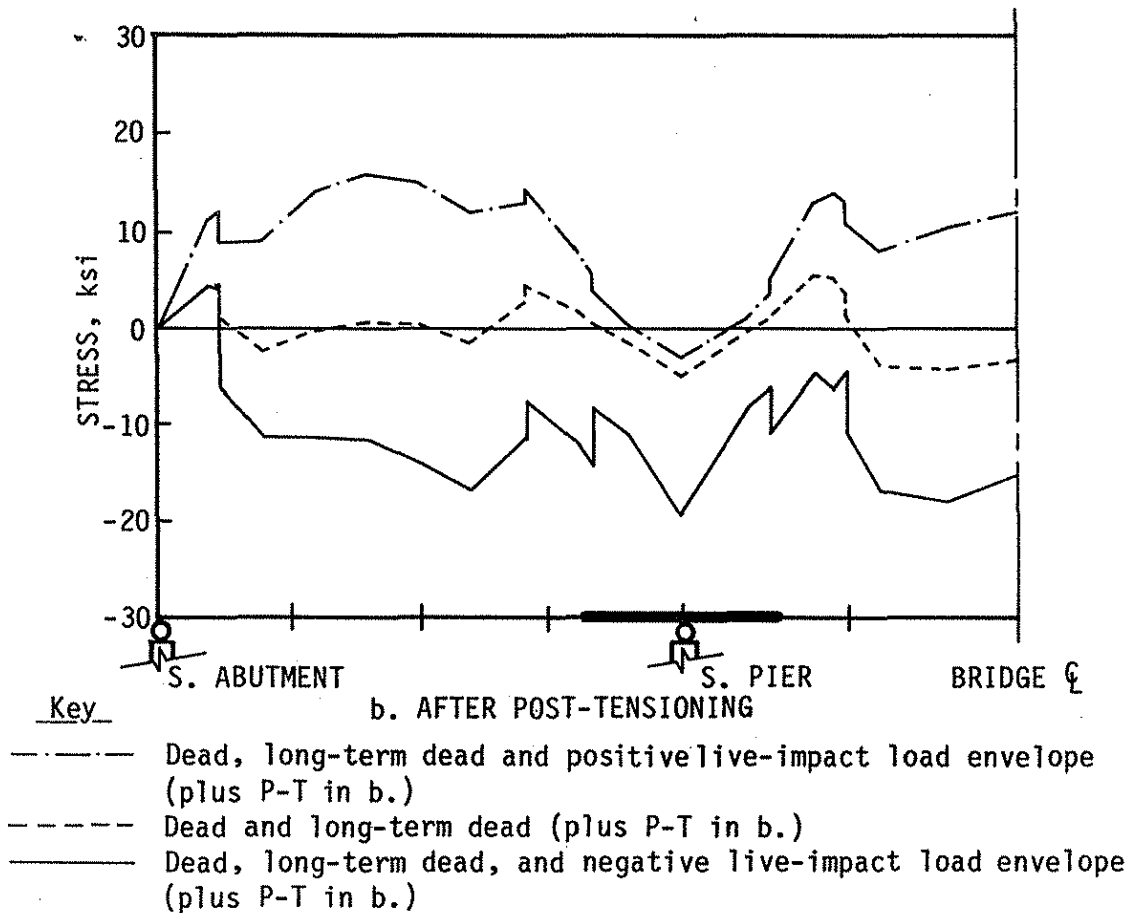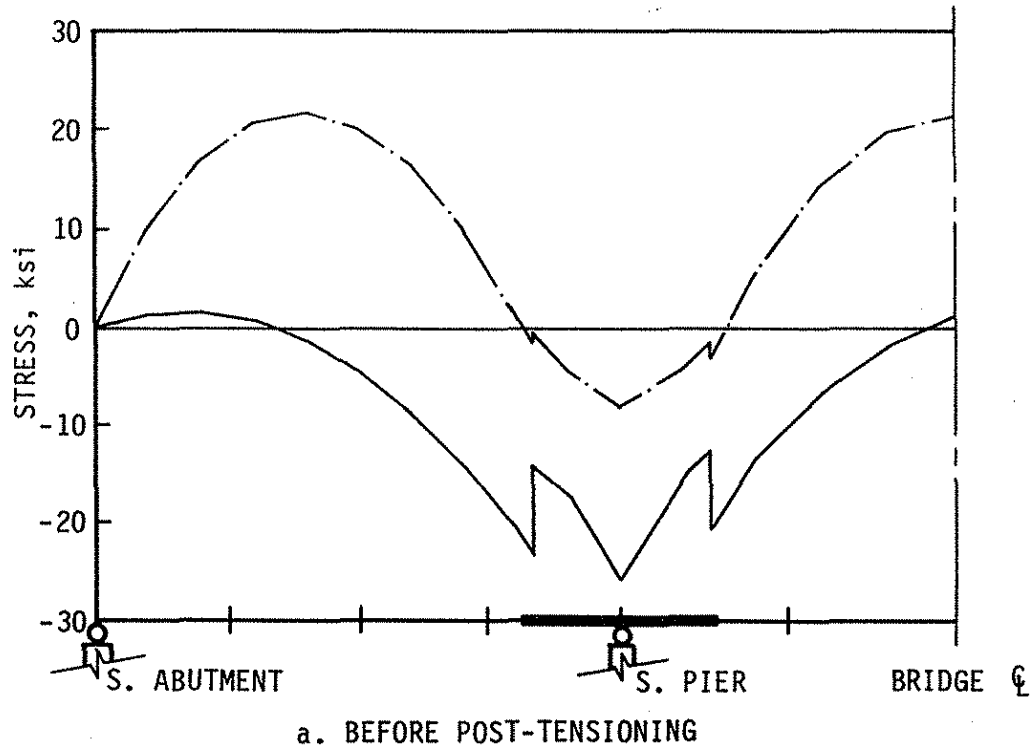
a. BEFORE POST-TENSIONING

b. AFTER POST-TENSIONING

Key

—·—·— Dead, long-term dead and positive live-impact load envelope (plus P-T in b.)

— — — — Dead and long-term dead (plus P-T in b.)

———— Dead, long-term dead, and negative live-impact load envelope (plus P-T in b.)

Fig. 2.11. Ext. bm bottom-flange stress envelopes for revised ld-behavior assumpt.

a. BEFORE POST-TENSIONING

b. AFTER POST-TENSIONING
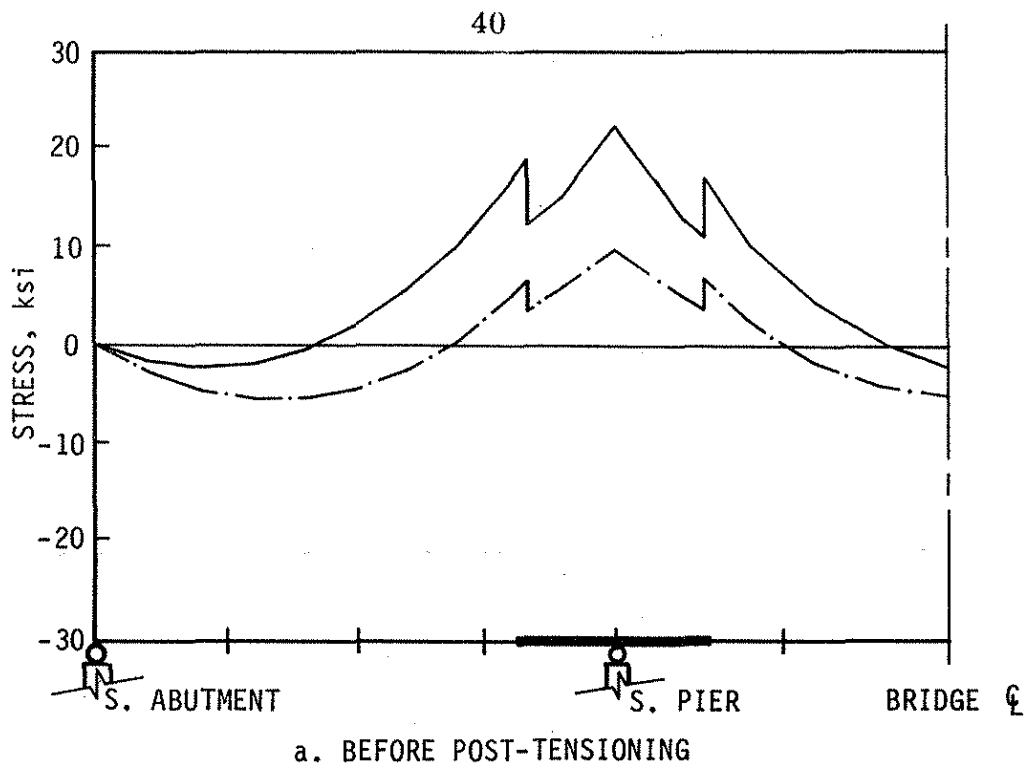
Key
———·—— Dead, long-term dead,and positive live-impact load envelope (plus P-T in b.)
———— Dead and long-term dead (plus P-T in b.)
———— Dead, long-term dead, and negative live-impact load envelope (plus P-T in b.)
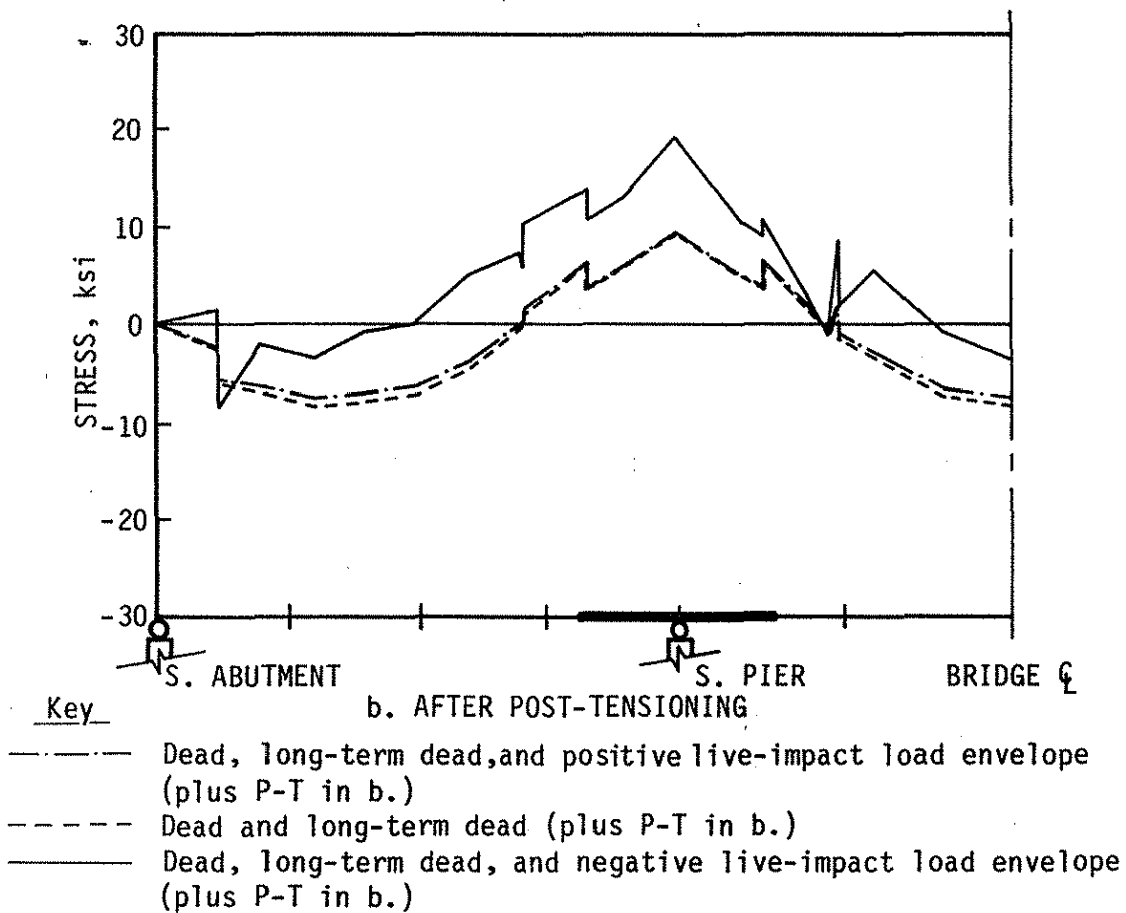
Fig. 2.12. Ext. bm top-flange stress envelopes for revised load-behavior assumpt.

41

a.   DECK BAR STRESS BEFORE POST-TENSIONING

S. ABUTMENT   S. PIER   BRIDGE ₵

b.   DECK STRESS BEFORE POST-TENSIONING

Key

—⋅——⋅—   Dead, long-term dead, and positive live-impact load envelope
          (plus P-T in d.)
————   Dead and long-term dead (plus P-T in c. and d.)
————————   Dead, long-term dead and negative live-impact load envelope
          (plus P-T in c. and d.)
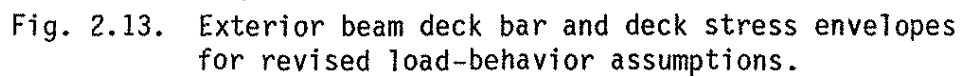
Fig. 2.13.   Exterior beam deck bar and deck stress envelopes
             for revised load-behavior assumptions.

42

c. DECK BAR STRESS AFTER POST-TENSIONING

d. DECK STRESS AFTER POST-TENSIONING

Fig. 2.13. Continued.

a. CURB BAR STRESS BEFORE POST-TENSIONING

b. CURB STRESS BEFORE POST-TENSIONING

S. ABUTMENT   S. PIER   BRIDGE ℄

Key

——·——— Dead,long-term dead, and postive live-impact load envelope (plus P-T in d.)

— — — — Dead and long-term dead (plus P-T in c. and d.)
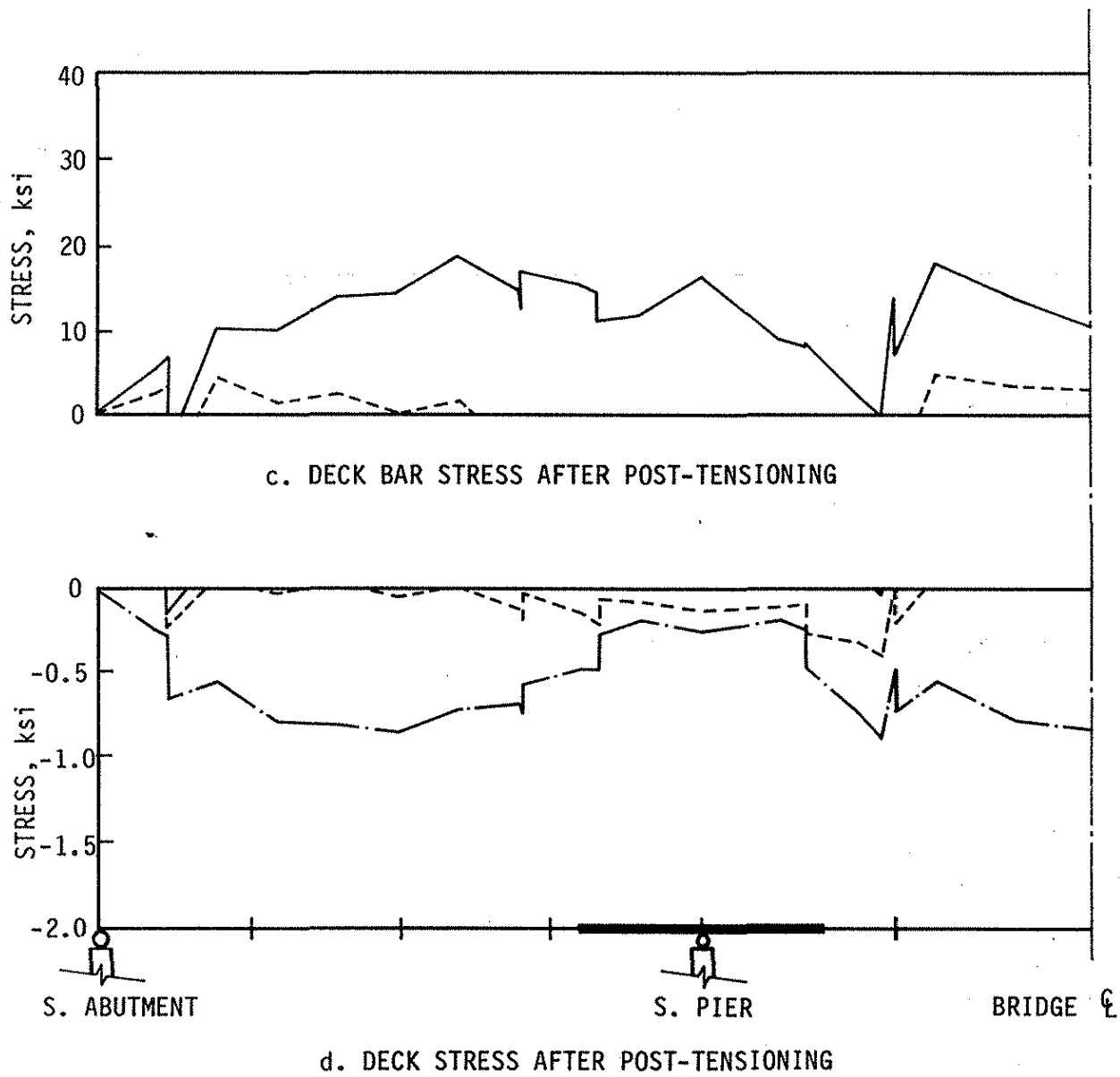
———————— Dead, long-term dead and negative live-impact load envelope (plus P-T in c. and d.)
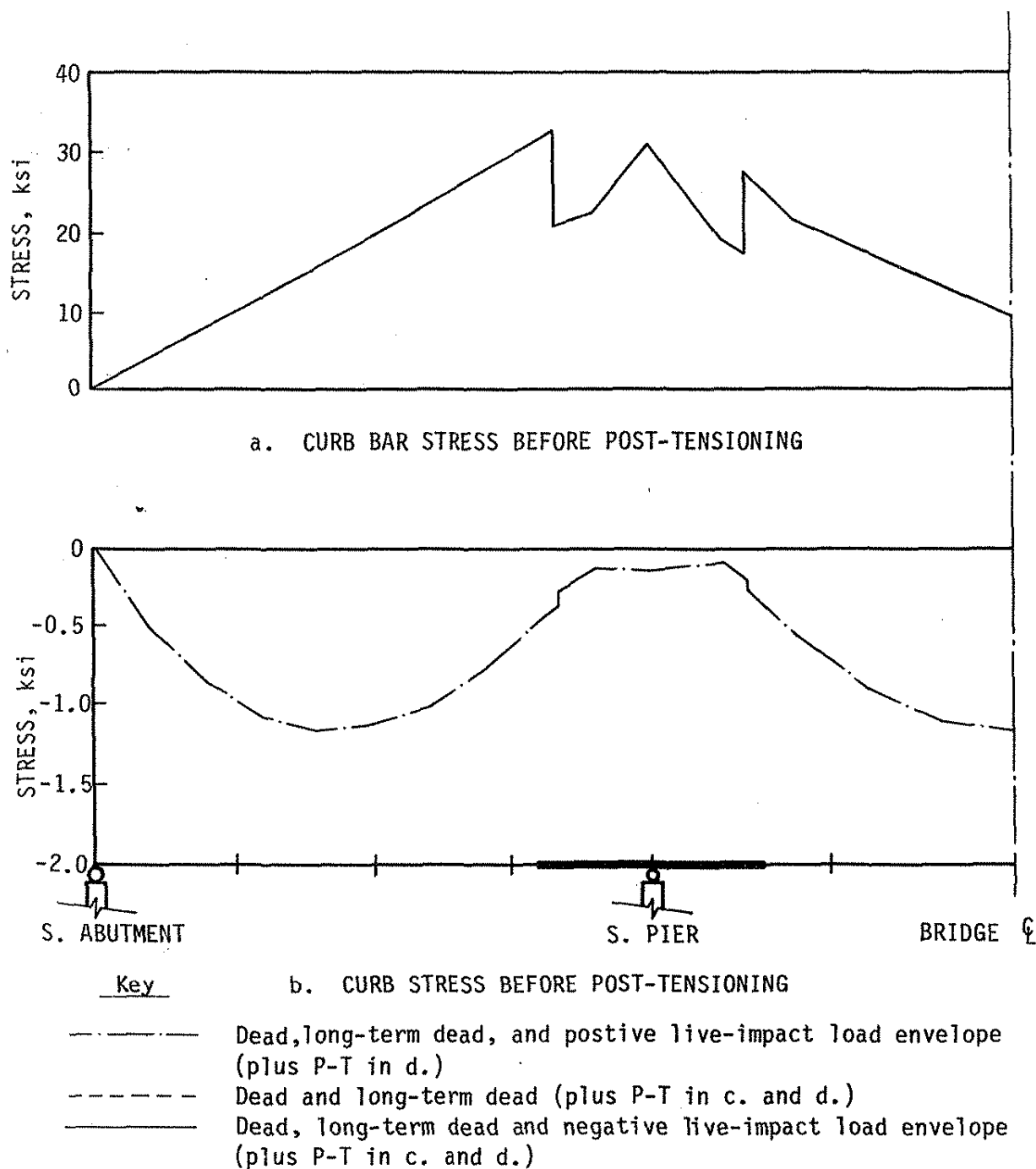
Fig. 2.14. Exterior beam curb bar and curb stress envelopes for revised load-behavior assumptions.

c. CURB BAR STRESS AFTER POST-TENSIONING

S. ABUTMENT

S. PIER

BRIDGE ₵

d. CURB STRESS AFTER POST-TENSIONING
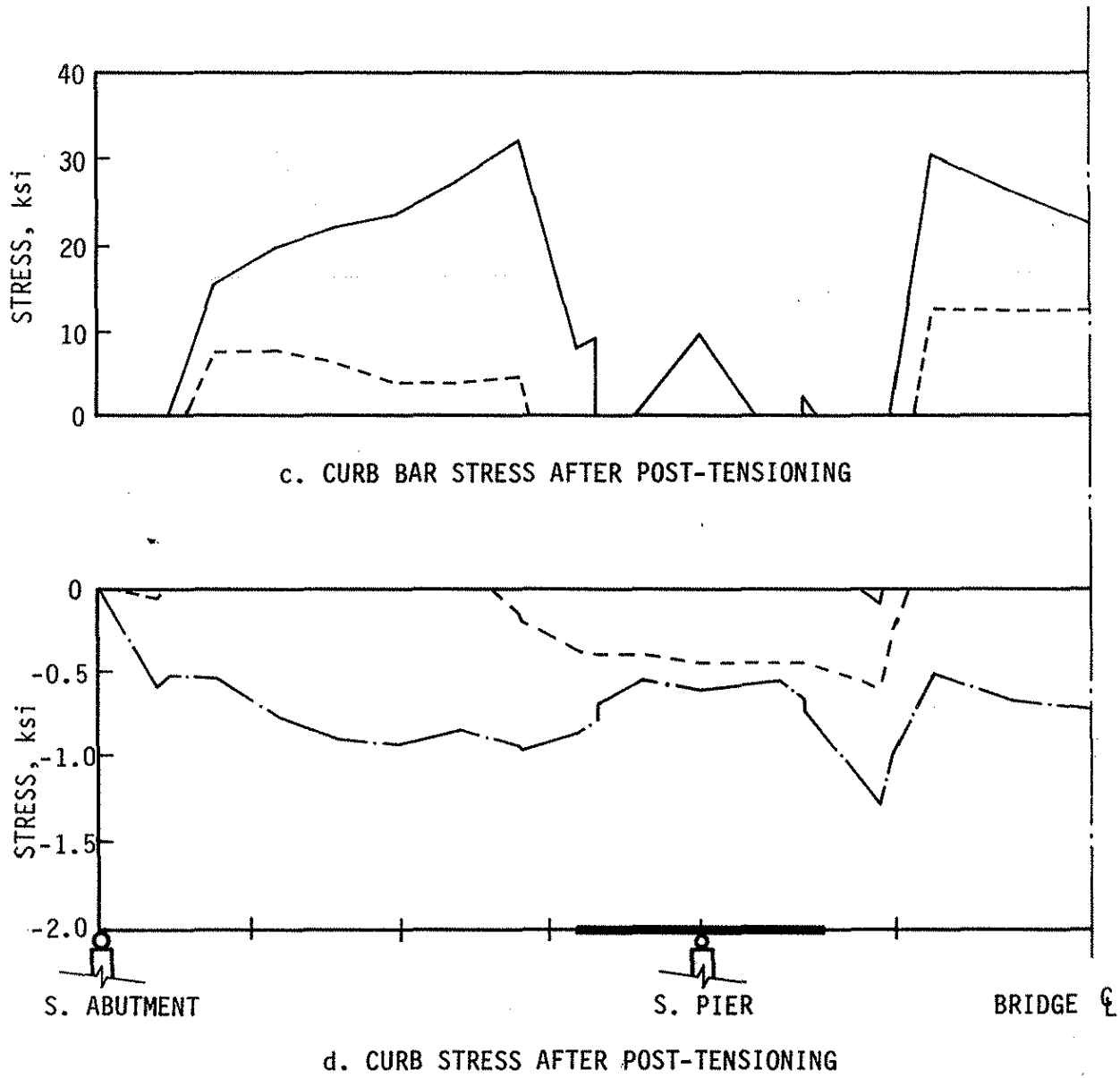
Fig. 2.14. Continued.

The lower part gives the compression stress envelope, to a different scale, for the most highly stressed part of the concrete, assuming that all loads after deck and curbs are placed are applied to the fully composite concrete and steel section.

Figure 2.13a shows deck bar overstresses near the piers in the region where the existing Fonda bridge deck was most heavily cracked. Figure 2.13c indicates that post-tensioning reduces the maximum bar stress to approximately 18.9 ksi, less than the allowable stress, but increases bar stresses on the end and center spans. These locations are where there was the most noticeable increase in cracking in the post-tensioned bridge deck. (See the deck crack patterns in Appendix C.) There are no concrete compression overstresses in either the existing or post-tensioned bridge deck.

For the curb, Fig. 2.14a shows overstresses in the reinforcing bars under existing conditions. Post-tensioning, as illustrated in Fig. 2.14c, does not significantly lower the maximum curb reinforcing stress. Post-tensioning does, however, increase the stresses in the end and center spans. In spite of these computed stress increases, the Fonda bridge curbs did not exhibit any significant additional cracking after the 1988 post-tensioning. Concrete compression stresses are within the allowable level (assuming 5000 psi concrete).

The stress envelopes for the interior beam under the revised load-behavior assumptions are quite similar to those for the exterior beam. Maximum stresses do not significantly exceed those for the exterior beam and deck; in some cases the maximum stresses are less.

The effect of the 1989 post-tensioning on the Fonda bridge generally was favorable in reducing stresses but unfavorable in increasing deck cracking. The magnitudes of the stress reductions are partially dependent on the analysis assumptions and the allowable operating stresses. Under the revised load-behavior assumptions, the only obvious steel beam inventory load

overstresses are at the piers. These overstresses of approximately 2 ksi are not severe enough to cause posting of the bridge, unless the compression overstress is unacceptable because of potential lateral buckling. There may be similar compression overstresses near the brackets, even though the total stress is less than 18 ksi.

Deck and deck reinforcing stresses under the revised load-behavior assumptions fall within the allowable inventory stresses, but curb bar stresses do not. In the post-tensioning computations for single span bridges [3], tension overstresses in the curb were neglected on the basis that, if the curb were disregarded, stresses in the deck and steel beams still would remain acceptable. Because there is no significant overcapacity in the Fonda bridge, disregarding the curb would increase deck and beam stresses above the inventory stress level but not to the operating level.

Based on flexural stress computations under the revised load-behavior assumptions, then, post-tensioning can reduce steel beam stresses below those allowable at the operating load level. Thus, a continuous bridge could be post-tensioned to remove the need for load posting. However, post-tensioning only the positive moment regions did not reduce all flexural stresses below those allowable at the inventory load level for this particular bridge.

2.2.2. Shear Connector Design

Shear connector design under present AASHTO bridge design specifications [21] requires design for both fatigue and strength. Because the number of load cycles for the Fonda bridge was unknown, it was not possible to check the existing connectors for fatigue. As was done for the single-span bridges previously strengthened, the existing angle plus bar connectors were checked only for strength [3,4].

The strength check indicated that existing shear connectors in the positive moment regions were insufficient and that additional shear connection capacity was required. The additional capacity was provided by one-inch-diameter, high-strength bolt connectors of the type developed and tested by the authors for single-span bridges [4].

The layout of the existing and new connectors is given in Fig. 2.15. A total of 220 new bolt shear connectors were added to the bridge. Because the top flanges of the bridge beams do carry large tensile stresses near the supports, the additional bolt connectors were located away from the piers. Two of the connectors were placed between the dead-load inflection point and the piers in each end-span beam, but the authors do not recommend that practice. If the loss of section at the bolt holes is considered, stresses will exceed the inventory allowable stress.

One option for reducing flange loss at bolt holes would be to stagger the pair of bolts rather than locate them both at the same section. Maximum section loss then would be a single bolt hole.

In view of the relatively high tension stresses in top flanges throughout the bridge, it would seem better to use additional welded connectors. The welded connectors do not have the potential for creating local stress concentrations as large as the bolted connectors.

2.2.3. Design Checks

The Fonda bridge additionally was checked for shear stress in the beams, deflection, and fatigue at the coverplate end welds. The shear stress check and approximate deflection check gave results within present AASHTO specifications [21].

The cover plate fatigue check indicated that the weld was acceptable for approximately 100,000 cycles. Because the fatigue history of the bridge is
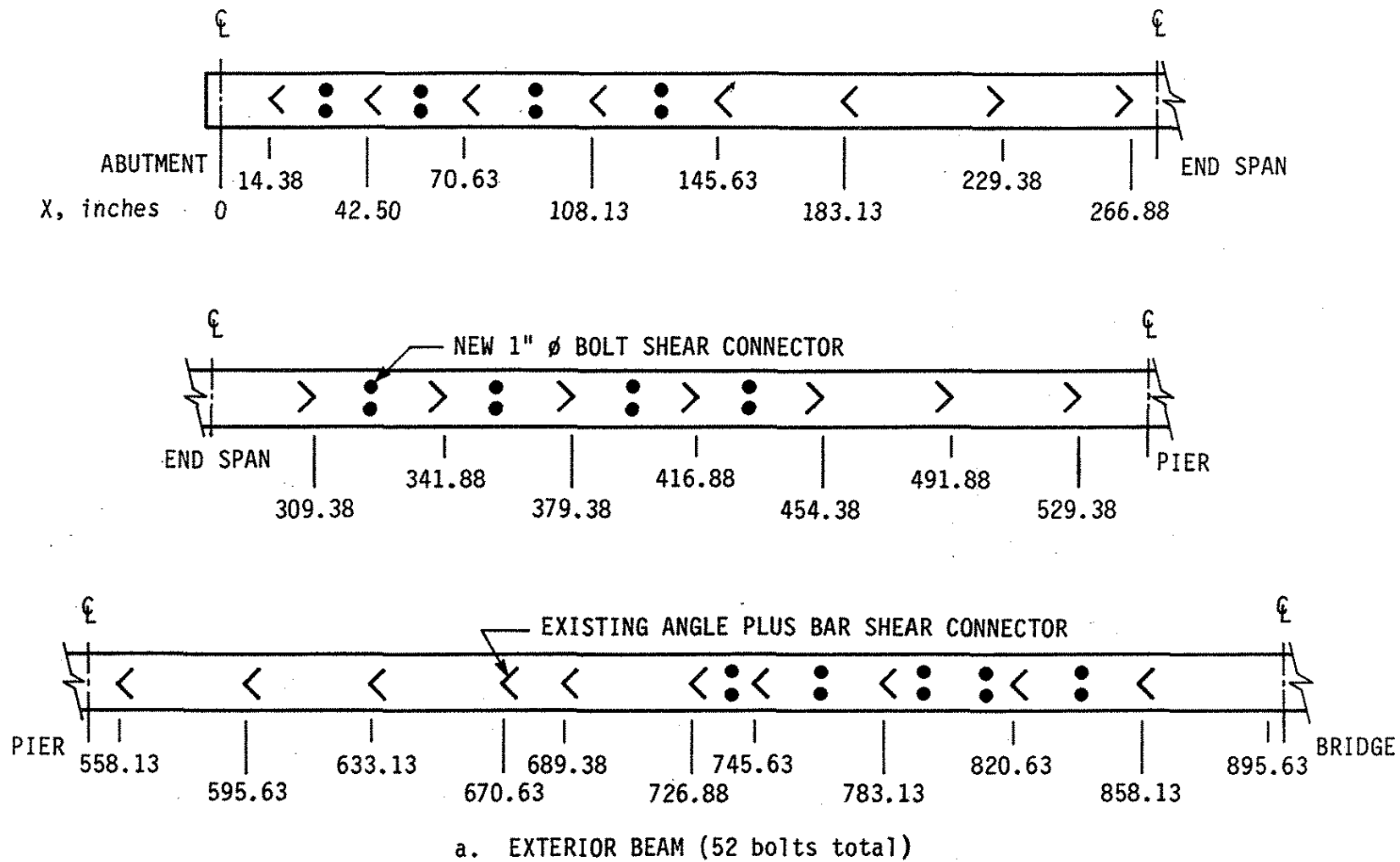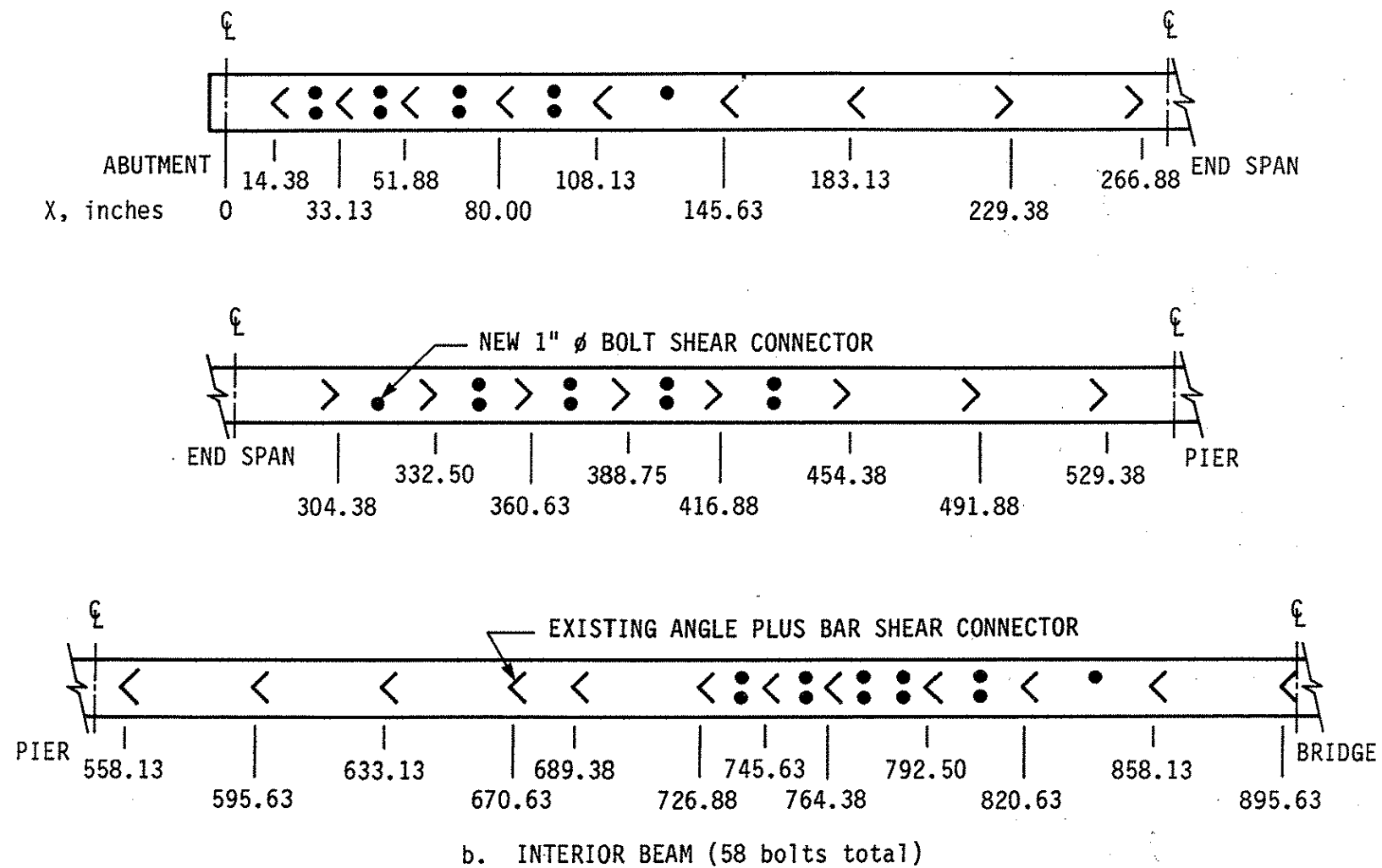
Fig. 2.15. New bolt shear connector layout.

48

ABUTMENT

X, inches

NEW 1" ø BOLT SHEAR CONNECTOR

END SPAN

PIER

EXISTING ANGLE PLUS BAR SHEAR CONNECTOR

PIER

BRIDGE

b. INTERIOR BEAM (58 bolts total)

Fig. 2.15. continued.

49

unknown, further checking was not performed. As noted in earlier work [3,4], fatigue of the post-tensioning brackets is not significant because the brackets are subjected only to fatigue from the variation in tendon force under truck load. The variation in tendon force is a small fraction of the total tendon force and thus causes minimal stress cycles.

With the continuous beam design of the Fonda bridge, the shear and deflection checks are closer to the allowable levels than for a single-span bridge. Although there is some margin between the computed and allowable values, these checks should not be neglected in strengthening design for continuous bridges.

3. TEST AND TEST PROCEDURES

The following sections outline the details of the specific tests that were conducted during the field strengthening and testing of the bridge. Only descriptions of the various tests, instrumentation used, and procedures followed during testing will be presented in this chapter; discussion and analysis of results, as well as the behavior of the bridge, will be presented in Chapter 4. For clarity, in the following sections, instrumentation, loadings, test procedures, and the like used in each year (1988 and 1989) are presented separately.

The instrumentation for the field tests consisted of electrical-resistance strain gages (strain gages), direct current displacement transducers (DCDT's), mechanical displacement dial gages (deflection dials), crack monitors, and temperature sensors.

Two different types of strain gages were used in this investigation: conventional strain gages and weldable strain gages. Conventional strain gages used on the post-tensioning tendons were attached by means of recommended surface preparations and adhesives. Weldable strain gages, which were used on the bridge, are essentially conventional strain gages that are laboratory-prebonded to a metal carrier and fully encapsulated. The gages are attached to the specimen, in this case the bridge beams, by spot welding with a portable hand-probe spot welder. The main advantages of the weldable gages are that they can be installed while the bridge is open to traffic and that they require only minimal surface preparation for installation. They are usable immediately after installation; no curing time is required. All strain gages were self-temperature compensated; however, time constraints (correct gages were back-ordered and would not be available for several months) forced the use of some weldable strain gages with incorrect compensation. As will be explained later, this constraint did not create any special problems. All strain

gages were waterproofed with appropriate protective coatings; three-wire leads were used to minimize the effect of the long lead wires (over 150 ft in some instances) and temperature changes.

The DCDT's were used in both years to measure the vertical movement of the bridge. Both the strain gages and the DCDT's were monitored and recorded with a computerized data acquisition system (DAS). Temperatures measured with temperature sensors (used in combination with the network system provided by the manufacturer) were monitored by using a standard switch-and-balance unit with a strain indicator and were recorded by hand.

The deflection dials (used the first year to determine longitudinal movement of the bridge) and crack monitors (used the second year to determine longitudinal and vertical movement of the bridge relative to the piers) were also read and recorded by hand.

3.1. Instrumentation

As has been previously noted, there are numerous differences in the instrumentation used each of the two years (1988 and 1989). Thus for clarity, the instrumentation used is presented by year.

3.1.1. 1988 Instrumentation

In the following paragraphs, the type of instrumentation, its location, purpose, and so forth are presented. Figure 3.1 indicates the location of the 64 strain gages mounted on the bridge. At each of the sections instrumented, there were two gages mounted on the upper surface of the bottom flange with their axes parallel to the axis of the beam. At six of the sections instrumented (see Fig. 3.1), in addition to the gages on the bottom flange, there were two gages on the lower surface of the top flange with their axes parallel to the axis
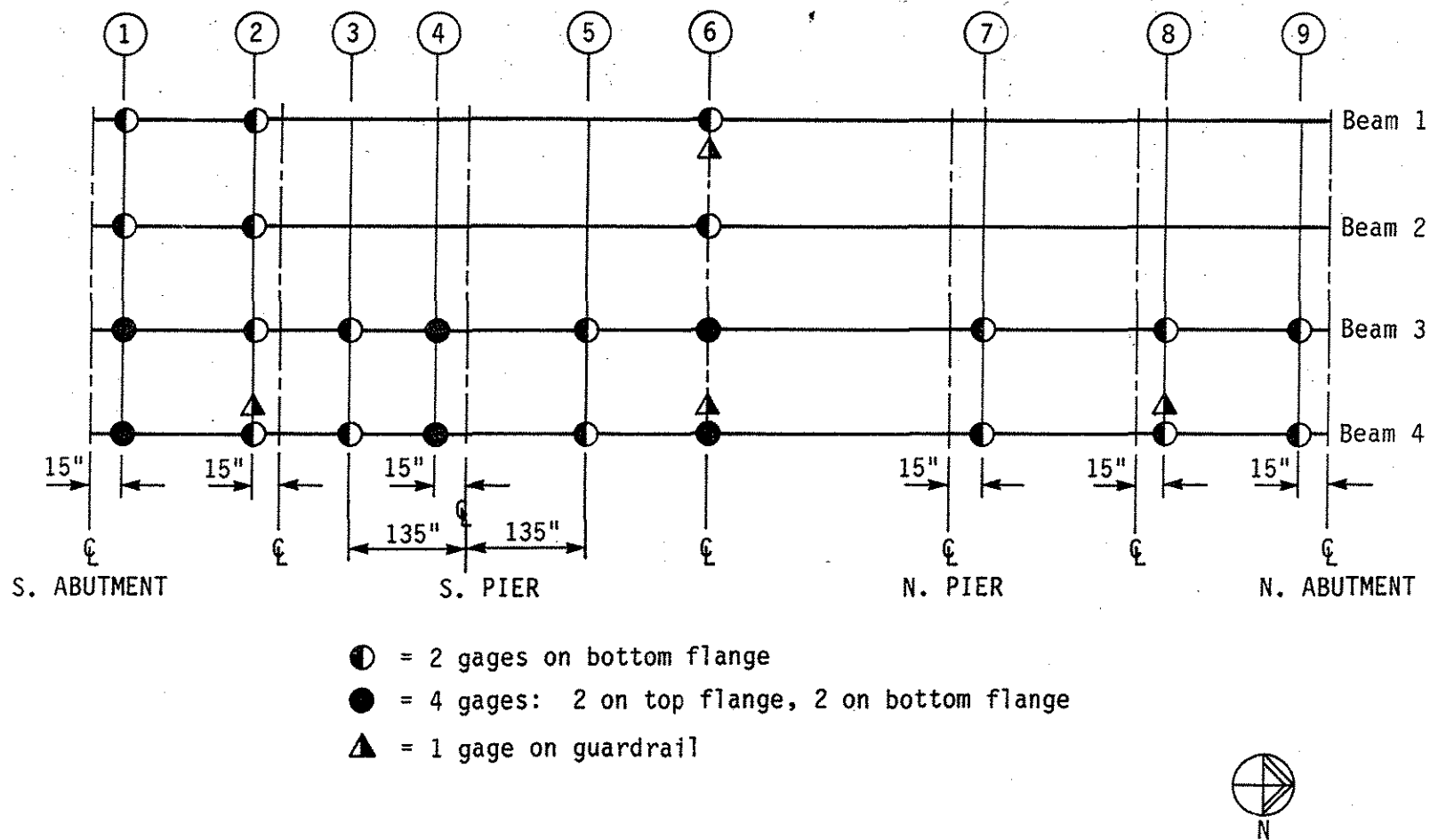
Fig. 3.1. Location of strain gages ∿ 1988.

63

of the beam. All beam strain gages were located 1 and 1/4 in. in from the beam flange edges, even at sections at which there were coverplates. As shown in Fig. 3.1, because of the presence of diaphragms it was necessary to offset the instrumentation at several locations (i.e., sections 1, 2, 4, 7, etc.). As may be noted in Fig. 3.1, beams 3 and 4 were "fully" instrumented while beams 1 and 2 only had three sections instrumented and thus were primarily used for check purposes. Instrumentation at sections 1 and 9 was employed for detecting the presence of end restraint while the instrumentation at Sections 3 and 5 was used to reveal composite action in these regions. Four strain gages were also positioned on the upper channel of the guardrails (see Fig. 3.1) with their axes parallel to the bridge beams. Although the four gages obviously were not sufficient to measure accurately the contribution of the guardrails to the load resistance of the bridge, they did provide some information.

For accurate force measurement, each of the Dywidag threadbars (2 1 and 1/4 in. required in the positive moment region of each beam) were instrumented with two longitudinal strain gages (wired to cancel bending and detect twice the actual axial strain).

For corrosion protection, all threadbars were given a fusion-bonded powder epoxy coating (thickness = 8 mils ± 2 mils) using 3M:SK213. Because the tendons were factory coated, all areas that were scratched during shipping or handling were recoated by hand using the same material. The post-tensioning brackets were painted in the laboratory with Iowa-DOT-approved red oxide Type 2 primer. After they were bolted in place, bolts were painted and the brackets "touched-up" with the primer. After the post-tensioning and testing were completed, the brackets, attaching bolts, and the like were painted with an Iowa-DOT finish coat: Foliage Green. In the end spans of the bridge, it was necessary to remove a portion of the interior diaphragm bracket for tendon clearance. Tendon vibratio (resulting from the dynamic loading of vehicles on the bridge) caused contact between the tendons and diaphragms in

these spans. Tendons in these regions were later covered with a portion of PVC pipe to protect the epoxy coating on the tendon.

Figure 3.2 illustrates the positions of the 10 DCDT's that were used for the measurement of vertical deflections on all four beams of the south and middle spans and the east exterior and interior beams of the north span. To support the DCDT's in the middle span, telescoping pipes were used to traverse the distance (approximately 26 ft) between the bottom of the bridge beams and the river bed. For stability the four individual pipe strands were stayed by means of a system of cables. Also shown in this figure are the locations of the four dial gages that were used for measuring longitudinal movement of the bridge. The dial gages at the end abutments were positioned to bear against the bearing stiffeners of the exterior beams; the dial gages on the piers were seated against the diaphragm between the east exterior and interior beams.

The positions of the six temperature sensors used to measure the temperature of the beams during the strengthening and testing are shown in Fig. 3.3. Note that two of the gages (nos. 4 and 6) were in the morning sun and one (no. 1) was in the late afternoon sun; the others were positioned under the bridge. Air temperature during testing was monitored with a regular thermometer located under the bridge out of direct sunlight.

3.1.2. 1989 Instrumentation

As a result of some of the data obtained in the 1988 testing, and the desire to obtain data at other locations, several modifications were made in the 1988 instrumentation. Shown in Fig. 3.4 are the locations of the 56 strain gages used in the 1989 testing program. As may be determined by comparing Figs. 3.1 and 3.4, 40 of these gages were used in the 1988 testing program, while 16 were added to sections previously not instrumented. The new gages were oriented and positioned (i.e., on the upper surface of the lower flange

= Dial gage for horizontal displacements

= DCDT's for vertical displacement
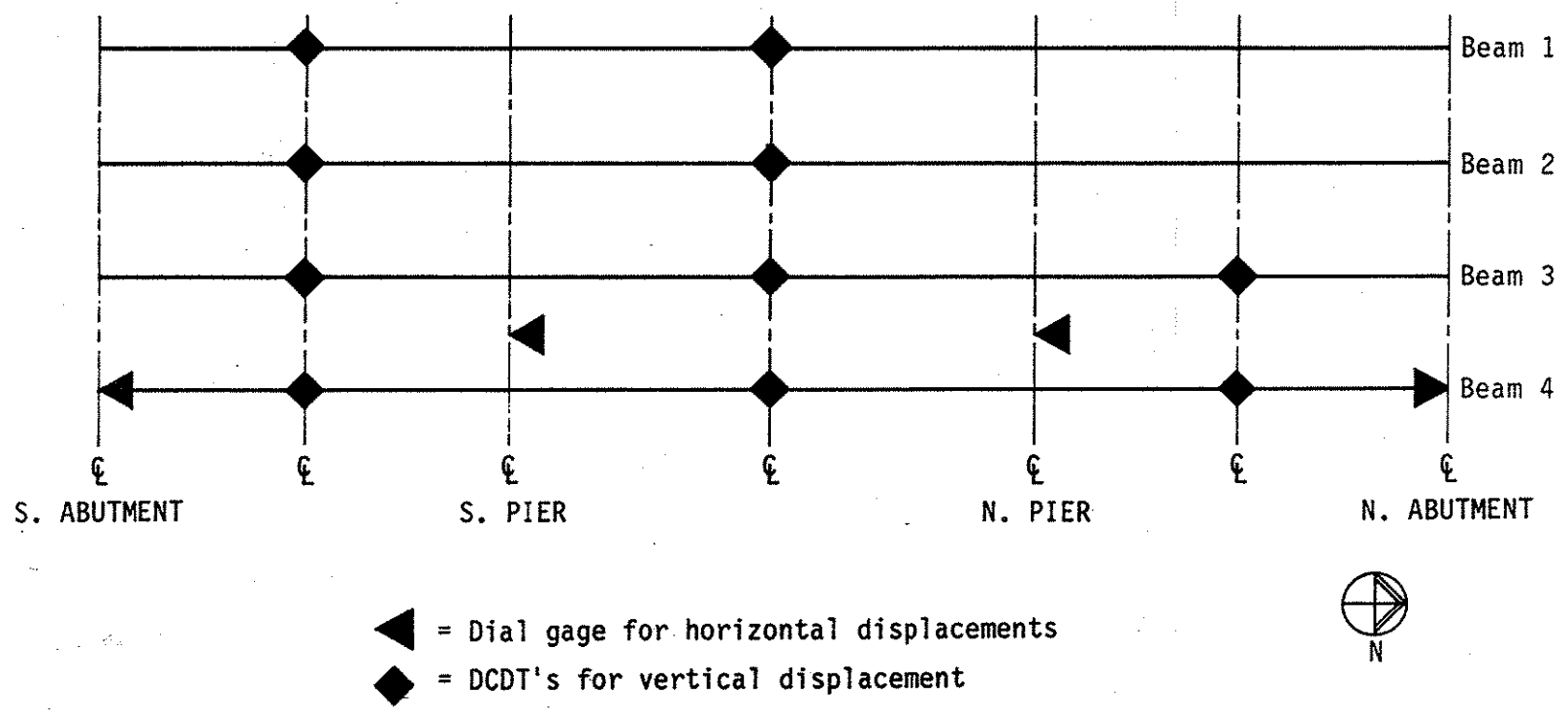
Fig. 3.2. Location of displacement instrumentation ∿ 1988.
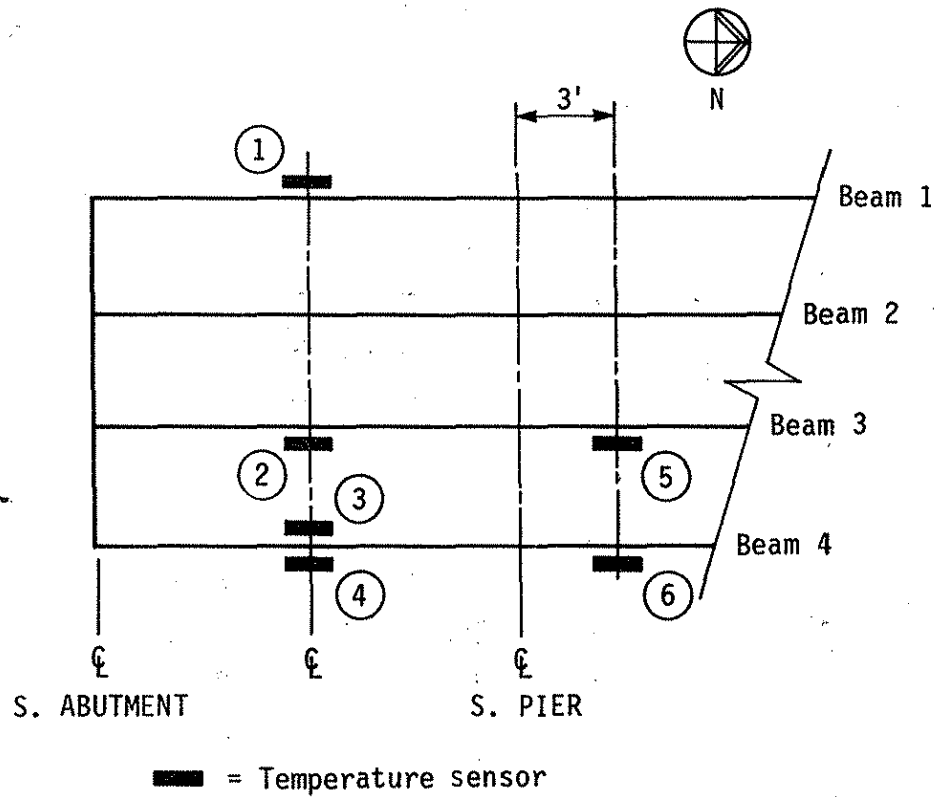
Fig. 3.3. Location of temperature sensors ∿ 1988 & 1989.
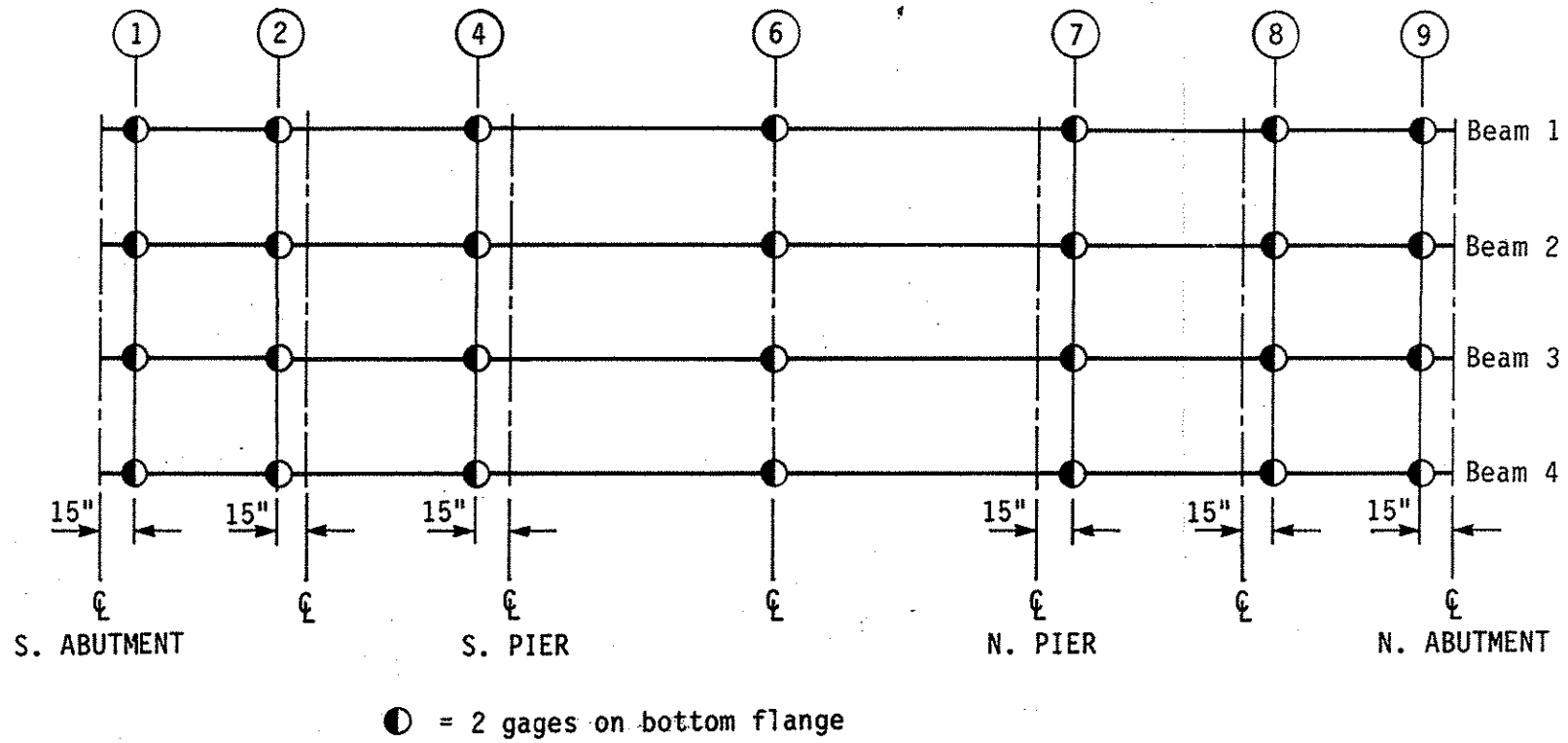
Fig. 3.4. Location of strain gages ∿ 1989.

58

1 and 1/4 in. in from the flange edge) the same as in 1988. For accurate force measurement, the same instrumentation (two strain gages per tendon) was used in 1989 as in 1988.

As was the case with the strain gages, additional instrumentation was added in 1989 for deflection measurements. As may be seen in Fig. 3.5, two additional DCDT's were added so that centerline displacements of all four beams could be determined in each of the three spans. A review of this figure also reveals that the four dial gages used in 1988 for measurement of longitudinal movements have been replaced with 16 crack monitors positioned to measure the movement of the four beams at each support point. Crack monitors consist of two acrylic plates. One plate, which was attached to the beams, is white with a black grid calibrated in millimeters; the overlapping transparent plate, which was attached to the abutments and piers, has red crosshairs centered over the zero lines of the grid. Because the two plates can move independently of each other, any vertical or horizontal movement of the beams relative to their supports will cause the crosshairs to change position on the grid, thus allowing the accurate determination of movements (vertical and/or horizontal).

Temperature sensors were again used to measure the bridge beam temperatures during testing (see Fig. 3.3 for location of sensors). In addition to the sensors and a standard thermometer for determining air temperatures, a Solomat portable thermocouple probe was used to measure the temperature of the concrete bridge deck, the post-tensioning tendons, beams, and the like at the centerline of the north span.

Beam 1

Beam 2

Beam 3

Beam 4

S. ABUTMENT   S. PIER   N. PIER   N. ABUTMENT

● = Crack monitors for vertical and horizontal displacement

◆ = DCDT's for vertical displacement

N
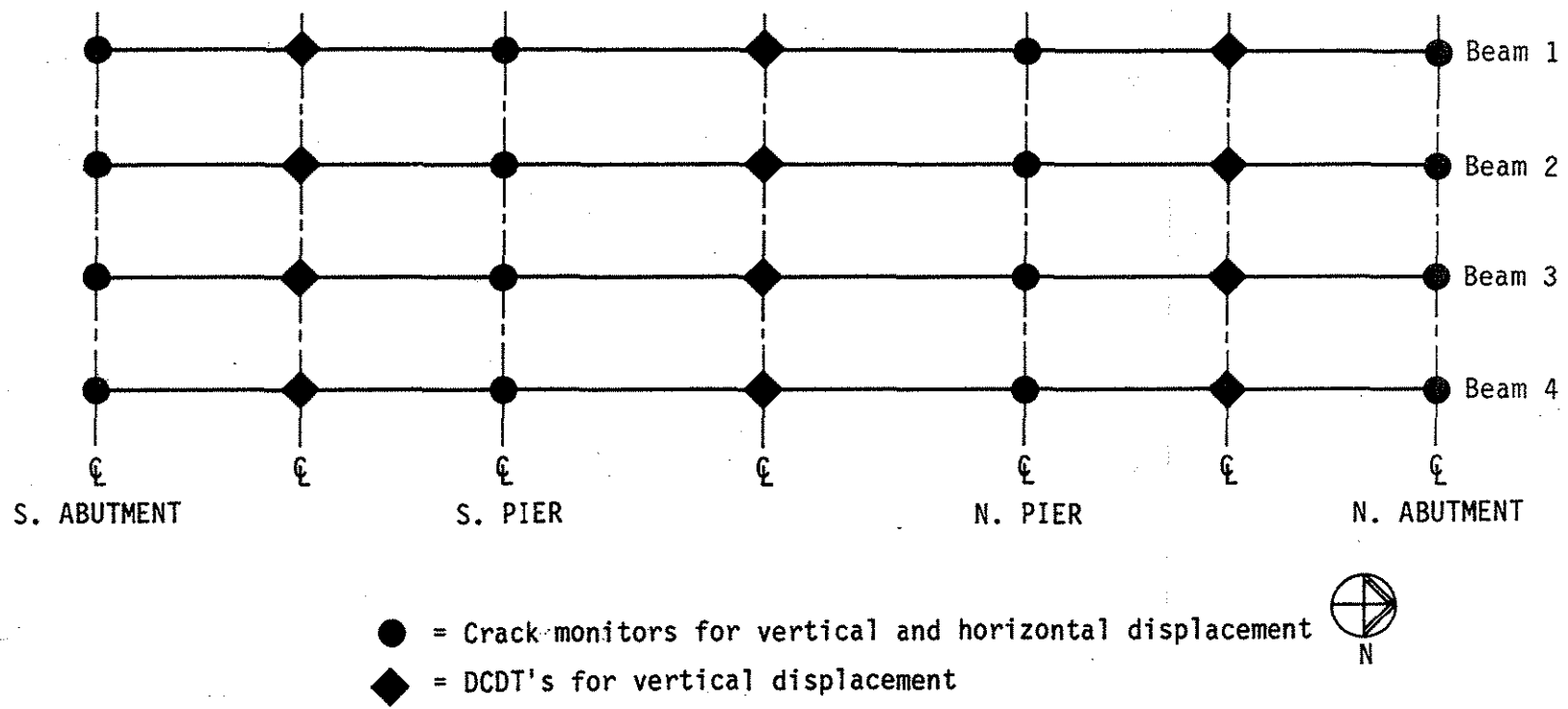
Fig. 3.5. Location of displacement instrumentation ∿ 1989.

3.2 Field Tests

The field testing program on each bridge consisted of determining the bridge's response, strains, and deflections to various loading, all of which will be described in the following sections.

The trucks (configuration and weights) used to load the bridge in 1988 and 1989 are shown in Fig. 3.6. Note that the trucks are essentially the same size (truck no. 2 in 1988 is actually the same truck that was used in 1989 and designated truck no. 1). However, the trucks had more load in 1989 than in 1988. Truck no. 1 in 1989 weighed approximately 8% more than truck no. 1 in 1988; truck no. 2 weighed approximately 12% more in 1989. Observe also in Fig. 3.6 the error in the center of gravity of truck no. 1 in 1988. This error of 6.2 in., however, is not significant when one considers that the length of the bridge is 150 ft (1800 in.).

The load points shown in Fig. 3.7 indicate where the center of gravity of trucks used in the loading the bridge were positioned. Note that these load points are at the 1/4 points of the south and middle span and at the middle point of the north span. These load points were used in the 1988 and 1989 testing programs with truck no. 1 each year being positioned at each of these 28 points (3 lanes: lanes 1, 2, and 3 with the truck heading north; 1 lane: lane 4 with the truck heading south).

When the truck was in lane 4 and positioned at load point 4.7, the front wheels of the truck were off the bridge; thus, data from this load point were disregarded. For easy reference, load positioned at one of the 28 points in Fig. 3.7 will be referred to as a load case. The load points are in ascending order as are the corresponding load case numbers. For example, in load case 1, load was applied at position 1.1; in load case 22, load was applied at position 4.1, and so on. The number of load points used made it possible to examine symmetry (i.e.,
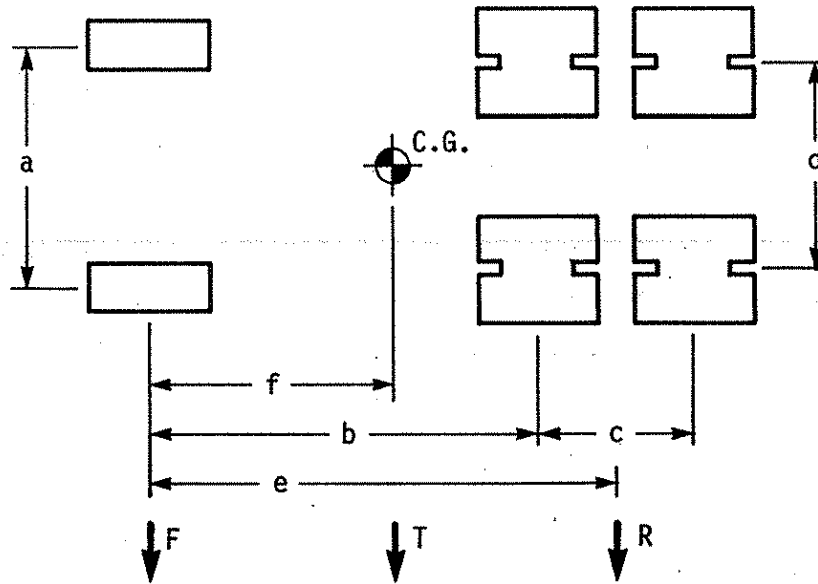
Yr	Trk	a (in)	b (in)	c (in)	d (in)	e (in)	f (in)	R(lbs)	F(lbs)	T(lbs)
'88	1	82	180.0	50.5	72	205.5	154.8*	44,440	14,580	59,060
	2	80	175.5	51	72	201	139.6	40,220	17,700	57,920
'89	1	80	175.8	51	72	201.2	149.6	47,200	16,470	63,760
	2	80	176.2	51	72	201.8	145.9	46,000	17,840	64,640

*Value actually used 148.6"

Fig. 3.6. Wheel configuration and weight
distribution of test vehicles.

a. PLAN VIEW

b. SECTION VIEW
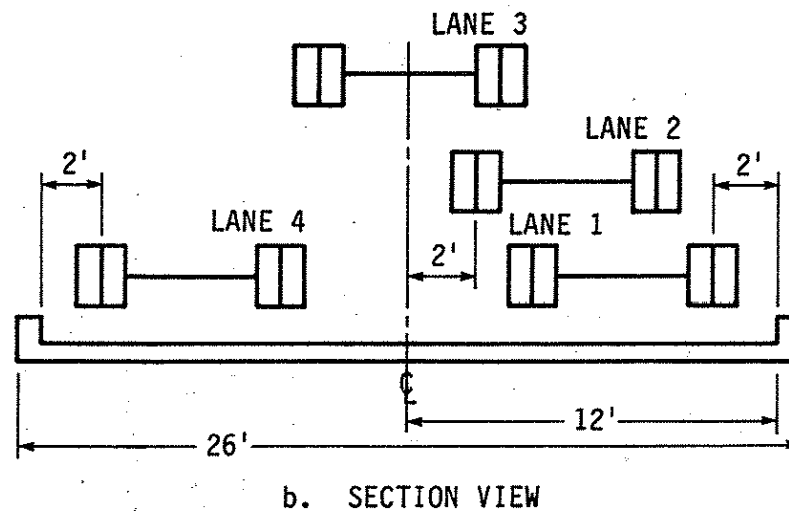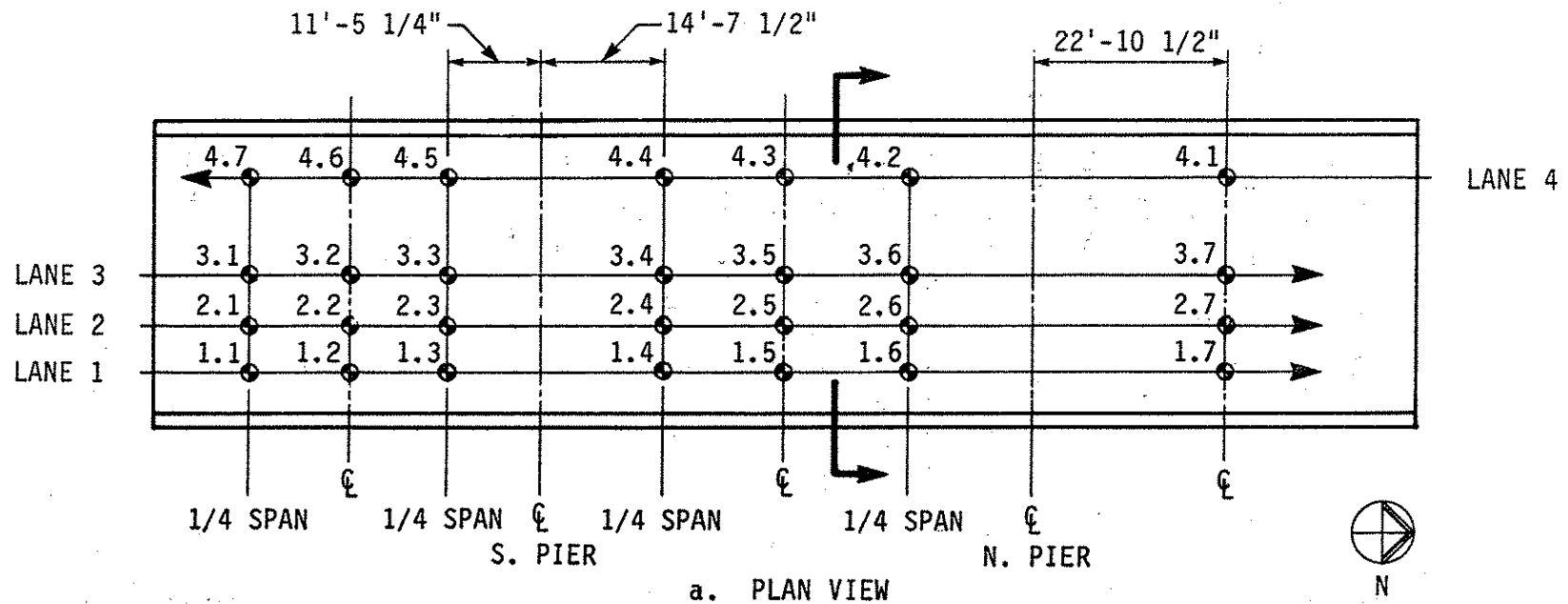
Fig. 3.7. Location of test vehicles.

load points 1.2 and 1.7, lanes 1 and 4, lane 3 on the longitudinal centerline of the bridge, etc.).

In addition to the loading of the bridge with one truck, various cases of pattern loading were applied to the bridge by using two trucks. A total of twelve different pattern loading cases were employed each year; these are presented as loading cases 29-40 in Table 3.1. The points referenced in this table correspond to the load points shown in Fig. 3.7. For example in Load case 36, load was applied at points 3.2 and 3.7, which obviously will tend to maximize the positive moment in both the north and south span. The term "tend to maximize" is used because the positions of the trucks are obviously not exactly at the positions that influence lines would indicate for maximizing positive moments in these spans. Figure 3.8 illustrates the trucks in position for two of the loading cases investigated. Post-tensioning was applied to (and removed from) the bridge using four 120-kip capacity, 6-in.-stroke, hollow-core-hydraulic cylinders, 6 and 1/4 in. in diameter. As noted in Chapter 2, the diameter of the cylinders controlled the position of the tendons relative to the bottom beam flange. Because each beam required two tendons in the positive moment region for strengthening and there were only 4 cylinders available, only two beams could be post-tensioned at a time. Thus, it was necessary to post-tension the bridge in stages; the required six stages are shown in Fig. 3.9. Several considerations are apparent in this figure:

- beams were post-tensioned in pairs so that transverse symmetry was always present.
- exterior beams in each span were post-tensioned before the interior beams.
- end spans were completely post-tensioned before post-tensioning was applied to the middle span.

The order used to remove the post-tensioning force from the bridge in the summer of 1989 was the reverse of that shown in Fig. 3.9 (i.e., post-tensioning

Table 3.1. Pattern loading vertical load points.

Load Case	Vertical Load Points																												
	Lane 1							Lane 2							Lane 3							Lane 4						
	1	2	3	4	5	6	7	1	2	3	4	5	6	7	1	2	3	4	5	6	7	1	2	3	4	5	6	7
29		•			•																							
30		•					•																					
31					•		•																					
32									•			•																
33									•					•														
34												•		•														
35																•			•									
36																•					•							
37																			•		•							
38																						•		•				
39																						•					•	
40																								•			•	

• = Loaded.

*See Fig. 3.7 for location of load points.
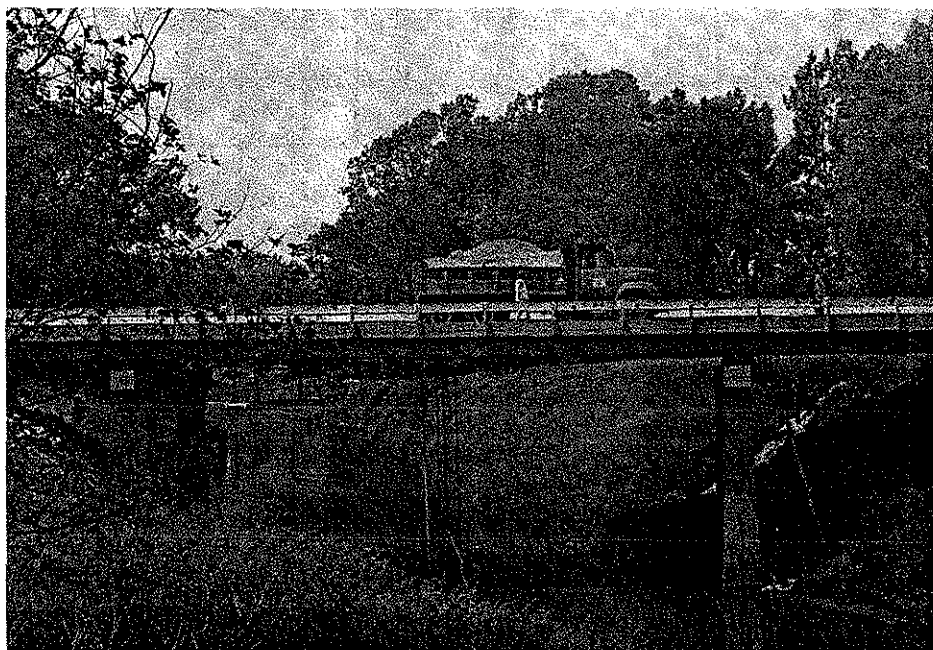
a. TRUCK NO. 1 IN LOAD POSITION 4.4
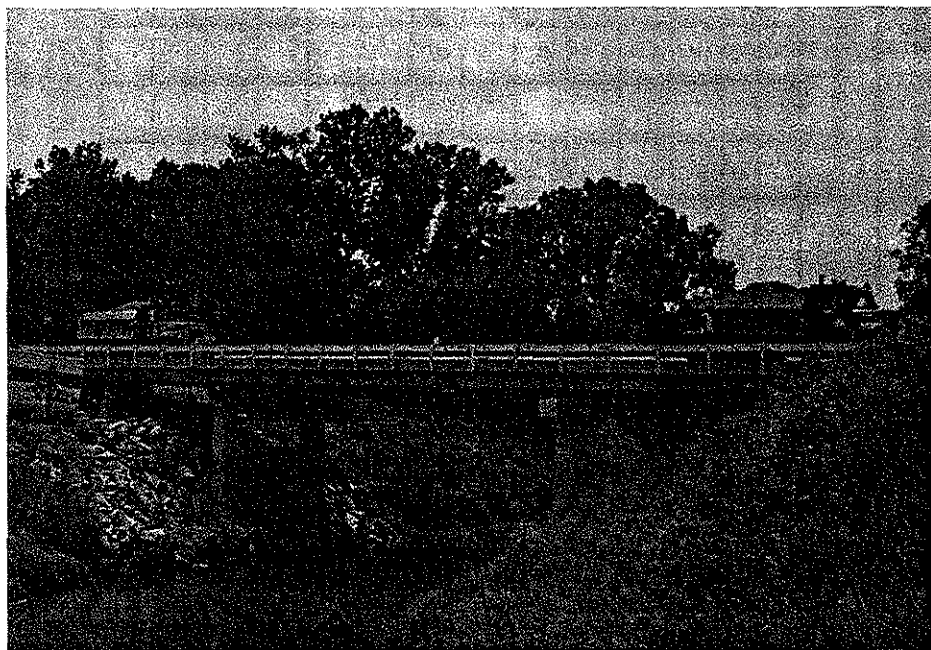
b. TRUCK NOS. 1 AND 2 IN POSITION
FOR LOAD CASE 30

Fig. 3.8. Field test vehicles on bridge.
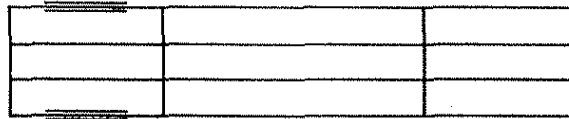
a. STAGE 1
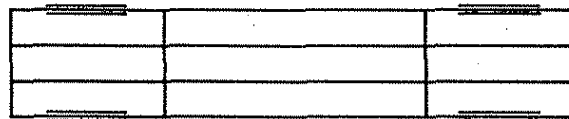
b. STAGE 2
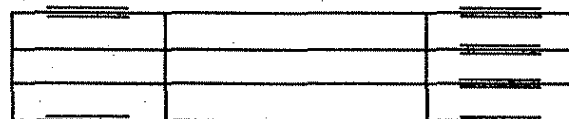
c. STAGE 3
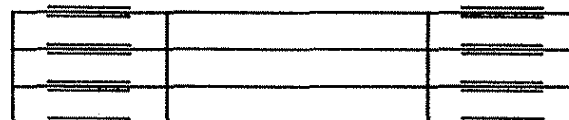
d. STAGE 4
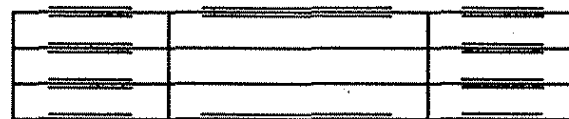
e. STAGE 5
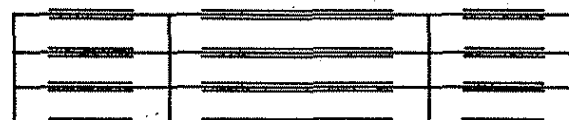
f. STAGE 6

Fig. 3.9. Order post-tensioning was applied to bridge.

force was first removed from the middle span interior beams, then middle span exterior beams, etc.). Shown in Fig. 3.10 are the theoretical forces required to strengthen the bridge. Obviously, the effects of post-tensioning beams of one span on the other beams in that span as well as on beams in adjacent spans (elastic shortening, etc.) have been taken into account. The actual post-tensioning forces applied to the individual beams in each of the two years are presented in Chapter 4.

The procedure used to obtain data on the bridge for the trucks in the various locations (see Fig. 3.7), as well as for the various stages of post-tensioning (see Fig. 3.9) or removal of post-tensioning forces, follows:

1. Record "zero" strain readings, "zero" deflection reading, and temperatures. (As previously noted, the majority of the data was collected using the DAS; however, some data were recorded by hand).

2. Apply loading (one truck, post-tensioning, truck plus post-tensioning, etc.) at predetermined locations.

3. Record strain, post-tensioning force, temperature, and deflection readings as in step 1; note any changes in the bridge behavior.

4. Remove loading from bridge and take "zero" strain and deflection readings as well as temperature, as was done in step 1. Obviously, when post-tensioning forces were applied to the bridge, this could not be done.

5. Repeat steps 1 through 4 for all loading conditions.

It was previously noted that because of time constraints it was necessary to use some strain gages that had an incorrect temperature compensation. Because the procedure just described–that is, taking new "zeros" before each loading case and a second "zero" when the loading was removed–was used, and because the time required for each test was approximately 15 minutes and thus minimal temperature change occurred, potential temperature compensation problems were essentially eliminated.
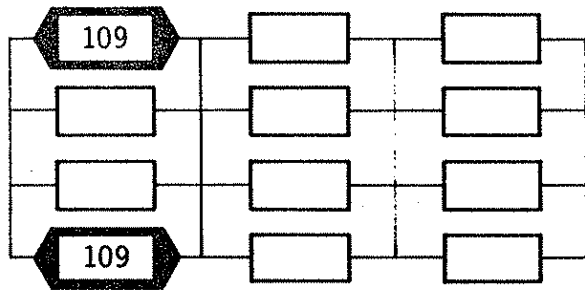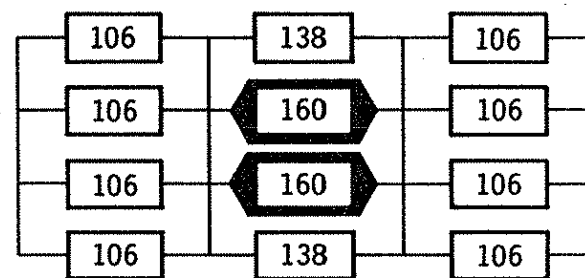
a. STAGE 1
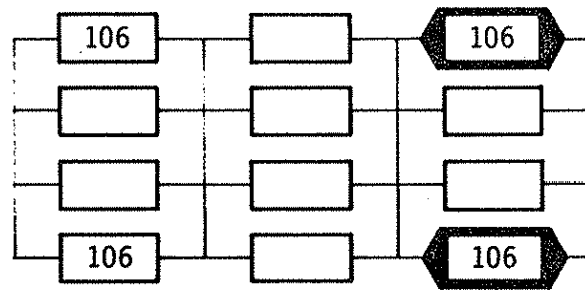
b. STAGE 2
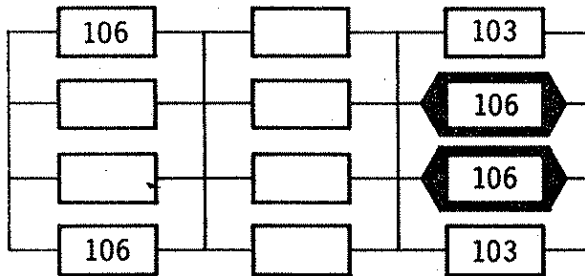
c. STAGE 3
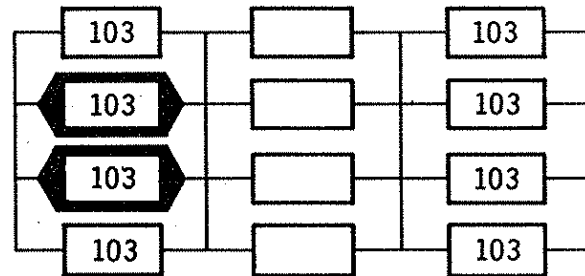
d. STAGE 4
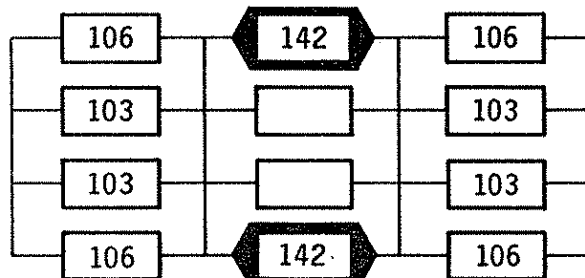
e. STAGE 5

f. STAGE 6

= Location of force being applied
  in each stage.

Fig. 3.10. Post-tensioning force required per
            beam: force in kips.

For clarity, the testing program and loadings used in 1988 and 1989 will be presented separately in the following sections.

3.2.1. 1988 Tests

On August 10, 1988 after approximately three months of preparation—installation of the strengthening system as well as the required instrumentation—the bridge was strengthened and tested. Initially the bridge was tested in an "as is" condition (except for the shear connectors, which were added (see section 2.2.2)). Loading (truck no. 1) was applied at the previously described 28 points (28 loading cases–see Fig. 3.7). After data were obtained from these loadings, as previously described, the bridge was post-tensioned in six stages (see Fig. 3.9). After each stage of post-tensioning, data were taken. Upon completion of the post-tensioning sequence, the strengthened bridge was loaded again with truck no. 1 at the same 28 load points; again, data were taken after each loading case. The final loading applied to the bridge was the 12 pattern loading cases described in Table 3.1. Data were obtained after each of these cases. In all of these pattern loading cases, truck no. 1 was always the lead truck. After completion of the testing, the bridge was left in the strengthened condition. Approximately every three months, between the 1988 and 1989 testing, the bridge was visually inspected.

3.2.2. 1989 Tests

Preparation time was considerably shorter in 1989 than in 1988 because the post-tension strengthening system was already in place, as was the majority of instrumentation. As has been previously noted and described, additional instrumentation was installed for the 1989 testings; it was also necessary to replace some of the strain gages that had been damaged. The 1989 testing program was undertaken on June 27 and 28, 1989. On the first

day, truck no. 1 was positioned on the strengthened bridge at the same 28 points (see Fig. 3.7) that had been used the previous year. Data were taken for each of the 28 load cases. To determine the losses in post-tensioning forces over the one-year period, the post-tensioning was removed from the bridge in six stages. Post-tensioning was removed from the bridge in reverse order to that in which it was applied (see Fig. 3.9). In other words, post-tensioning was first removed from the interior beams of the middle span, then the exterior beams of the middle span, and so forth. Data were taken after each stage of the un-tensioning. The final test of day one was to position truck no. 1 at the 28 load points and to obtain data on the bridge for the truck in each of these positions.

Day two of the testing was essentially the same as that completed in 1988 after data were obtained with a truck on the bridge in the "as is" condition (except for the added shear connectors). Thus, on day two, the bridge was post-tensioned in six stages. Truck no. 1 was then positioned at the 28 positions, and trucks no. 1 and 2 were positioned on the bridge for load cases 29-40. For each one of these load cases, strain, displacement, and temperature data were obtained.

4. TEST RESULTS

A detailed description of the bridge that was strengthened, as well as a description of the finite element analysis that was used to design the post-tension strengthening system, were presented in Chapter 2. The instrumentation used in the field testing as well as a description of the various loadings that were applied to the bridge were described in Chapter 3. In the following sections of this chapter, experimental results of the various tests performed will be presented. In several instances the experimental results will be compared with theoretical results. Because the theoretical analysis used has been well documented in Chapter 2, no additional details will be provided in this chapter.

As was previously noted, at several sections during the 1988 field testing, beam strains were measured on the top of the bottom flange (bottom-flange strains) and on the bottom of the top flange (top-flange strains) while at other instrumented sections strains were only measured on the bottom flanges. Strains were measured on both flanges so that the position of the neutral axis could be determined. In 1989, the bottom beam flanges at several additional sections were instrumented. Because of the number of instrumented sections and the limited capacity of the DAS, it was possible to measure and record only bottom-flange strains in the 1989 field tests. As only bottom-flange strains were obtained in the second-year tests, only these strains are reported in this report. However, top-flange strains obtained in the first year indicate similar behavior.

Although, as previously noted in Chapter 3, there were some differences in the weights of the trucks used in 1988 and 1989 and, also (as will be documented in this chapter), although the post-tensioning forces applied in 1989 were slightly larger than those applied in 1988, there was still very good agreement in the data obtained in 1988 and that obtained in 1989. This

agreement indicates that the post-tensioning that was on the bridge for approximately one year did not alter the behavior of the bridge. This agreement is documented in some of the results presented; however, the majority of the data presented is from the 1989 tests. Because of the vastness of the field tests and the fact that the bridge was tested two times approximately one year apart, an enormous amount of data was collected. Only the most significant portions of the data will be presented in this report; however, in the authors' opinion, sufficient data have been presented to document the bridge response and behavior.

For clarity, in the following sections the results of the various tests performed on the bridge will be presented and discussed separately.

4.1. Post-Tensioning

As stated in Section 3.2, the post-tensioning forces were applied to the bridge in six stages (See Fig. 3.9). In Fig. 3.10 the magnitude and sequence of post-tensioning forces required on each beam were presented. The forces that were actually applied in 1988 are presented in Fig. 4.1. In this figure, the effect of post-tensioning two beams on the post-tensioning force on beams that have been previously post-tensioned is apparent. This effect is more significant on beams in the same span and on beams in adjacent spans that are "in-line" with those being post-tensioned. It also may be seen that, in some instances, there is an increase in the post-tensioning forces on beams that have been previously tensioned, while in other cases there is a decrease. Shown in Fig. 4.2 are the initial forces applied to each beam (Fig. 4.2a), the final force resulting on each beam (Fig. 4.2b), and the difference in magnitude between what was initially applied and what resulted (Fig. 4.2c), as well as the percent change (Fig. 4.2d). As may be seen, the greatest loss was 5.9%, while the greatest gain was 2.9%. The average change was a loss of 2.6%. This was
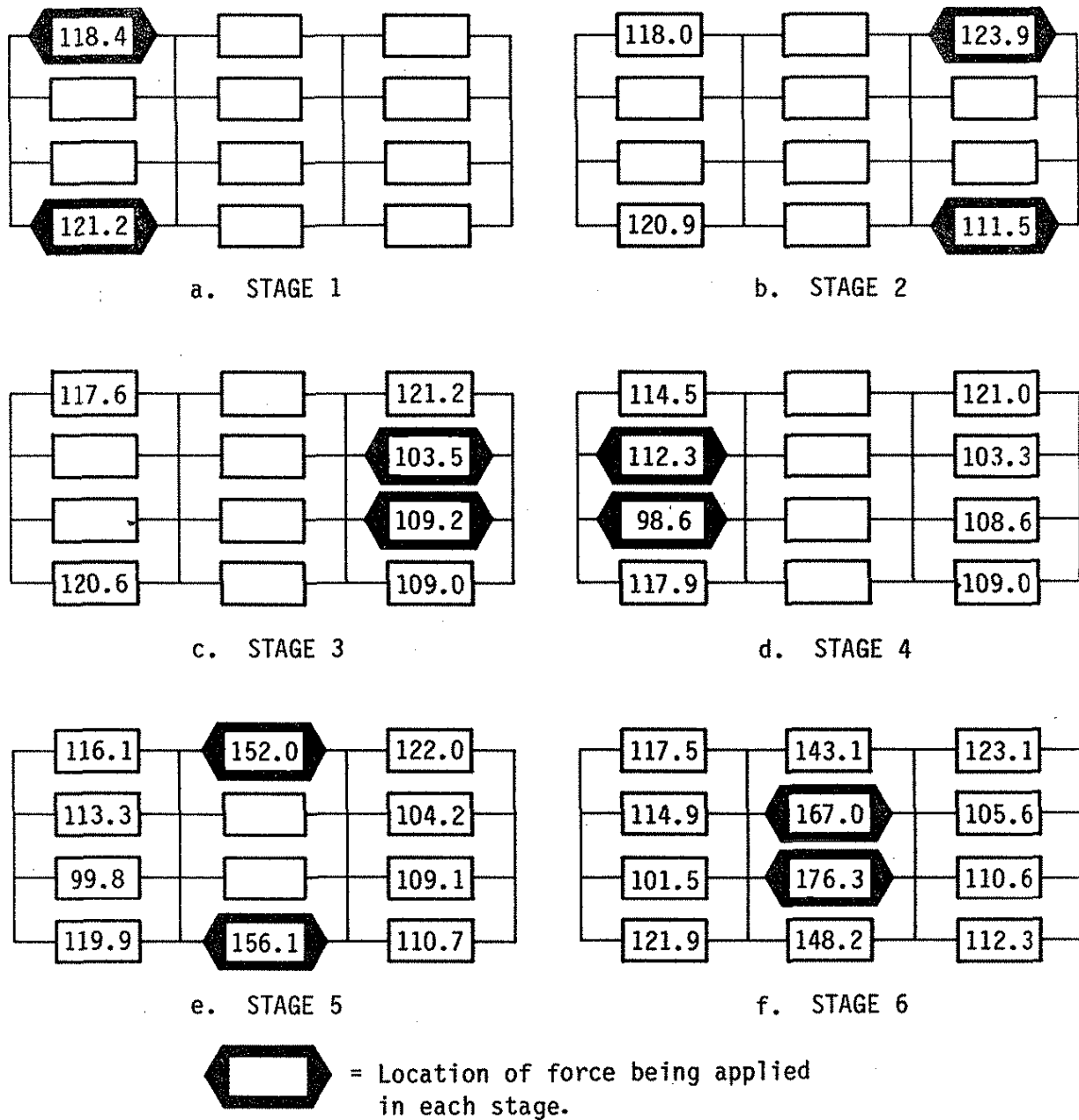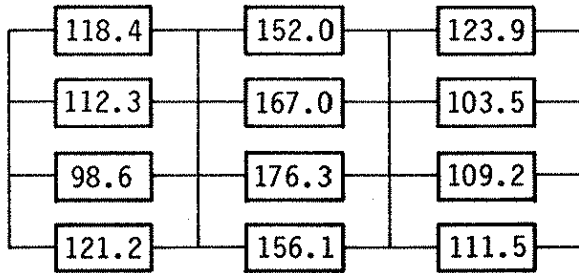
a. STAGE 1

b. STAGE 2

c. STAGE 3

d. STAGE 4

e. STAGE 5

f. STAGE 6

= Location of force being applied
  in each stage.

Fig. 4.1. 1988 - Post-tensioning forces applied
to each beam: force in kips.

76

118.4	152.0	123.9
112.3	167.0	103.5
98.6	176.3	109.2
121.2	156.1	111.5

a. 1988 INITIAL FORCE APPLIED

122.7	148.5	129.4
113.4	176.4	120.6
103.8	174.0	116.8
119.4	144.4	116.2

e. 1989 INITIAL FORCE APPLIED

117.5	143.1	123.1
114.9	167.0	105.6
101.5	176.3	110.6
121.9	148.2	112.3

b. 1988 FINAL FORCE

122.8	140.4	128.7
114.6	176.4	122.5
107.0	174.0	119.2
120.5	137.3	118.0

f. 1989 FINAL FORCE

-.9	-8.9	-.8
2.6	0	2.1
2.9	0	1.4
.7	-7.9	.8

c. CHANGE IN INDIVIDUAL P-T FORCES
DUE TO APPLICATION OF ADDITIONAL
FORCE ∿ 1988.

.1	-8.1	-.7
1.2	0	1.9
3.2	0	2.4
1.1	-7.1	1.8

g. CHANGE IN INDIVIDUAL P-T FORCES
DUE TO APPLICATION OF ADDITIONAL
FORCE ∿ 1989.

-.8	-5.9	-.6
2.3	0	2.0
2.9	0	1.3
.6	-5.1	.7

d. % CHANGE ∿ 1988

0	-5.5	-.5
1.0	0	1.6
3.1	0	2.1
.9	-4.9	1.5
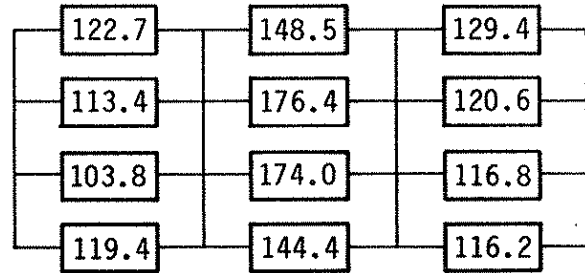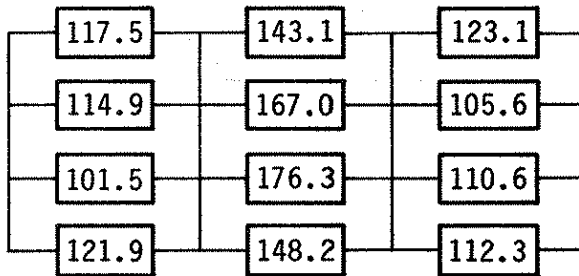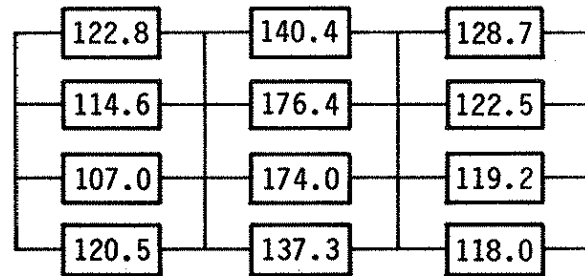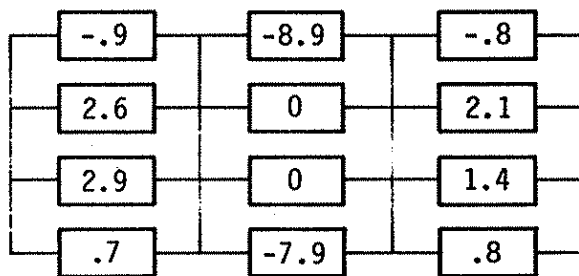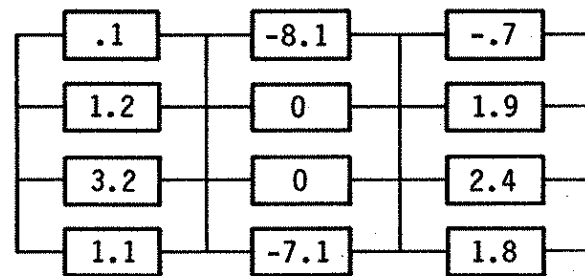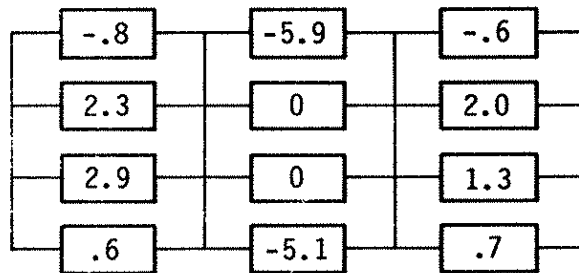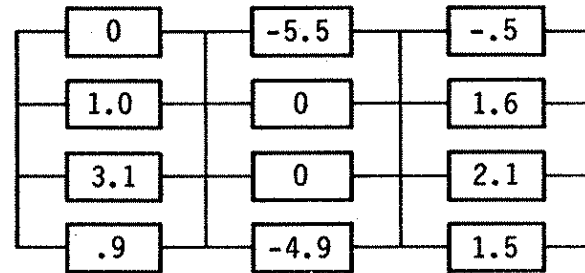
h. % CHANGE ∿ 1989

Fig. 4.2.   Change in various post-tensioning forces
due to post-tensioning of other beams.

based on ten beams; as when the last two beams were post-tensioned, there was obviously no change in the force on these beams due to post-tensioning. The bridge was subjected to a total post-tensioning force of 1542 kips--455.8 kips, 634.6 kips, 451.6 kips on the south, middle, and north spans, respectively.

Figure 4.3 indicates the difference between the force that theoretically was required on each beam and that which was actually applied in 1988. As may be seen, only two beams were tensioned slightly less than what was theoretically desired, while the force on the majority of the beams was larger than what was theoretically required. In Fig. 4.3b it is seen that the largest "understress" was 4.2%, while the largest "overstress" was 16.1%. The average "overstress" was 6.8%. As was noted in Chapter 3, in 1989 after some initial testing, the post-tensioning force applied in 1988 was removed so that losses (or possibly gains) that took place in the one-year period could be determined. The forces that were removed from the bridge in 1989 are given in Fig. 4.4; in comparison with the 1988 final forces (Fig. 4.2b) the magnitude of losses and gains can be determined (Fig. 4.4b). The greatest loss was 11.8 kips while the greatest gain was 5.5 kips. Because the magnitude of force in each beam varied (See Fig. 4.2b), it is more significant to review the percent change (Fig. 4.4c). The largest loss was 10.3%, while the largest gain was 3.8%; the average change was a loss of 2.1%, which is slightly less than the 3.7% assumed in Chapter 2.

After several truck loading tests on the bridge in the unstrengthened condition (except for the shear connectors, which were added in 1988), the bridge was post-tensioned with the six-stage sequence previously described. The forces that were applied in 1989 are presented in Fig. 4.5. The south, middle, and north spans were subjected to 464.9 kips, 628.1 kips, and 488.4 kips of post-tensioning force, respectively; total post-tensioning force on bridge thus was 1581.4 kips. The influence of post-tensioning beams on beams that
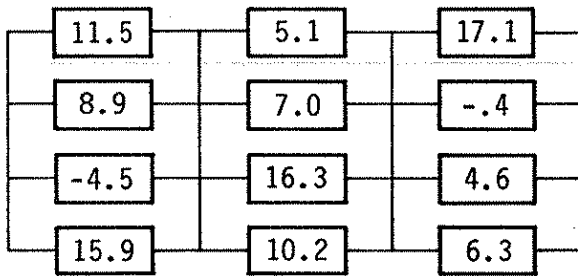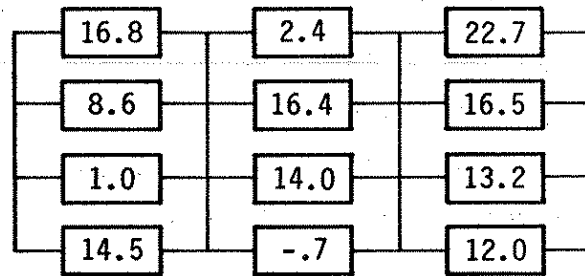
11.5	5.1	17.1
8.9	7.0	-.4
-4.5	16.3	4.6
15.9	10.2	6.3

a. DIFFERENCE (IN KIPS) BETWEEN
    THEO. REQUIRED AND ACTUALLY
    APPLIED ∿ 1988

16.8	2.4	22.7
8.6	16.4	16.5
1.0	14.0	13.2
14.5	-.7	12.0

c. DIFFERENCE (IN KIPS) BETWEEN
    THEO. REQUIRED AND ACTUALLY
    APPLIED ∿ 1989

10.8	3.7	16.1
8.4	4.4	-.4
-4.2	10.2	4.3
15.0	7.4	5.9

b. % DIFFERENCE ∿ 1988

15.8	1.7	21.4
8.1	10.3	15.6
.9	8.8	12.5
13.7	-.5	11.3
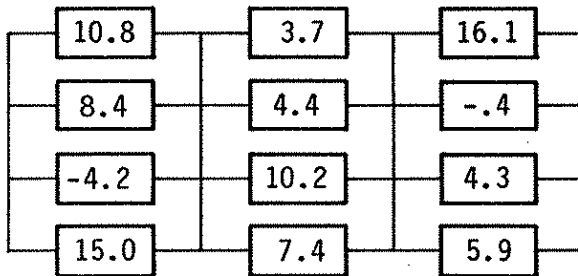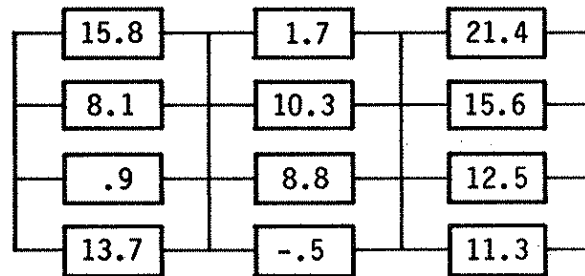
d. % DIFFERENCE ∿ 1989

Fig. 4.3.   Post-tensioning force actually applied to bridge
            vs magnitude of force theoretically required
            for strengthening.

111.0	148.6	125.7
103.1	169.5	98.9
96.6	171.7	106.4
119.0	152.6	111.8
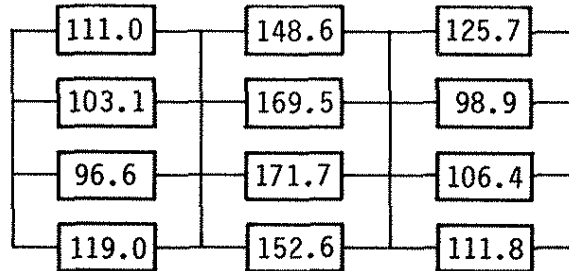
a. FORCE RELEASED IN 1989

-6.5	5.5	2.6
-11.8	2.5	-6.7
-4.9	-4.6	-4.2
-2.9	4.4	-.5
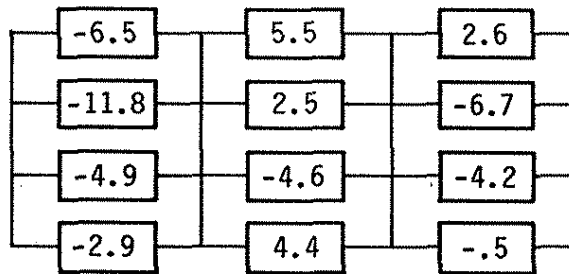
b. MAGNITUDE (IN KIPS) OF
DECREASE IN P-T FORCE

-5.5	3.8	2.1
-10.3	1.5	-6.3
-4.8	-2.6	-3.8
-2.4	3.0	-.4
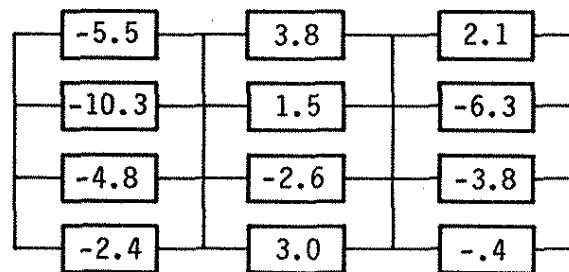
c. % LOSS FROM 1988 TO 1989

Fig. 4.4. Change in post-tensioning force from 1988 to 1989.

a. STAGE 1

b. STAGE 2

c. STAGE 3

d. STAGE 4

e. STAGE 5

f. STAGE 6

= Location of force being applied in each stage.
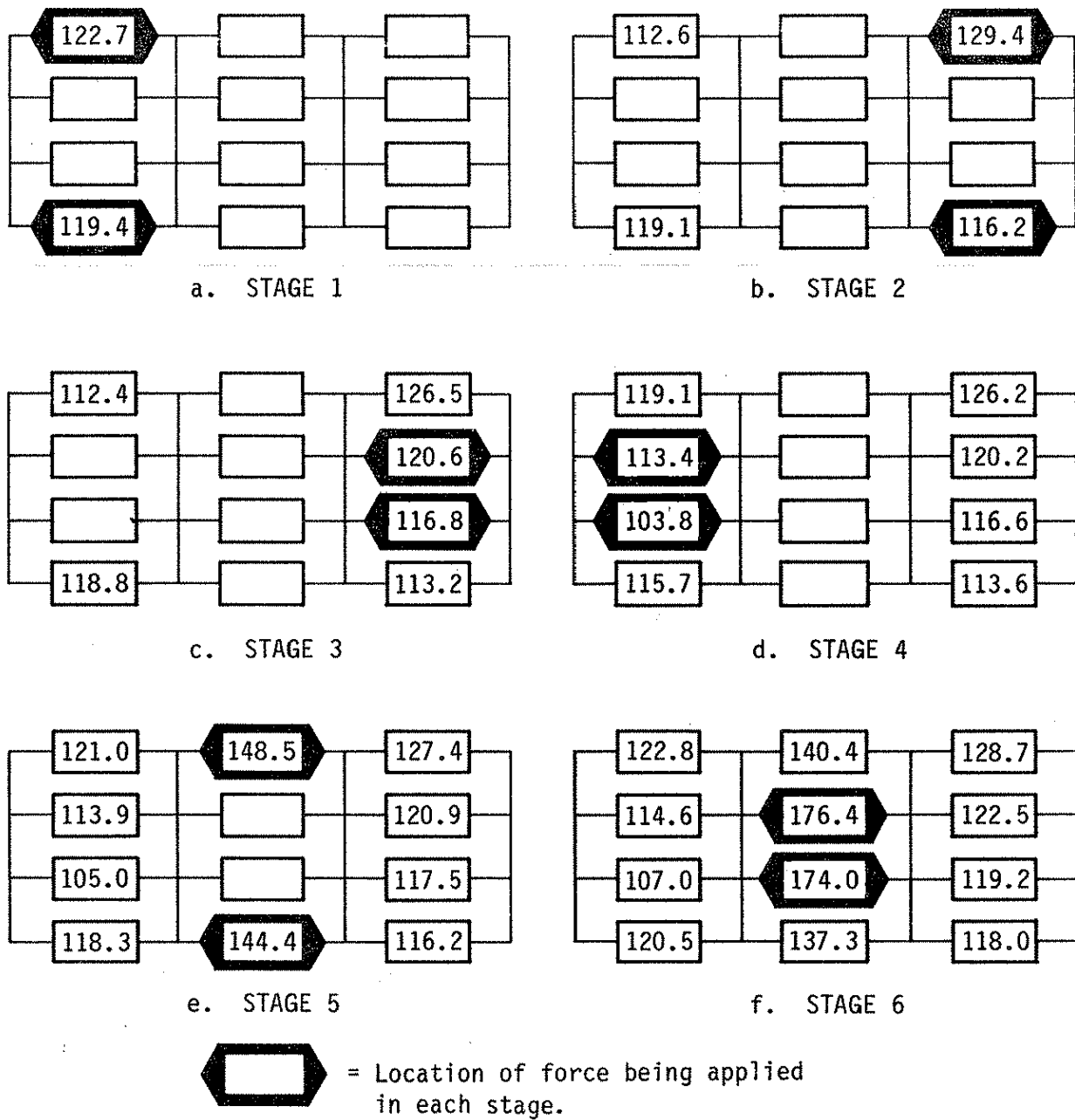
Fig. 4.5. 1989 - Post-tensioning forces applied to each beam: force in kips.

had been previously post-tensioned--which was documented in 1988--was again observed.

The differences in the forces that were initially applied to the beams (Fig. 4.2e) and the final force (Fig. 4.2f) are given in Fig. 4.2g. The percentage difference is given in Fig. 4.2h. The greatest loss was 5.5%, while the greatest gain was 3.1%. It is interesting to note that the greatest loss occurred on the same beam in 1988 and 1989, while the greatest gain also occurred on the same beams in 1988 and 1989. The average change was a loss of approximately 0.1% (based on ten beams). In comparing Figs. 4.2d and h, one notes very little difference between the losses and gains in 1988 and 1989.

The difference between the force that was actually applied to the individual beams in 1989 and that which was theoretically required is shown in Fig. 4.3c. Note only one beam was slightly "undertensioned," while the remaining beams were provided with post-tensioning forces greater than those theoretically required. In Fig. 4.3d it is seen that the largest "understress" was 0.5%, while the largest "overstress" was 10.5%. Shown in Fig. 4.6 are the differences between the final forces applied in 1988 and 1989. As may be noted, the force applied in 1989 was greater on 7 of the 12 beams. A total of 39.4 kips more was applied to the bridge in 1989 than in 1988. The percentage differences on individual beams are presented in Fig. 4.6b. The differences ranged from -7.4% to +16.0%.

Midspan deflections (south, middle, and north spans) that occurred at each stage of the 1989 post-tensioning are shown in Fig. 4.7. Note that for all stages of post-tensioning there is excellent symmetry in the deflection patterns. In the one case (stage two post-tensioning, north span) where this is not true, the authors question the validity of the deflection on beam 3, because for all other stages of loading this span exhibits excellent symmetry in the deflection patterns. A review of the deflection patterns in this figure indicates that the beams deflected upward or downward depending on where the

5.3	-2.7	5.6
-.3	9.4	16.9
5.5	-2.3	8.6
-1.4	-10.9	5.7
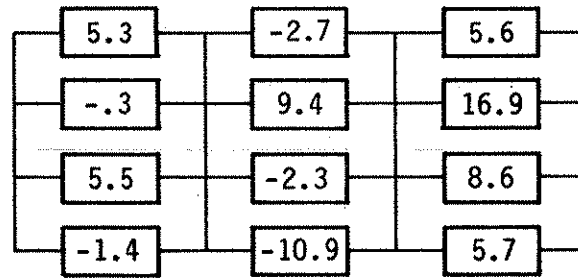
a. DIFFERENCE (IN KIPS) IN APPLIED
FORCE IN 1988 AND 1989.

4.5	-1.9	4.5
-.3	5.6	16.0
5.4	-1.3	7.8
-1.1	-7.4	5.1
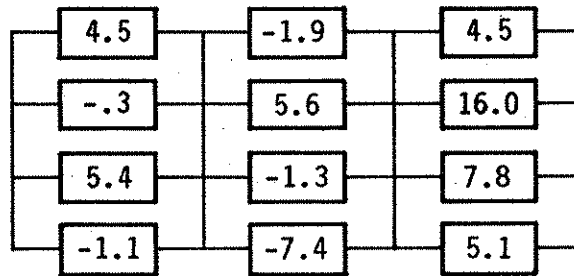
b. % DIFFERENCE

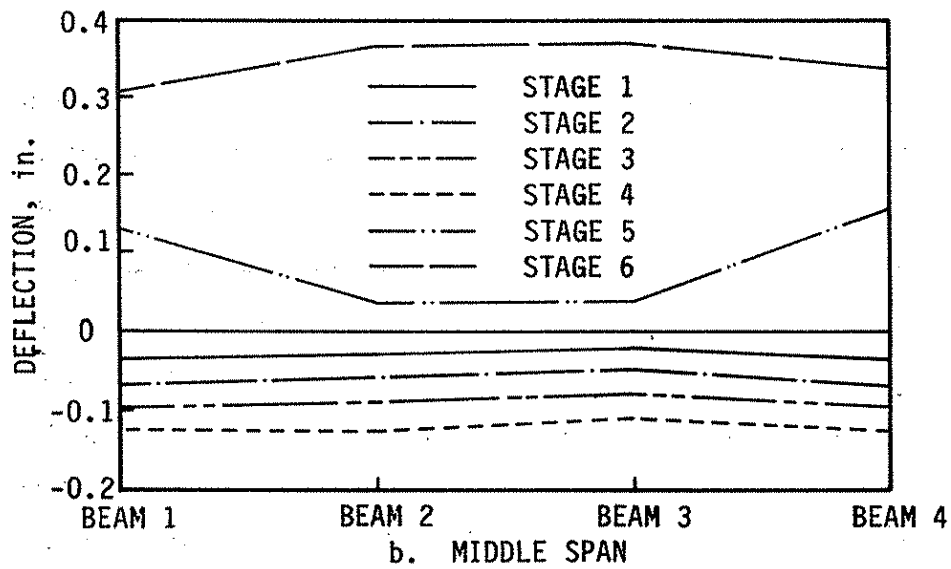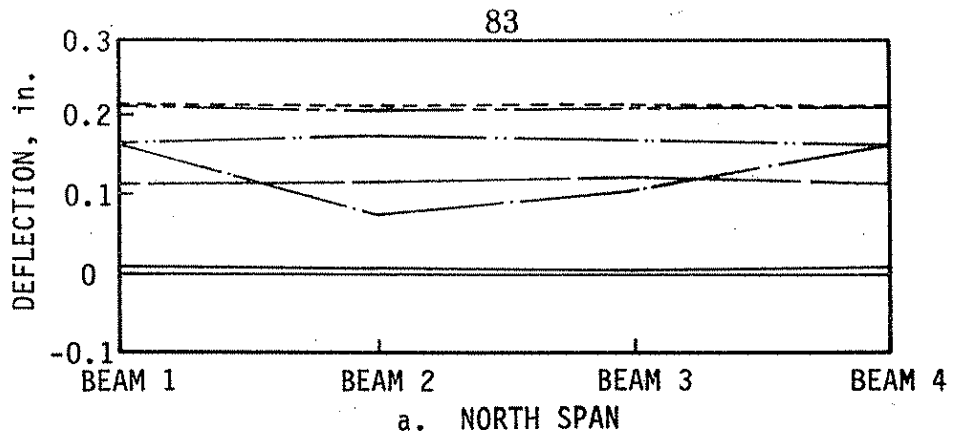Fig. 4.6. Difference in post-tensioning forces
applied in 1988 and 1989.
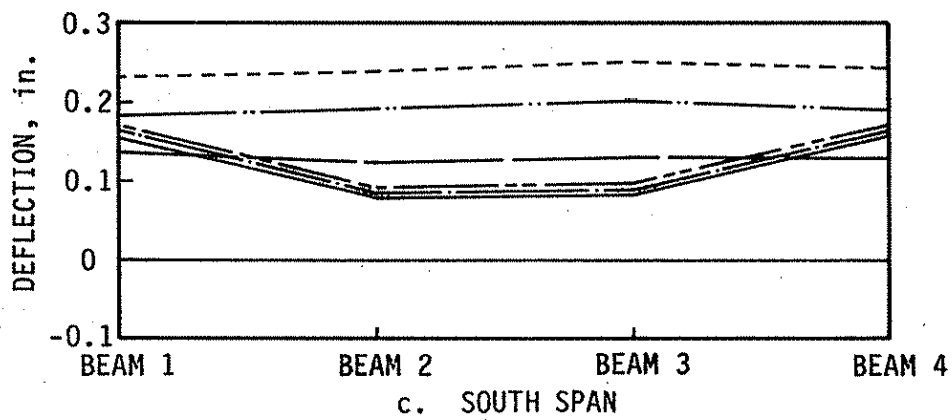
Fig. 4.7. Variation in midspan deflections as six stages of
post-tensioning are applied - 1989.

post-tensioning is being applied. The maximum final displacements (0.376 avg) occurred on the interior beams of the middle span. Final beam displacements in the end spans were essentially the same for the interior and exterior beams, with the interior beams only deflecting slightly more than the exterior beam. Note that the mid-span deflections in the end spans were larger in the south span than in the north span because of the presence of more end restraint at the north abutment. This end restraint will be discussed in more detail later in this section.

Final midspan deflections for each of the three spans resulting from post-tensioning the bridge are presented in Fig. 4.8. Also presented in this figure are theoretical deflection curves, which were obtained from finite element analysis that assumed the ends of the bridge were simply supported or fixed. In the end spans (Fig. 4.8a and c) the measured deflections were bracketed by the simple support and fixed-end conditions, indicating the presence of end restraint. An examination of these figures indicates there was slightly more end restraint present at the north abutment. In the middle span, the measured deflections are less than the theoretical deflections obtained by assuming either end condition. However, they are relatively close to the theoretical curve assuming simple support conditions–19.8% and 13.2% low on the exterior and interior beams, respectively. Other than experimental error, the only explanation the authors have for this discrepancy is the contribution of the guardrails or possibly the compressive strength of the concrete in the deck being higher than what was assumed. Figures 4.9-4.16 give 1989 bottom beam strains for the symmetrical post-tensioning stages: 2, 4, 5, and 6 (see Fig. 3.9), for exterior beams (Figs. 4.9-4.12), and interior beams (Figs. 4.13-4.16). The experimental strains plotted in Figs. 4.9-4.12 are an average of the strain at a particular section in the two exterior beams, while the experimental strains plotted in Figs. 4.13-4.16 are an average of the strains at a particular section in the two interior beams. Also shown in these eight figures is the theoretical
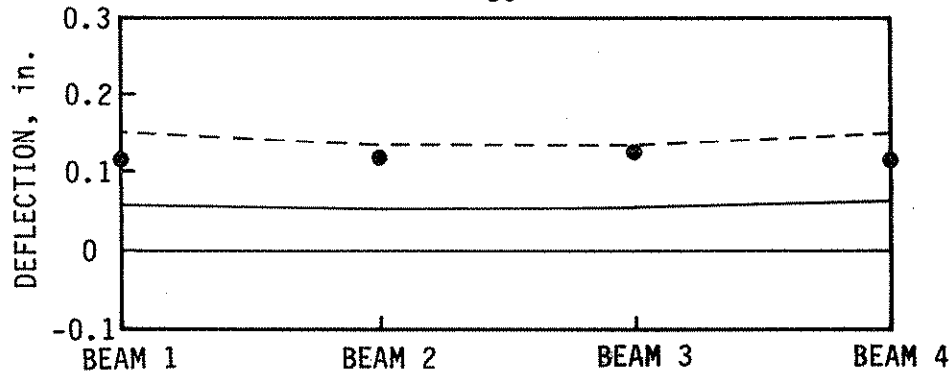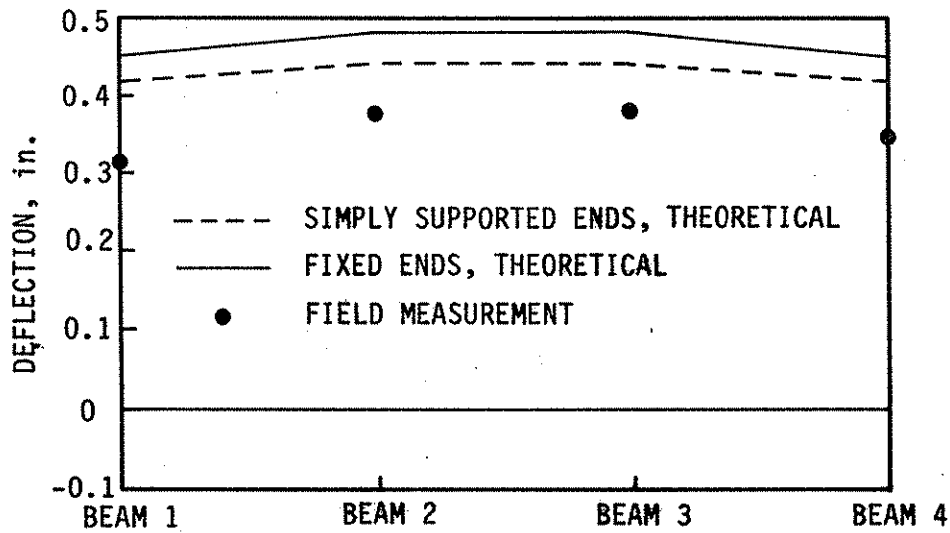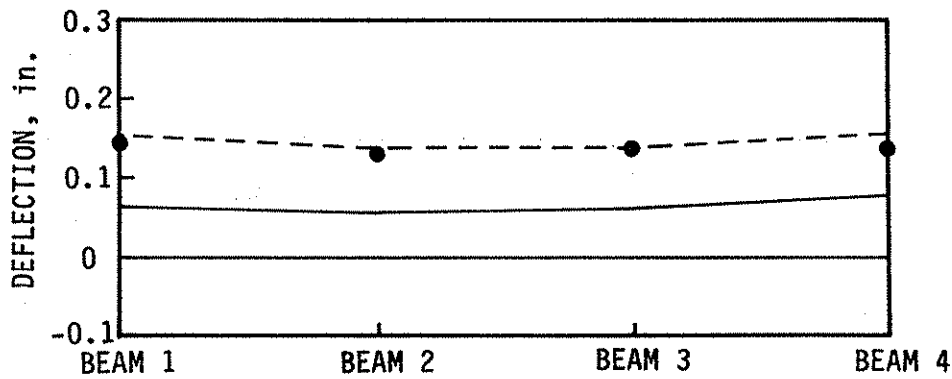
Fig. 4.8.   Comparison of experimental and theoretical
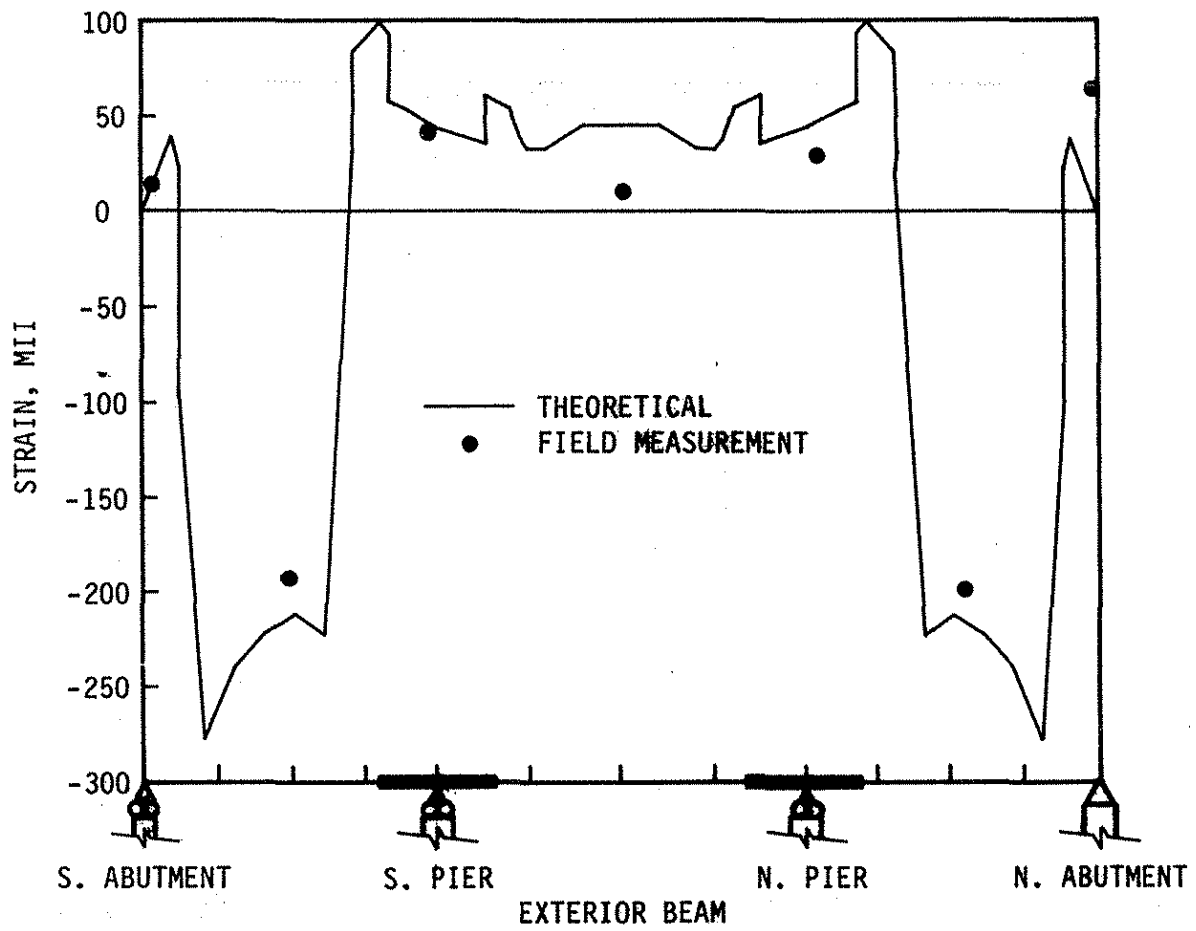post-tensioning deflection data - 1989.

Fig. 4.9. Exterior beam bottom-flange beam strains: Stage 2
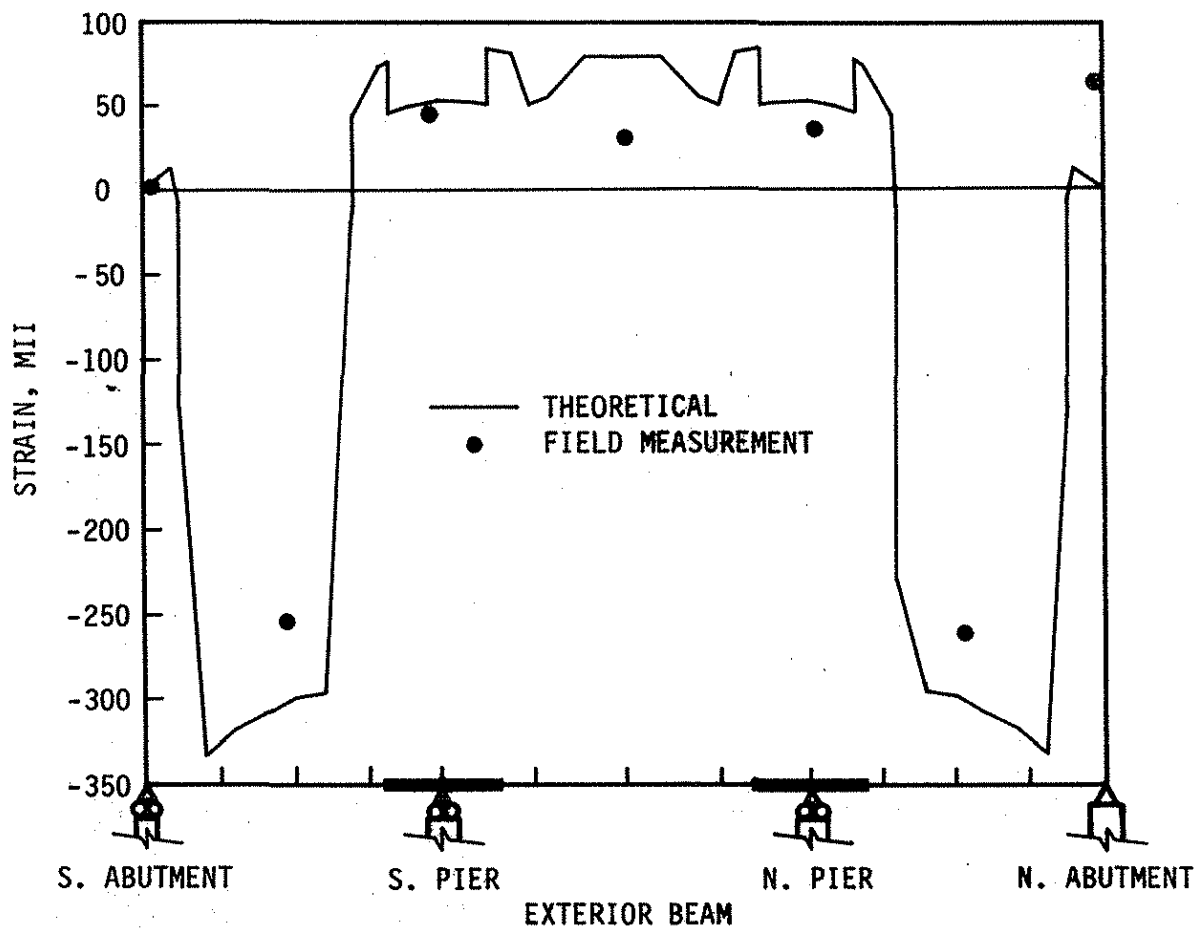post-tensioning - 1989.

Fig. 4.10. Exterior beam bottom-flange beam strain: Stage 4
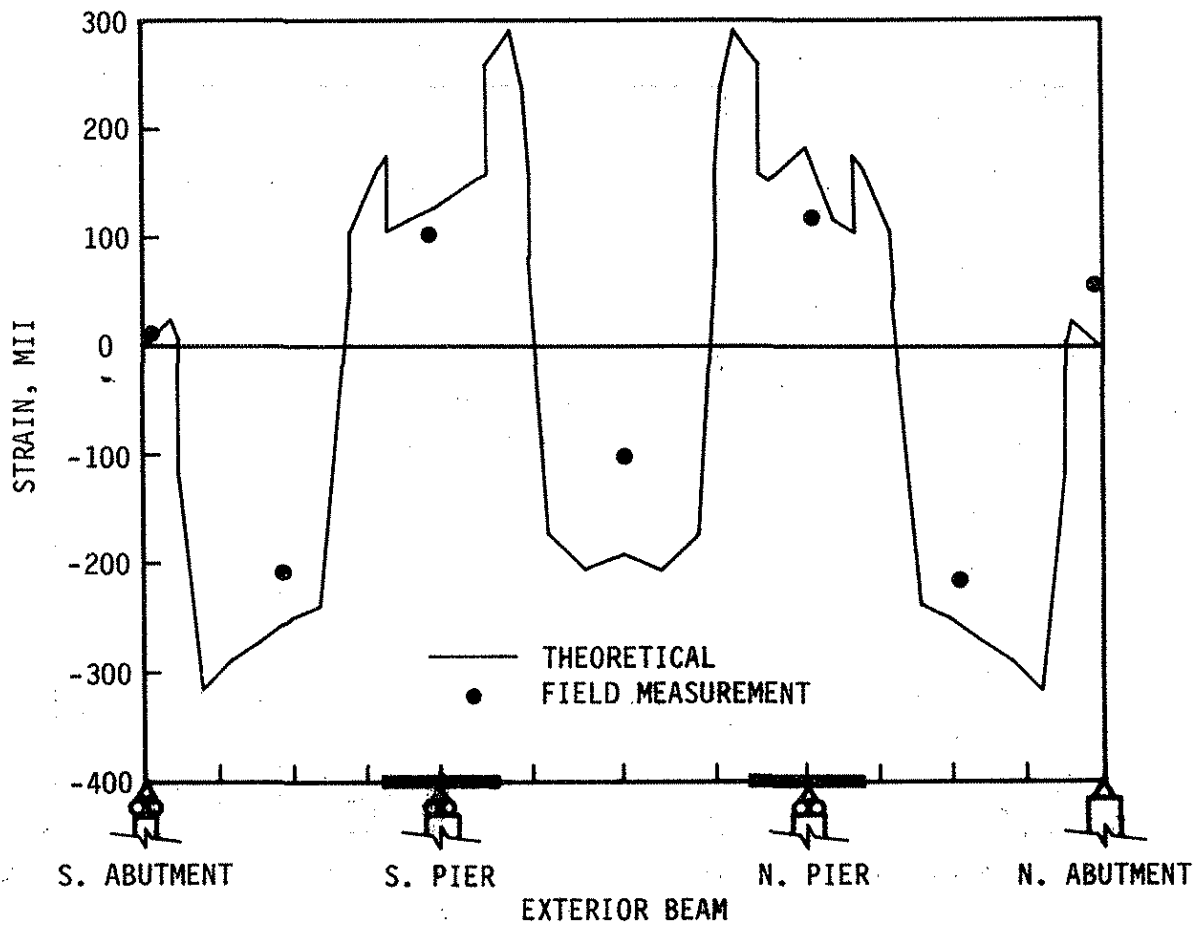post-tensioning - 1989.

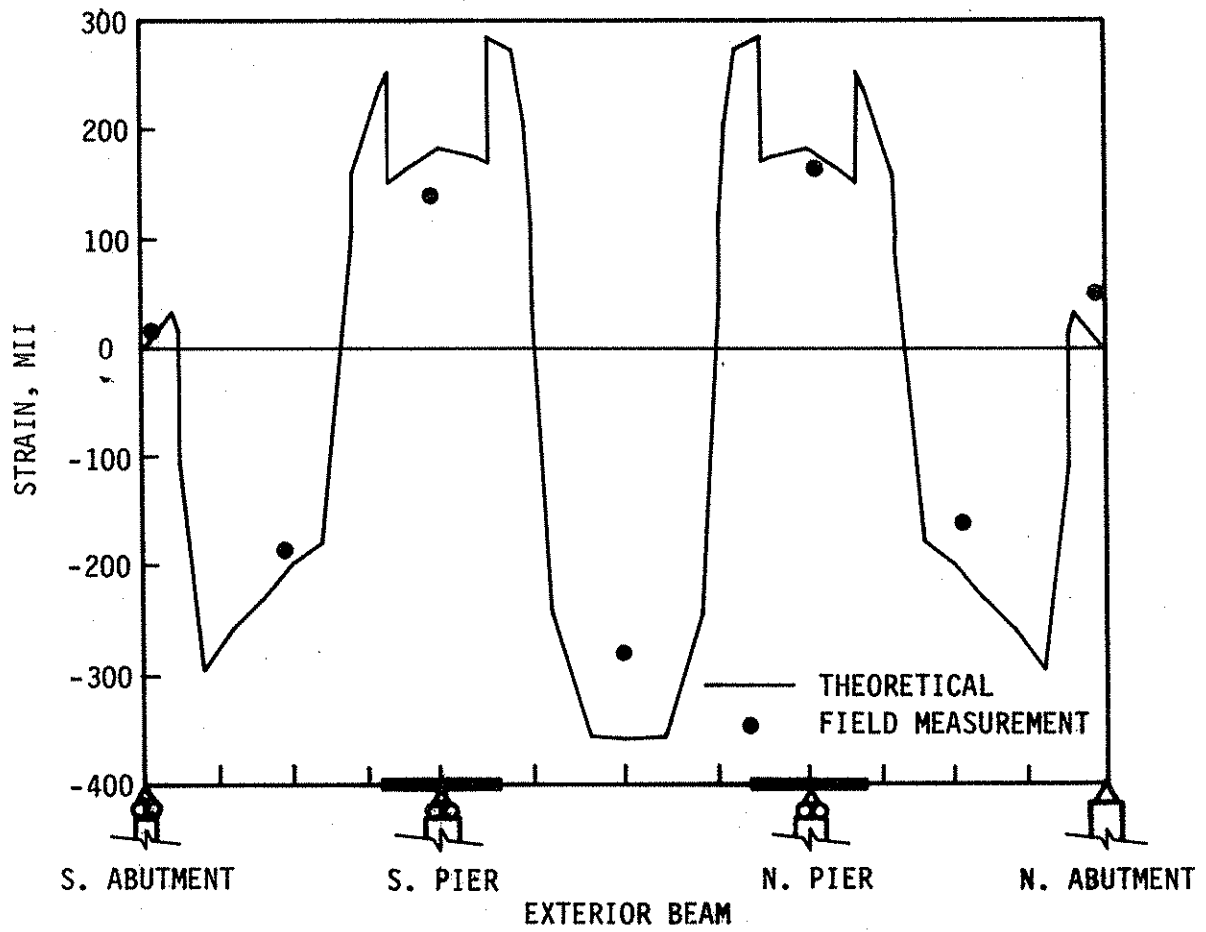Fig. 4.11. Exterior beam bottom—flange beam strains: Stage 5
post-tensioning - 1989.

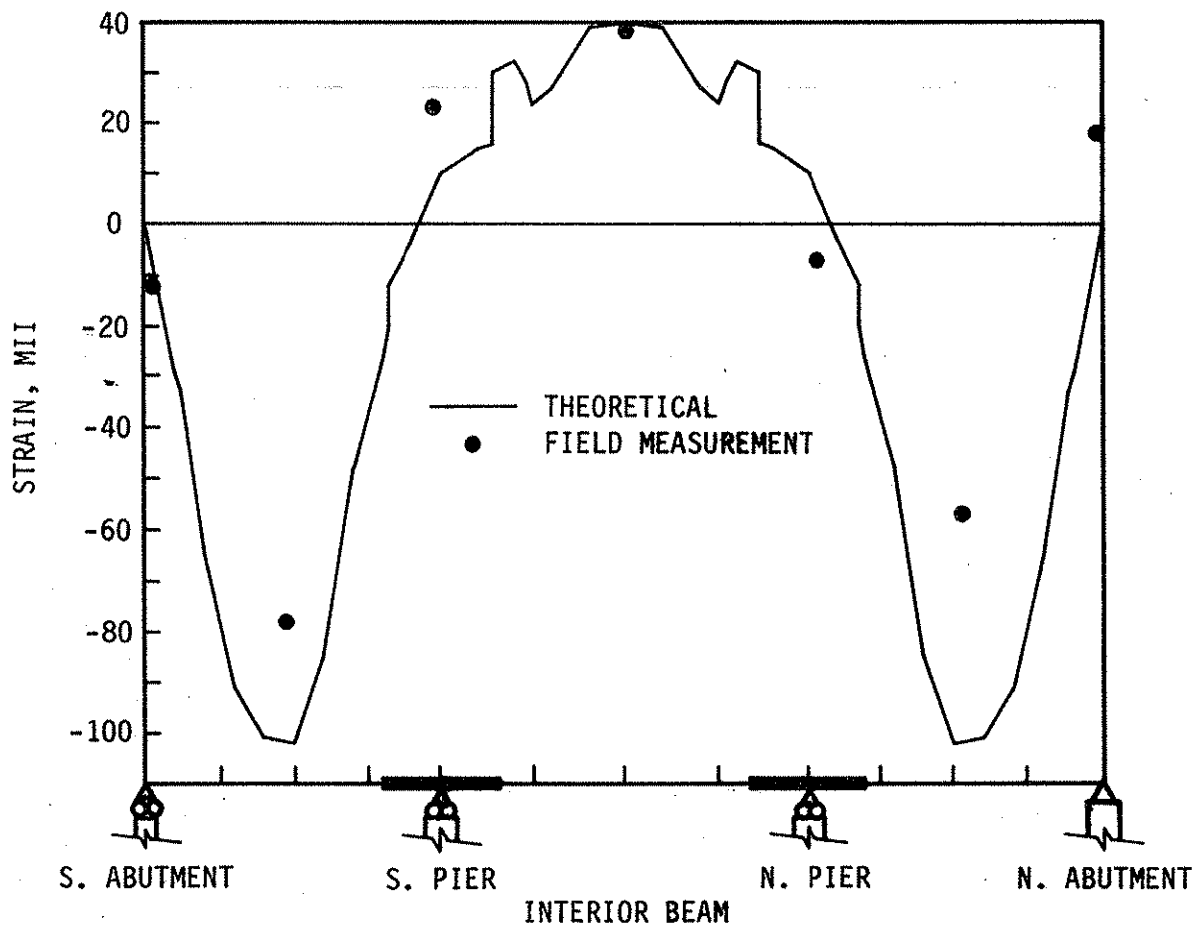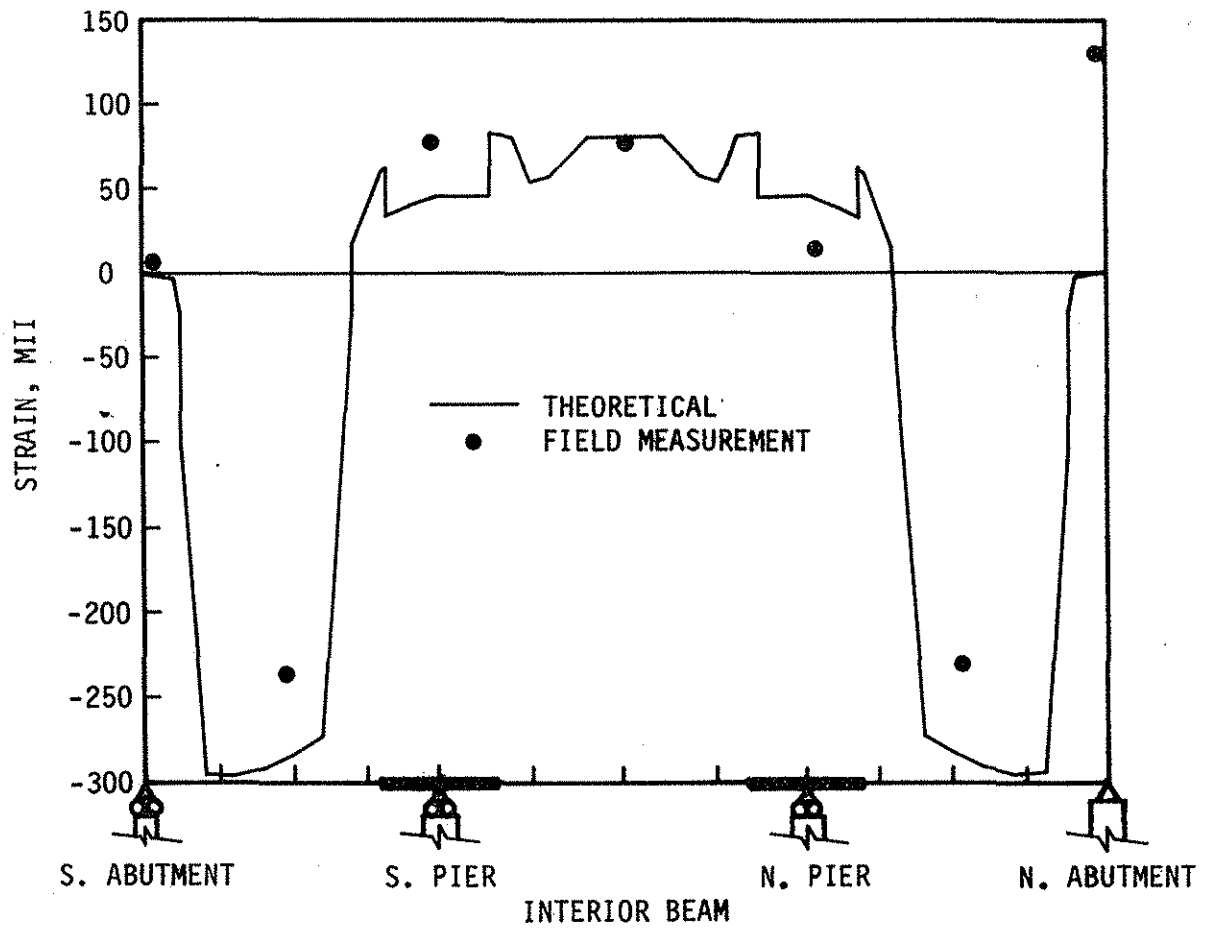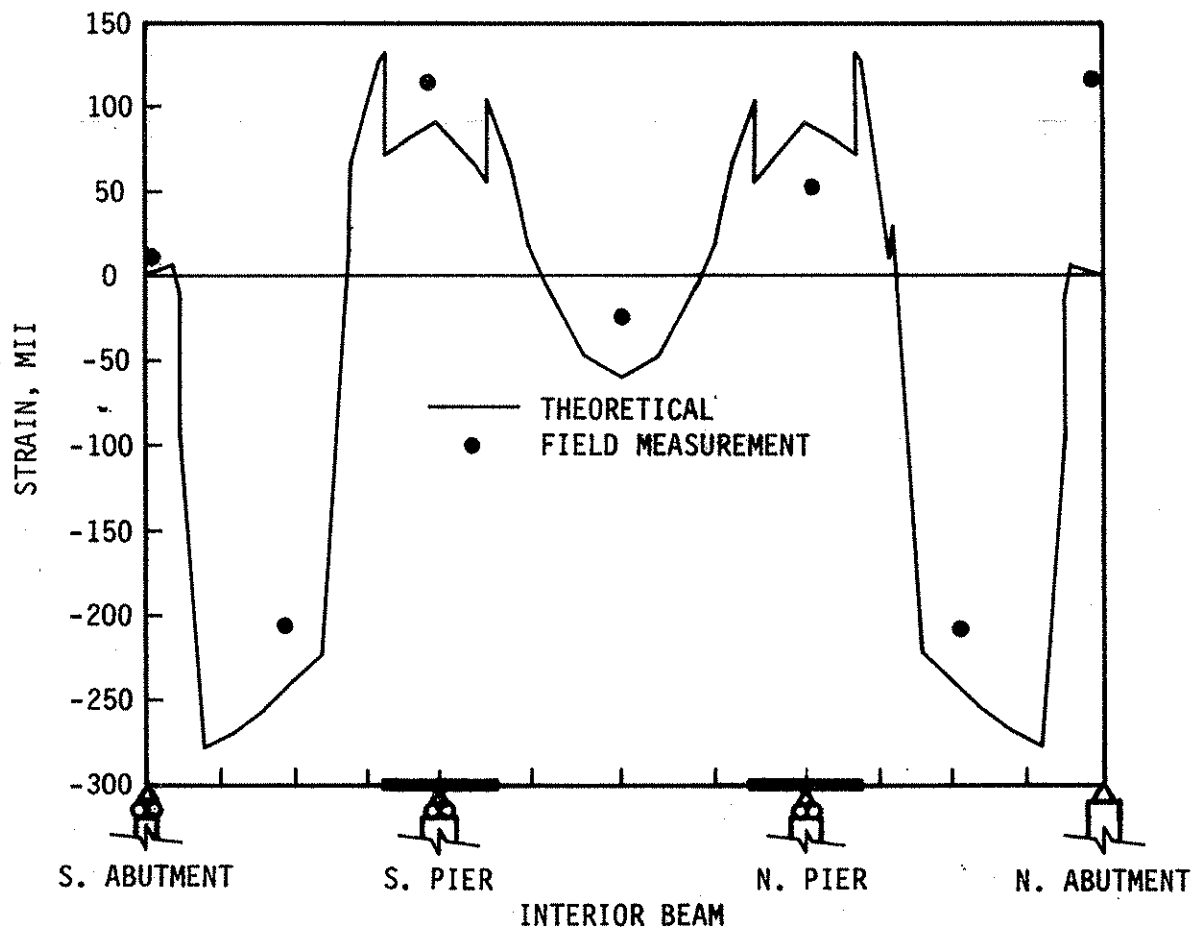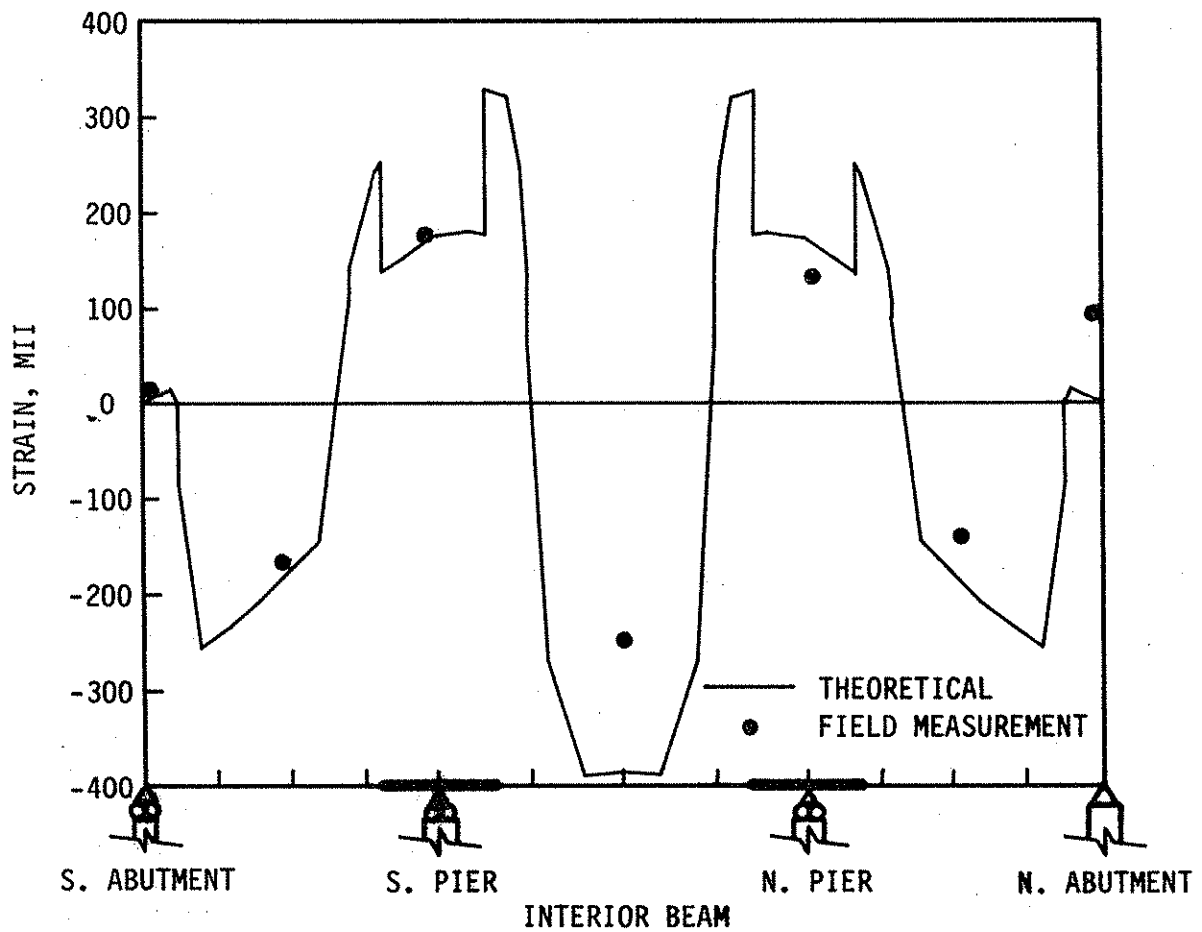Fig. 4.12. Exterior beam bottom-flange beam strains: Stage 6 post-tensioning - 1989.

Fig. 4.13. Interior beam bottom-flange beam strains: Stage 2 post-tensioning - 1989.

Fig. 4.14. Interior beam bottom-flange beam strains: Stage 4
post-tensioning - 1989.

Fig. 4.15. Interior beam bottom-flange beam strains: Stage 5
post-tensioning - 1989.

Fig. 4.16. Interior beam bottom-flange beam strains: Stage 6
post-tensioning - 1989.

variation of bottom-flange beam strains for the previously noted four stages of post-tensioning. Simple supports were assumed in the finite element analysis; thus the bottom flange beam strains at the north and south abutments in all these theoretical curves are zero.

A review of the bottom flange strains in the exterior beams when subjected to post-tensioning (Figs. 4.9-4.12) reveals considerably more end restraint at the north end (a pinned end) than at the south end (a roller support). Considerably more end restraint is observed when the end spans are post-tensioned (stages 1-4); in these stages the top of the beam is rotated into the approach span. When the middle span is post-tensioned (stages 5 and 6) the ends of the beams in the north and south spans rotate so that the top of the beam rotates away from the approach spans, thus reducing end restraint strains.

Post-tensioning stages 1-4 (bottom flange strains from stages 1 and 2 are illustrated in Fig. 4.9 while bottom flange strains from stages 3 and 4 are illustrated in Fig. 4.10) produce positive bottom flange strains at midspan of the middle span as well as at the desired positive strains over the two interior supports. As only the positive moment regions of the beams in the end spans have been post-tensioned, the strain observed at the interior supports and at midspan of the middle span are the result of longitudinal distribution. When the last two stages (stages 5 and 6 on the middle span) of post-tensioning are applied to the bridge, the desired negative strains are obtained in the bottom flanges of the middle-span beams. However, stages 5 and 6 do produce a reduction in the negative bottom flange strain of the end spans (compare Figs. 4.10 and 4.12). Except for the midspan, bottom-flange, middle-span strains, there is excellent agreement between the experimental and theoretical post-tensioning bottom flange strains shown in Fig. 4.12. The experimental bottom flange strain in the middle span is approximately 80% of the theoretical strain. The end strains illustrated in Fig. 4.12 verify the presence of more end

restraint at the north end of the bridge than at the south end. Assuming E_s = 29,000 ksi, the experimental exterior beam bottom-flange strains shown in Fig. 4.12 indicate a stresses change of -5.1 ksi, 4.0 ksi, -8.2 ksi, 4.8 ksi, and -5.5 ksi at south midspan, south pier, middle midspan, north pier, and north midspan, respectively.

Shown in Figs. 4.13-4.16 are the bottom flange strains in the interior beams for the various stages of post-tensioning (stages 2, 4, 5, and 6). A review of these strains reveals behavior very similar to that of the exterior beam; however, there are a few differences. As was true with the exterior beams, there is more end restraint at the north end of the interior beams than at the south end. Although the end restraint at the south end of the interior and exterior beams was essentially the same, there was significantly more end restraint at the north end in the interior beams than in the exterior beams. The largest difference between experimental and theoretical bottom flange strains occurs at the midspan of the south and north span during stage 2 post-tensioning. These strains result from lateral distribution in stage 2 when only the exterior beams of the end spans have been post-tensioned. Shown in Fig. 4.16 are the bottom flange strains, which resulted from stage 6 post-tensioning. As was the case with the exterior beams, the largest difference between the theoretical and experimental strains occurred at the midspan of the middle span. At all other sections (except for the end restraint strains at the north abutment) there was very good agreement between theoretical and experimental strains. Assuming E_s = 29,000 ksi, the experimental interior beam bottom-flange strains shown in Fig. 4.16 indicate a stress change of -4.7 ksi, 5.1 ksi, -7.1 ksi, 3.9 ksi, and -5.0 ksi at the south midspan, south pier, middle midspan, north pier, and north midspan, respectively.

The previous strain results verify that a continuous bridge distributes post-tensioning both longitudinally and transversely. Post-tensioning all beams in the positive moment regions of the three spans reduced the

transverse distribution effects. However, the difference in the sizes of the interior and exterior beams (thus a difference in their stiffnesses) did influence transverse distribution. Longitudinal distribution was very apparent as only the positive moment regions of the beams were post-tensioned; however, very significant strain reductions were measured in the negative moment regions.

4.2. Truck Loading

As described in Chapter 3, the bridge was subjected to truck loading before and after post-tensioning in 1988 and 1989. In both years after post-tensioning, the bridge was pattern loaded (see Table 3.1). The following sections documented the bridge's response and behavior when subject to the previously described vertical loading.

4.2.1. Single Truck

The weights and dimensions of the trucks used to load the bridge each year were given in Fig. 3.6; the loading points referred to in the following paragraphs were given in Fig. 3.7. Bottom flange beam strains for the truck in lanes 1, 2 and 4 (see Fig. 3.7), and at midspan of the south, middle, and north spans, are plotted in Figs. 4.17 through 4.19. In each of these figures the experimental points are joined with lines in order to show the pattern of the strains from beam to beam. In Fig. 4.17 the strains are plotted for three loading positions: 1.2, 3.2, and 4.6. A review of these locations, shown in Fig. 3.7, reveals that 3.2 should produce symmetrical strains, while 1.2 and 4.5 should produce strains that are "opposite handed." The strains shown in Fig. 4.17b exhibit this behavior.
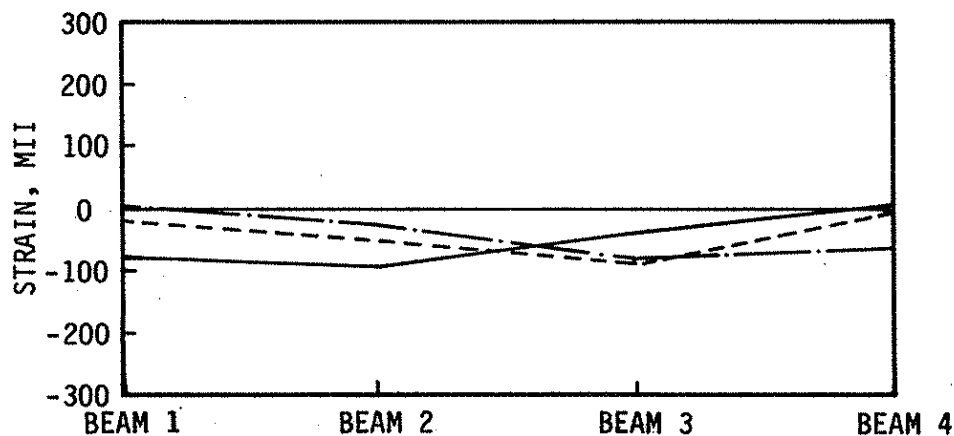
The patterns of strains illustrated in Fig. 4.17b are very similar to those for a simple-span bridge. Some of the differences between the load at loading positions 1.2 and 4.6 are due to the fact that the truck is actually applying six
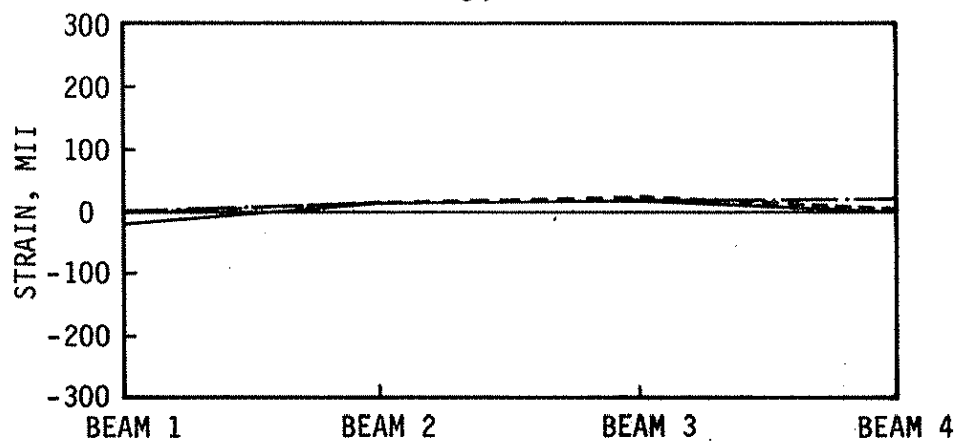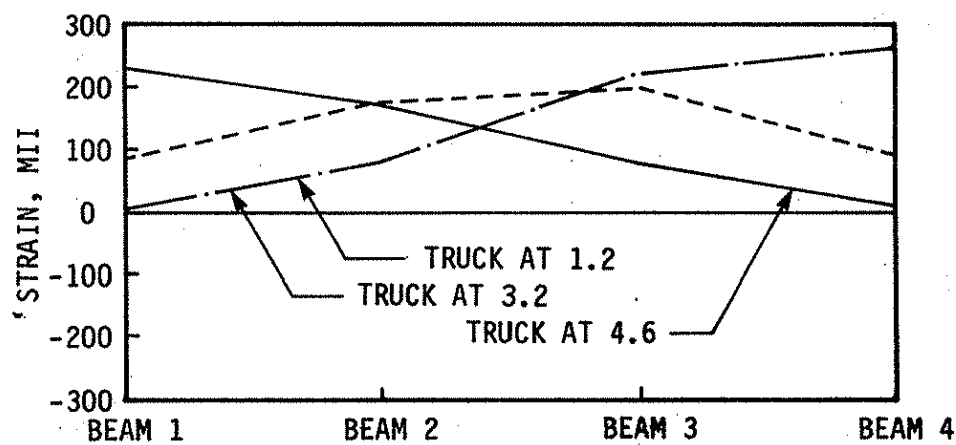
TRUCK AT 1.2
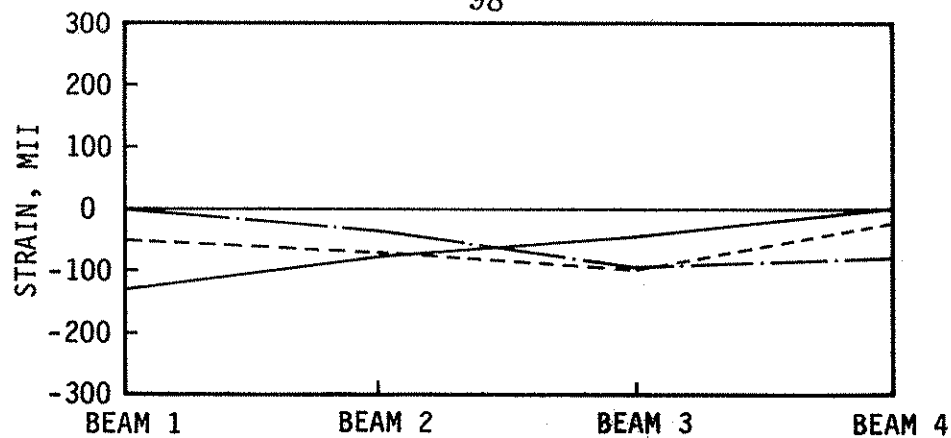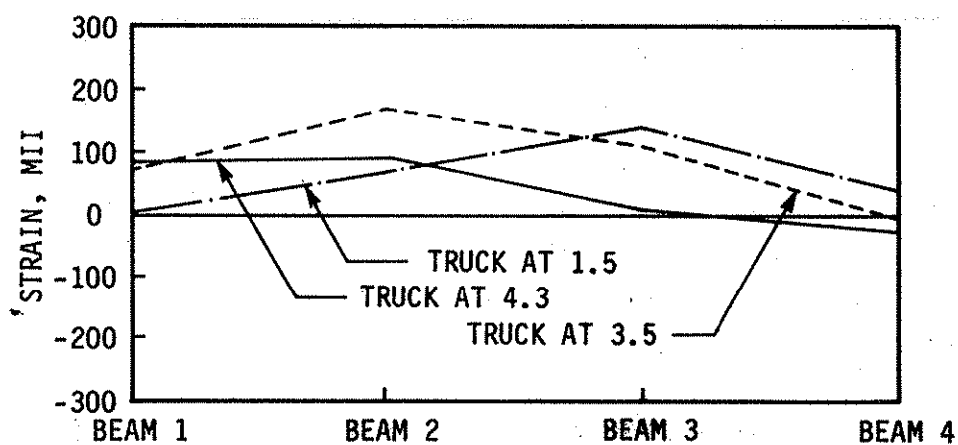TRUCK AT 3.2
TRUCK AT 4.6
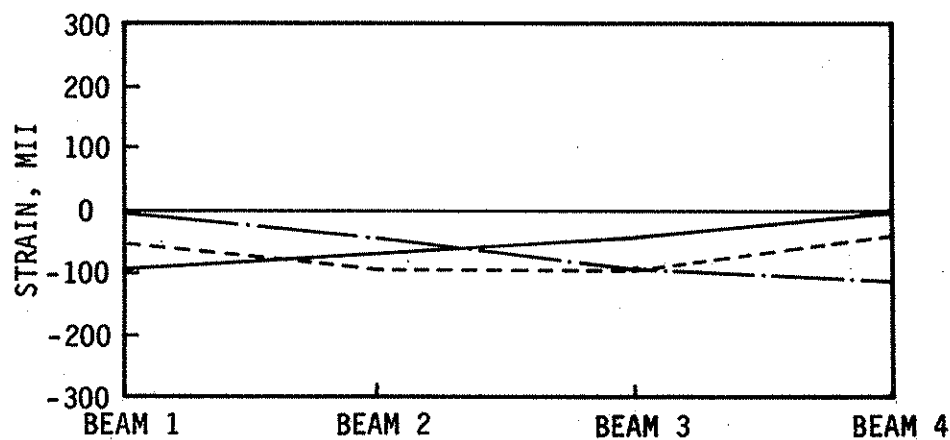
Fig. 4.17. Bottom-flange beam strains, truck at various locations in south span, no post-tensioning - 1989.

a. SOUTH PIER

b. MIDSPAN

TRUCK AT 1.5
TRUCK AT 4.3
TRUCK AT 3.5

c. NORTH PIER

Fig. 4.18. Bottom-flange beam strains, truck at various locations
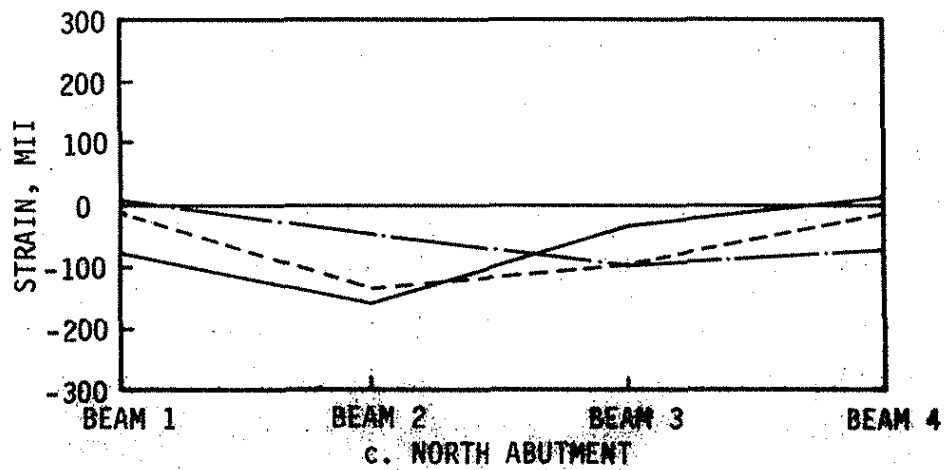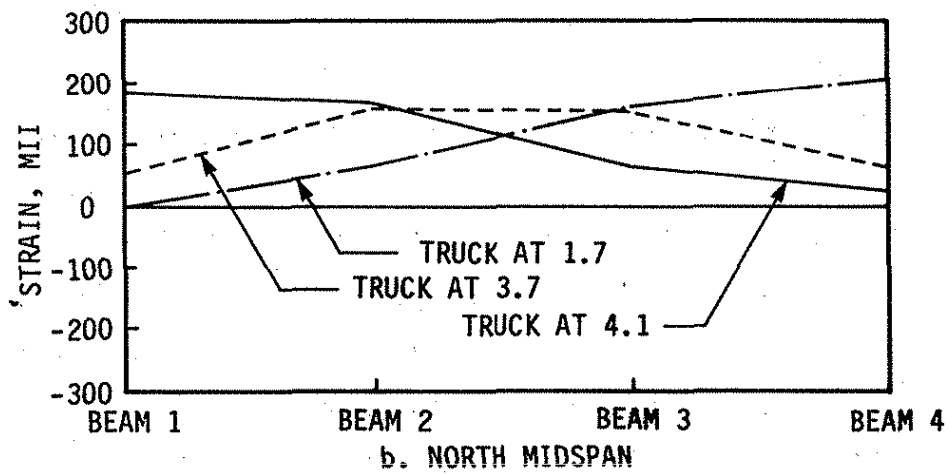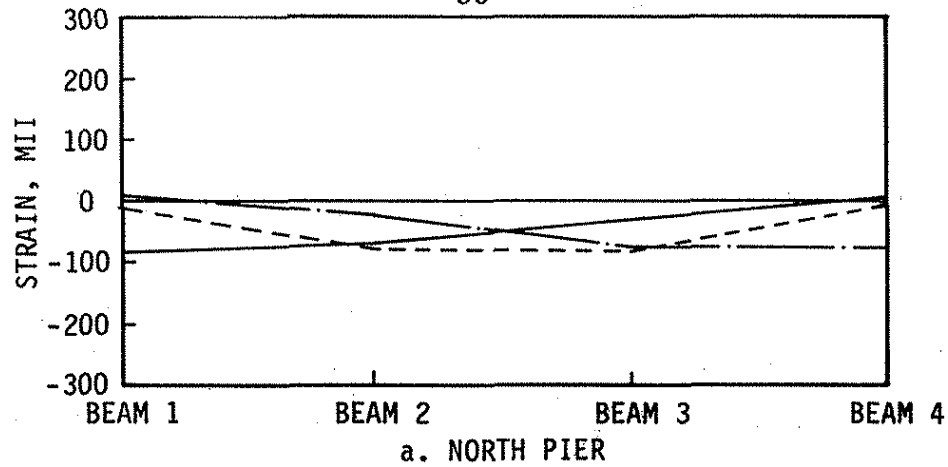in middle span, no post-tensioning - 1989.

Fig. 4.19. Bottom-flange beam strains, truck at various locations in north span, no post-tensioning - 1989.

concentrated loads to the bridge rather than applying the load at the center of gravity, which is positioned at the two load points. The position of the six concentrated loads relative to the centerline of the span thus varies depending on which direction the truck is moving. Obviously, positioning the truck in the south span will produce strains in the other two spans; however, because the instrumented sections in these two spans are far removed from the applied loads, the strains produced will be very small and thus are not shown. Only strains at the loaded section (Fig. 4.17b) and on the sections at the ends of the loaded span (Figs. 4.17a and c) are illustrated. Strains shown in Fig. 4.17a indicate the presence of some end restraint, while the strains in Fig. 4.17c indicate the presence of negative moment over the south pier as one would expect.
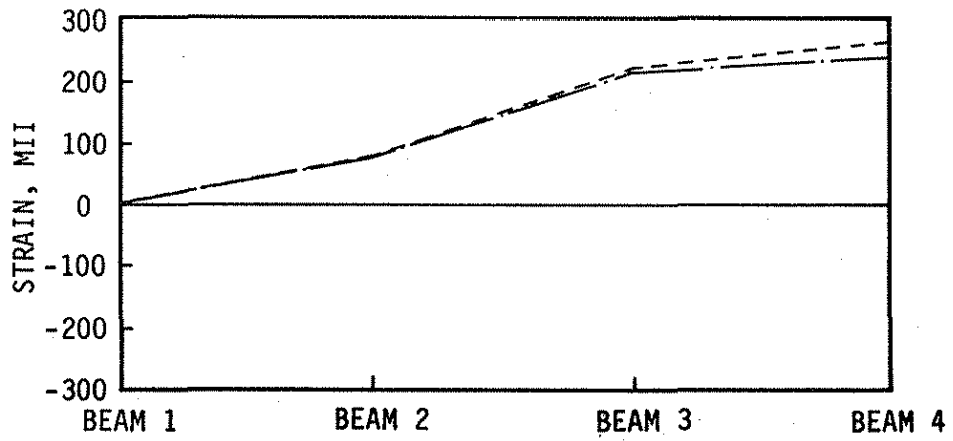
Strains for the truck at midspan of the bridge (loading positions 1.5, 3.5, and 4.3) are presented in Fig. 4.18. Behavior similar to that when the truck was in the south span was observed: symmetrical strain distribution when the truck was in lane 3 (except for one low reading at midspan (Fig. 4.18b)), negative moment over both south and north piers, and strain patterns at midspan (Fig.4.18b) similar to those for a simple-span bridge.

The pattern of strains shown in Fig. 4.19 for the truck in the north span (loading positions 1.7, 3.7, and 4.1) are essentially the same as the strain distribution shown in Fig. 4.17, which is for the truck in the south span, with one exception. There is considerably more end restraint at the north abutment (see Fig. 4.19c) than was observed at the south abutment when the truck was in the south span (see Fig. 4.17a). The only difference that is readily apparent between the support at the south and north abutments is the fact that the south support is a roller while the north support is a pin. There obviously could be construction differences (for example, slab steel extended into the wing walls) that are not visible. The data that were presented in the three figures just discussed was from the 1989 testing program. However, similar
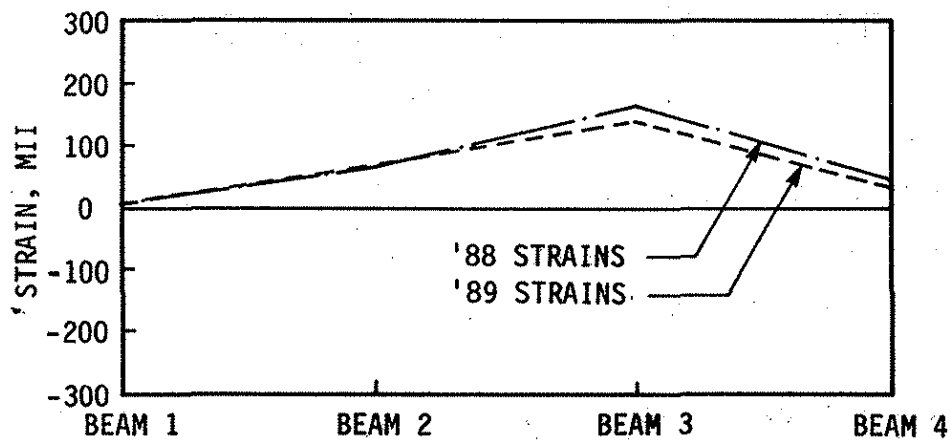
results were obtained in 1988 field testing programs. Verification of this is presented in the next paragraph where strains from the 1988 and 1989 testing programs are compared.

As was previously noted–taking into account the fact that the truck weights were slightly greater in 1989, as was the post-tensioning force applied to the bridge–there was excellent agreement between the 1988 and 1989 field results. Shown in Figs. 4.20 and 4.21 are midspan strains measured when the truck was positioned at midspan (two different lanes) of the span where strains were measured. For example, Figs. 4.20a and 4.21a illustrate the strains at the midspan of the south span when the truck is positioned at loading positions 1.2 and 3.2, respectively. The 1989 low strain reading on beam 3 at the midspan of the middle span is once again evident (see Fig. 4.21b). As there was instrumentation only on beams 3 and 4 at midspan of the north span in 1988, there are no strain readings available at this section for Beams 1 and 2 (see Figs. 4.20c and 4.21c).
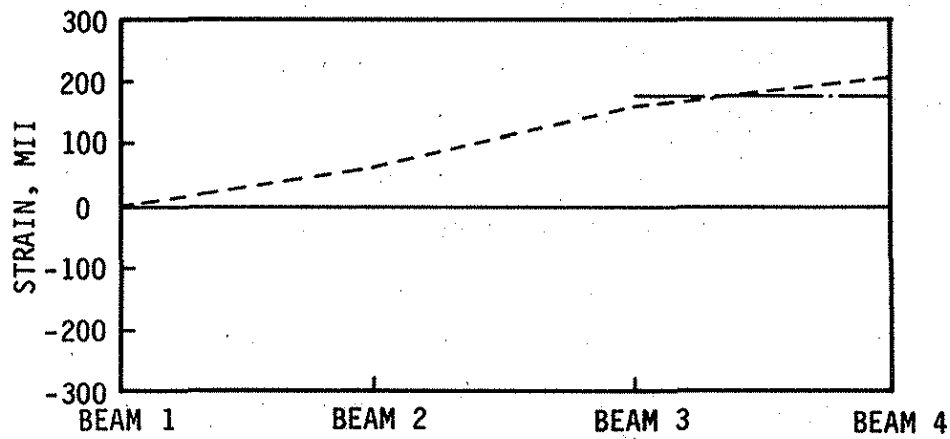
As has been shown in the testing of various post-tensioned, simply supported bridges, the post-tensioning adds very little to the stiffness of the bridge. Thus strains and deflections resulting from vertical loading do not change significantly when the post-tensioning system and forces are applied. Similar results were observed in post-tensioned, continuous-span bridges. Shown in Figs. 4.22 and 4.23 are strains that were obtained in 1989 from truck loading, which was applied to the bridge before post-tensioning and after post-tensioning. Note that the loading positions and sections being examined are the same as those in Figs. 4.20 and 4.21. Also to be noted is that the strains are due only to the truck loading and do not include the effects of post-tensioning. Although no attempt has been made to quantify the results at this time, the fact that–at three sections (midspan of the south, middle, and north spans) and for six different positions of the truck loading–strains due to truck loading after post-tensioning are noticeably less than the strains before
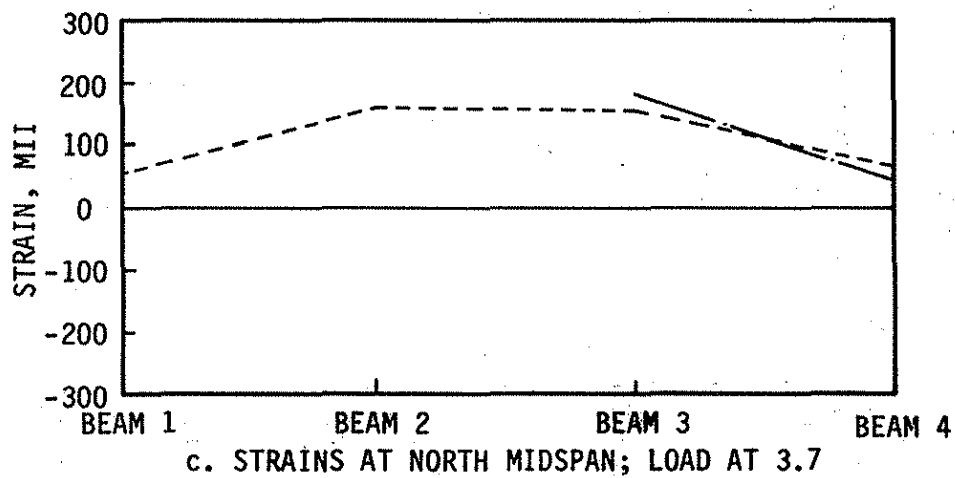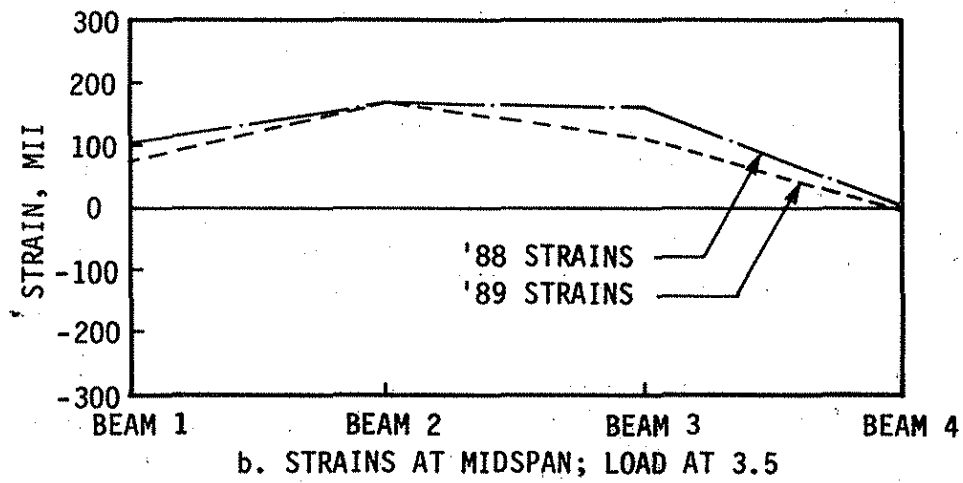
Fig. 4.20. Comparison of 1988 and 1989 bottom-flange beam strains
before post-tensioning at various sections with loading
in lane 1.

a. STRAINS AT SOUTH MIDSPAN; LOAD AT 3.2

b. STRAINS AT MIDSPAN; LOAD AT 3.5
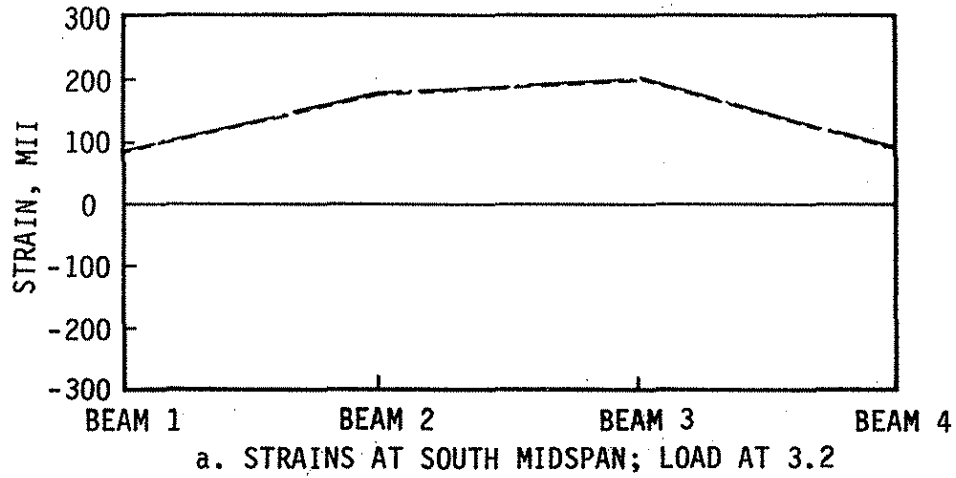
c. STRAINS AT NORTH MIDSPAN; LOAD AT 3.7

Fig. 4.21. Comparison of 1988 and 1989 bottom-flange beam strains before post-tensioning at various sections with loading in lane 3.

a. STRAINS AT SOUTH MIDSPAN; LOAD AT 1.2

b. STRAINS AT MIDSPAN; LOAD AT 1.5
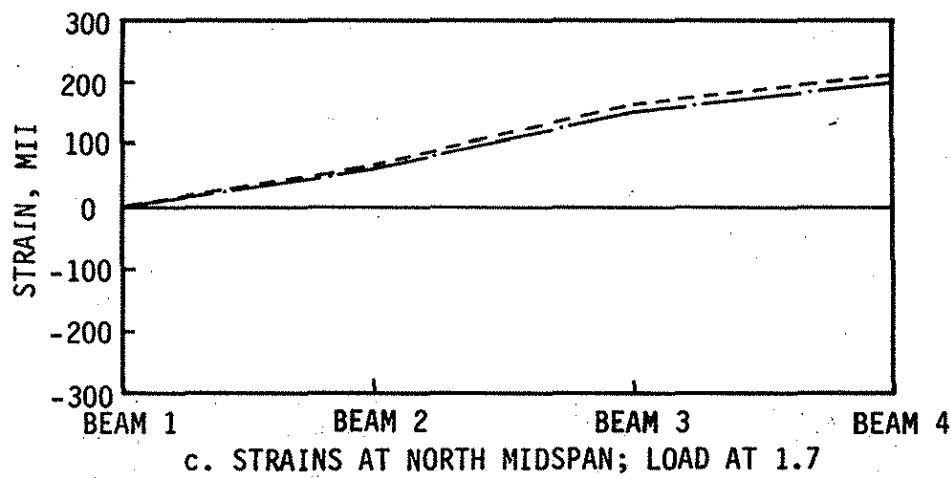
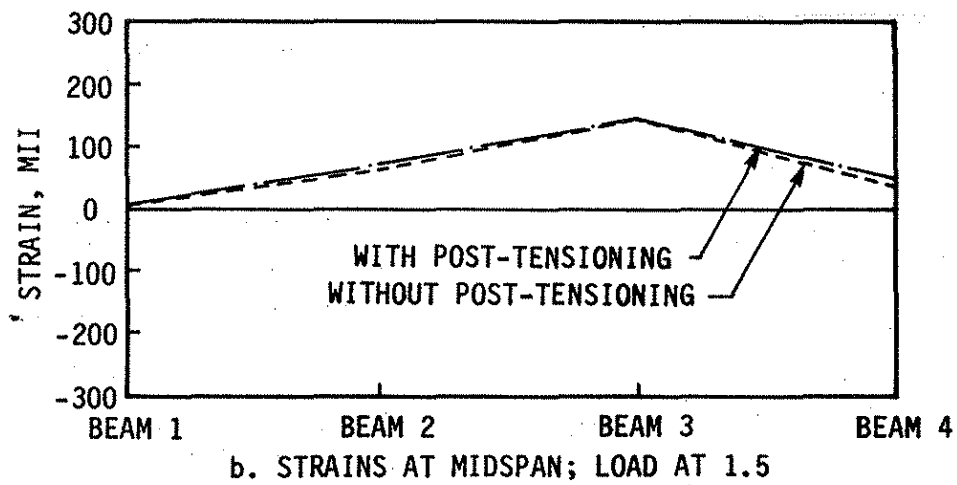c. STRAINS AT NORTH MIDSPAN; LOAD AT 1.7

Fig. 4.22. Effect of post-tensioning on bottom-flange beam strains
at various sections with loading in lane 1 - 1989.

a. STRAINS AT SOUTH MIDSPAN; LOAD AT 3.2

b. STRAINS AT MIDSPAN; LOAD AT 3.5

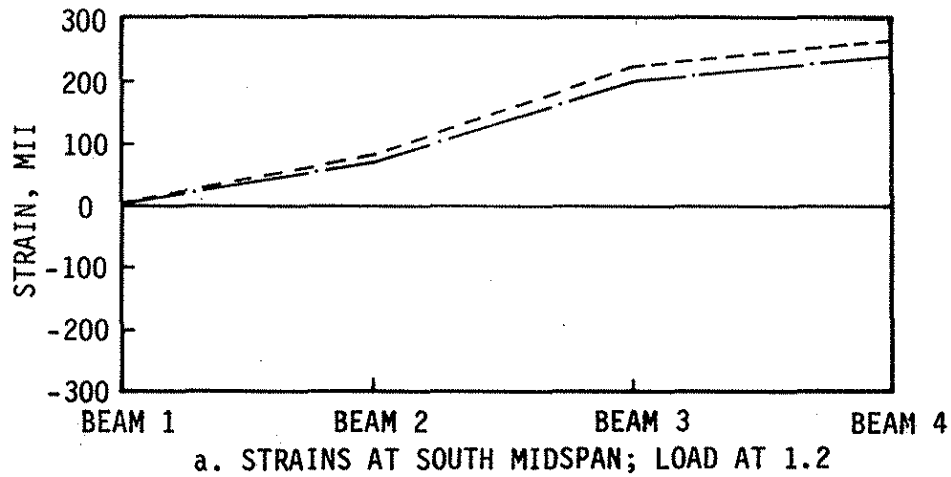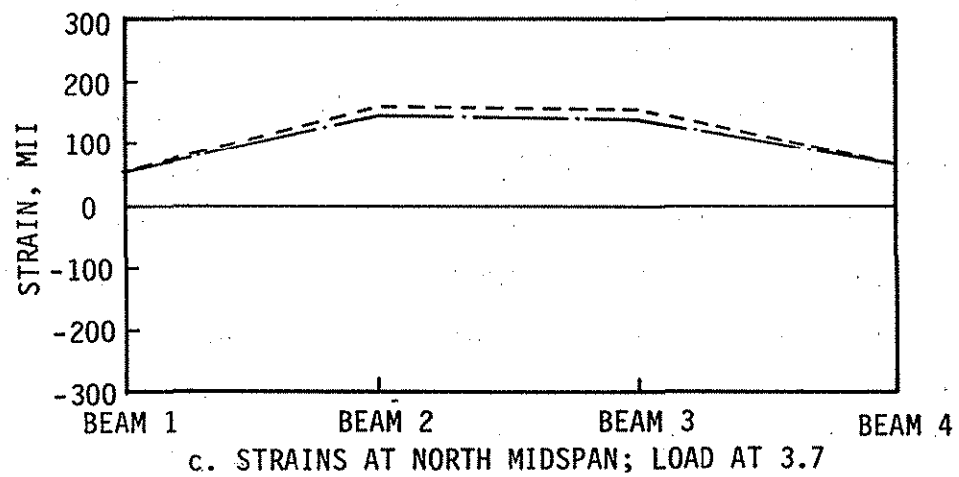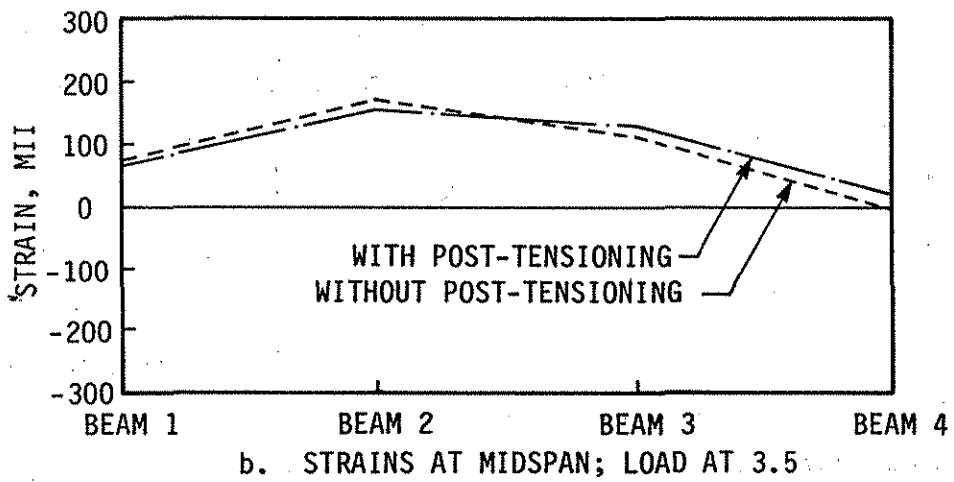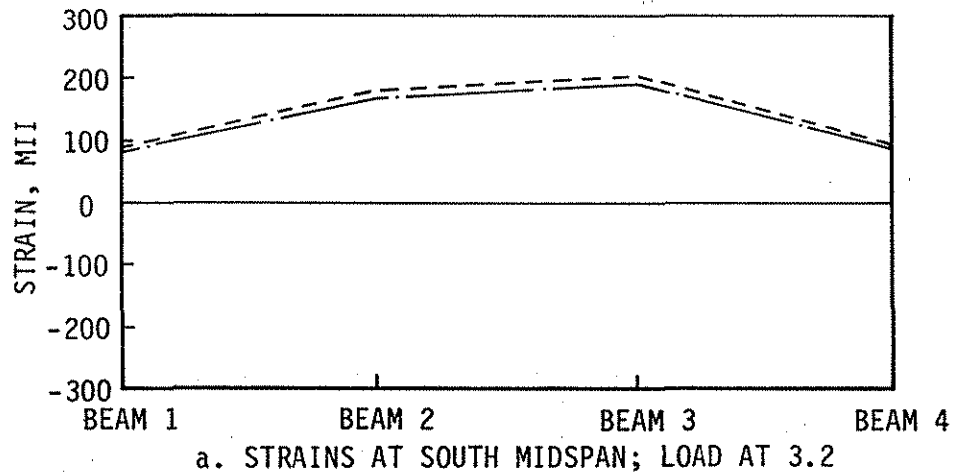c. STRAINS AT NORTH MIDSPAN; LOAD AT 3.7

Fig. 4.23. Effect of post-tensioning on bottom-flange beam strains
at various sections with loading in lane 3 - 1989.

post-tensioning indicates that the post-tensioning has slightly increased the bridge stiffness. Additional analysis is required to determine if this increase may be significant in certain situations.

4.2.2. Pattern Loading

As was described in Chapter 3 after the bridge was post-tensioned, it was subjected to 12 different pattern loading cases (see Table 3.1 and Fig. 3.7). The pattern loadings were intended to maximize the strains at various locations in the bridge. Because large strains can be measured more accurately than small strains, the pattern loading made it easier to determine the bridge's response to vertical loading. Because of space limitations, only representative samples of the pattern loading data are presented in this report. In Figs. 4.24 through 4.28, strains occurring at critical sections for particular loading cases are presented. Strain data along the four bridge beams are presented in Figs. 4.29 through 4.31 for load cases 30, 35, 36, and 37; thus, both the longitudinal and transverse strain distribution may be reviewed.

Each pattern loading case employed was selected to either maximize the positive moment near midspan in one of the bridge's three spans or maximize the negative moment at one of the two piers. In Figs. 4.24 through 4.28, strains are plotted for load cases 36, 35, 31, 30, and 38 respectively; the section in the figures corresponds to the section at which strains were maximized by the particular load case. In the figures that correspond to negative moment locations (Figs. 4.25, 4.26, and 4.28), strains for truck no. 1 at the two positions used in the particular load case are also included in the figure. For example, in Fig. 4.25, strains from load case 35 (truck no. 1 at 3.5 and truck no. 2 at 3.2) are plotted along with the strains from truck no. 1 at position 3.2 and position 3.5. As may be observed, the sum of the strains from the single load cases is
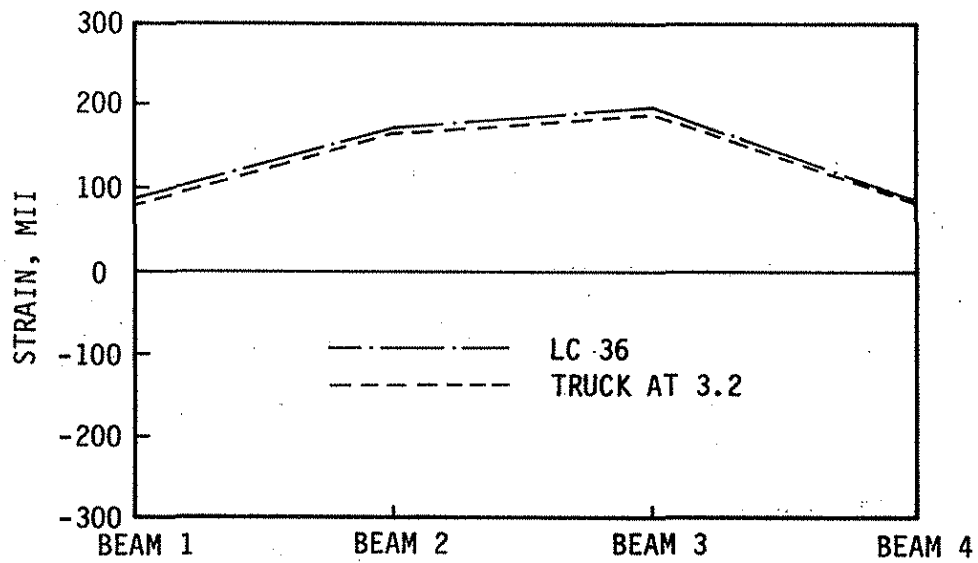
Fig. 4.24. South midspan, bottom-flange beam strains, LC 36 - 1989.

Fig. 4.25. South pier, bottom-flange beam strains, LC 35 - 1989.
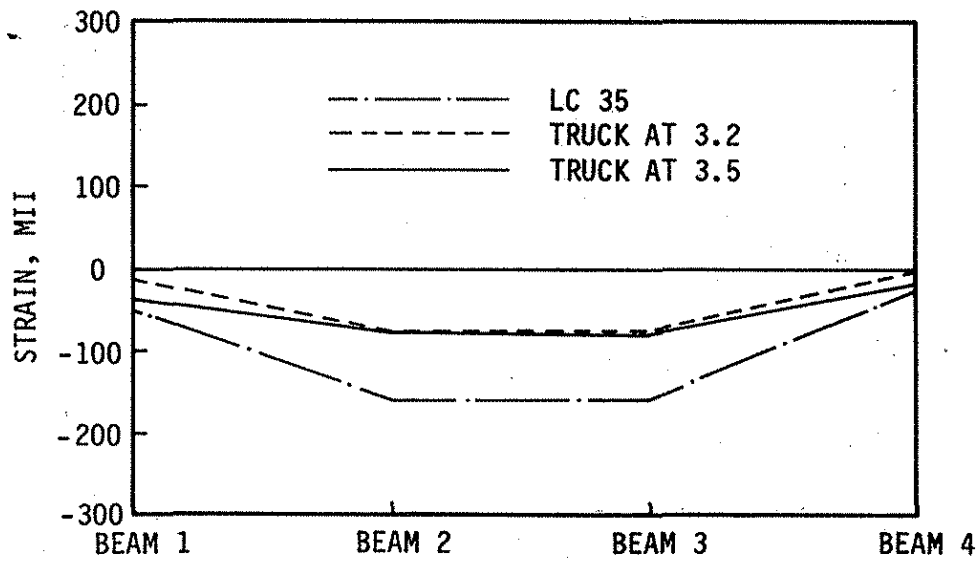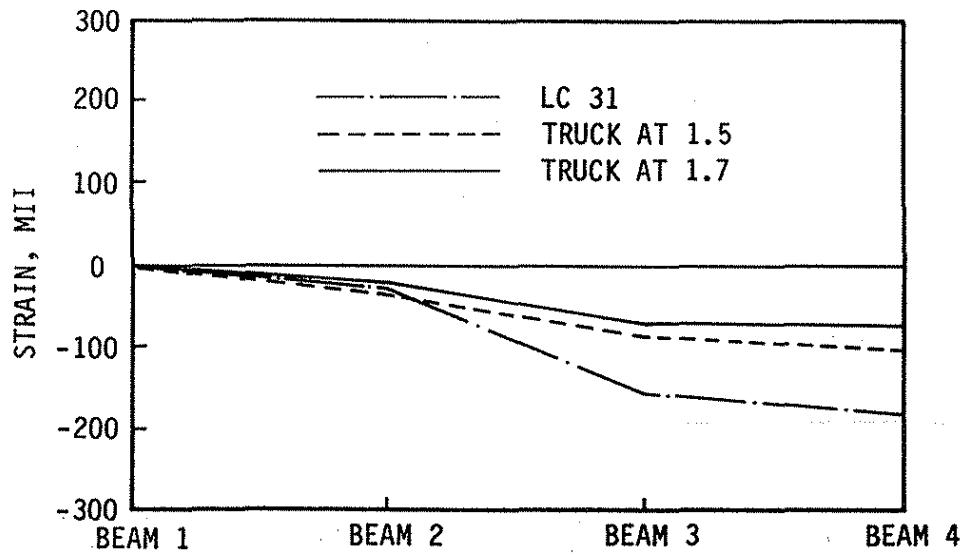
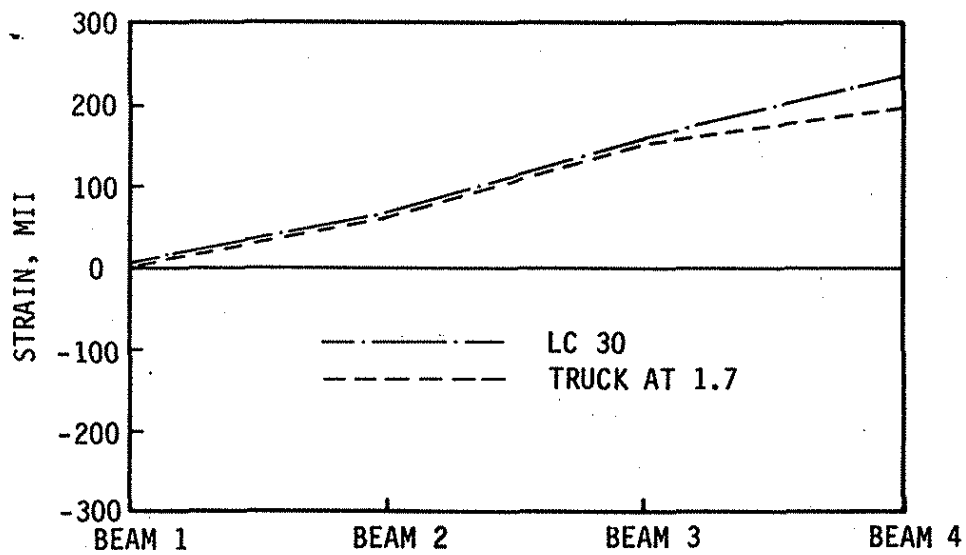Fig. 4.26. North pier, bottom-flange beam strains, LC 31 - 1989.

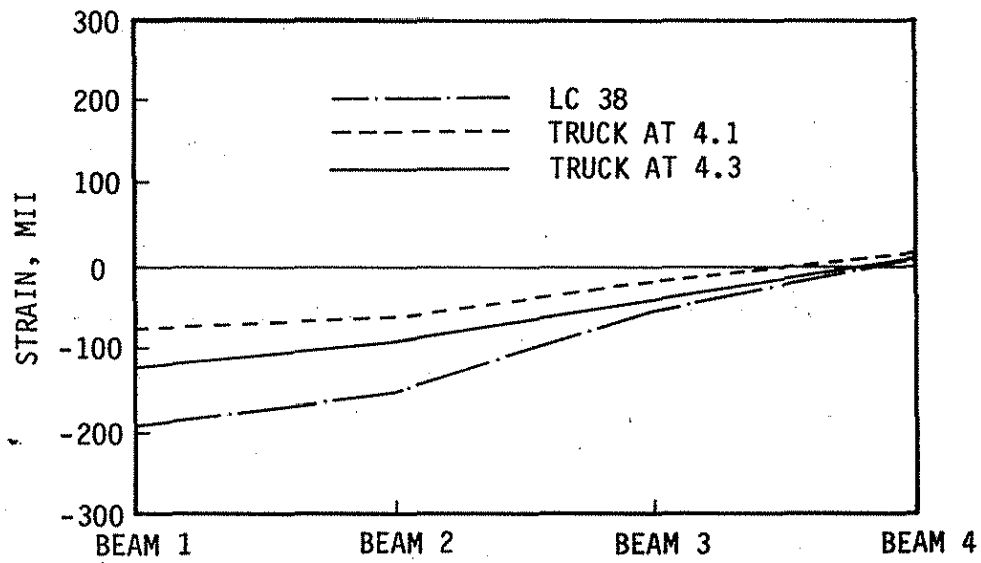Fig. 4.27. North midspan, bottom-flange beam strains, LC 30 - 1989.

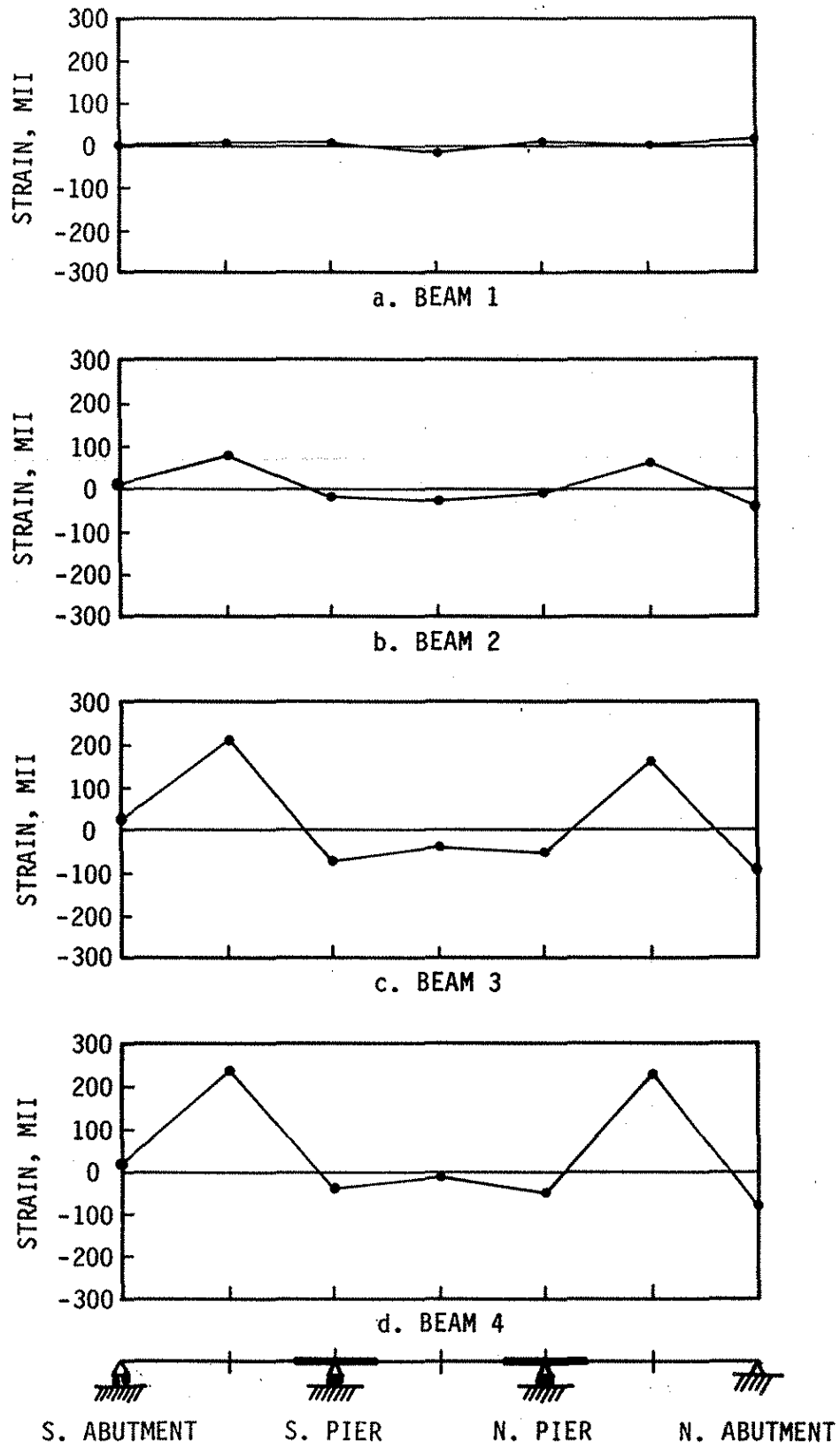Fig. 4.28. North pier, bottom-flange beam strains, LC 38 - 1989.

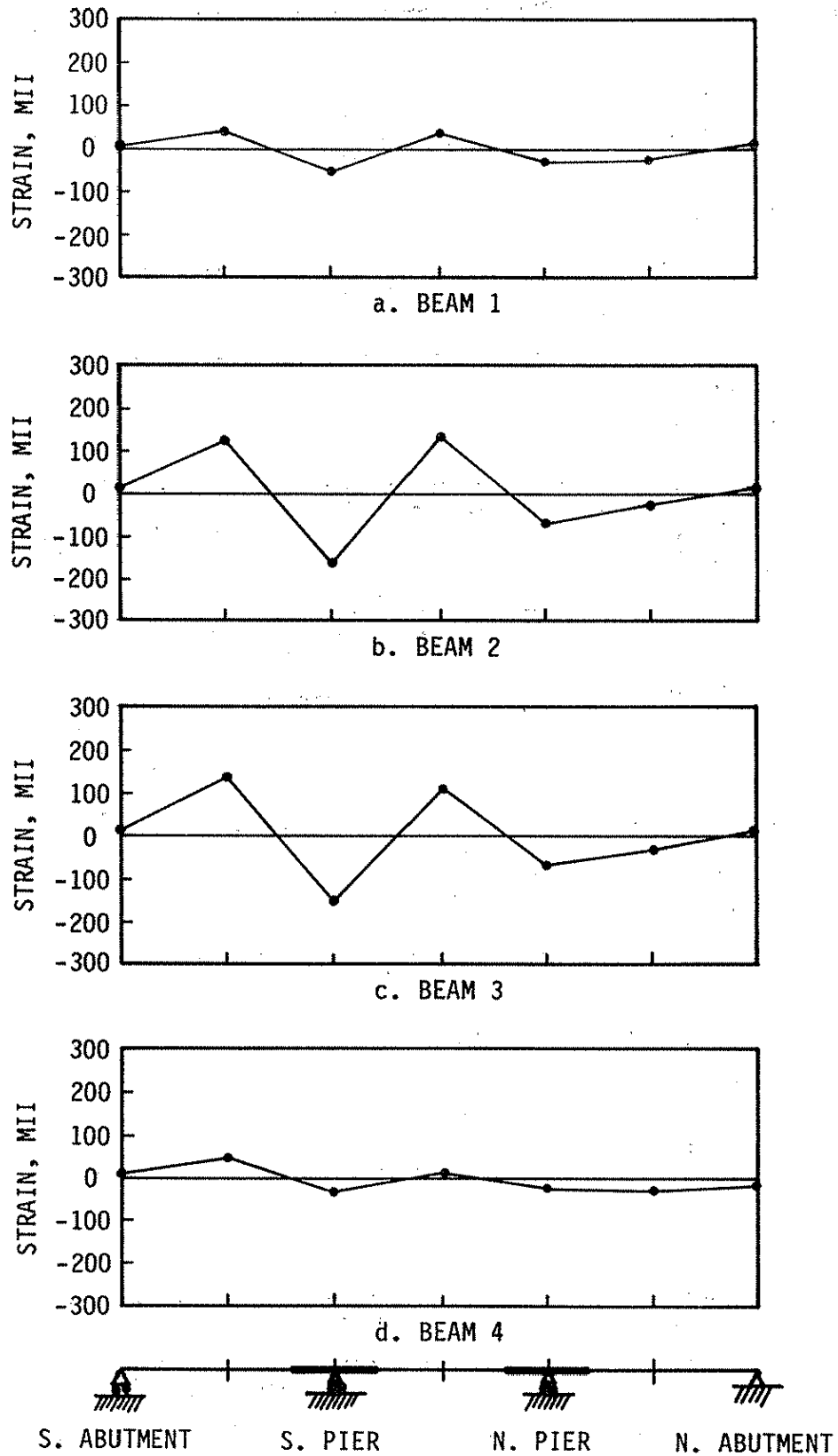Fig. 4.29. LC 30, bottom-flange beam strain distribution.

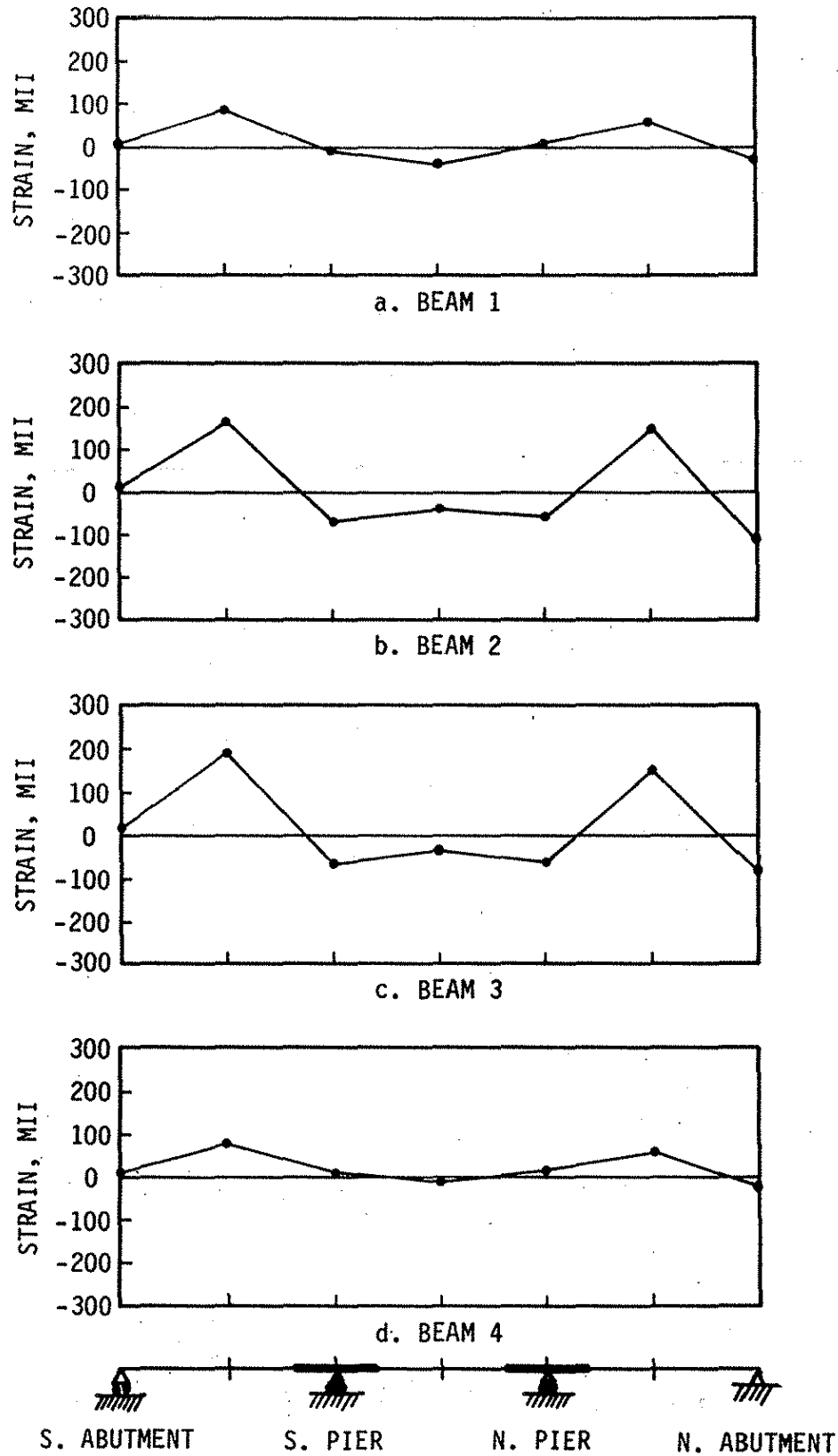Fig. 4.30. LC 35, bottom-flange beam strain distribution.

Fig. 4.31. LC 36, bottom-flange beam strain distribution.

essentially equal to the strains from load case 35. Similar statements can be made about the strains shown in Figs. 4.26 and 4.28.

In Fig. 4.24 strains from Load Case 36 (truck no. 1 at 3.7 and truck no. 2 at 3.2) are plotted plus strains for truck no. 2 at 3.2. The closeness of the two curves indicates that truck no. 1 in the far span (at position 3.7) has a very small effect on the positive moment in the south span. A similar statement may be made about the strains shown in Fig. 4.27–strains from truck no. 1 at position 1.7 are essentially the same as those from load case 30 (truck no. 1 at 1.7 and truck no. 2 at 1.2); thus, loading in the south span has minimal effect on strains in the north span.

In general, it may be stated that pattern loading has a significant effect on negative moments and a very small effect on positive moments.

Shown in Fig. 4.29 are the bottom strains along beams 1-4 that result from loading case 30 (truck no. 1 at 1.7 and truck no. 2 at 1.2), which, as may be seen, maximize the positive moment in the end span. A review of this figure reveals: considerably more end restraint at the north abutment than at the south abutment, including even a difference in signs; minimal strains in beam 1 farthest from the truck loading; negative strain at the midspan of beams 3 and 4; and more end restraint on the interior beam than on the exterior beams.

Figures 4.30 through 4.32 are for load cases 35, 36, and 37, respectively. As these load cases all have the trucks centered on the longitudinal centerline of the bridge (lane 3) one would expect the symmetry that may be observed in all of these figures. Observations similar to those made about the results illustrated in Fig. 4.29 may be made about the results in these figures. In addition, one may observe the significant changes in the north abutment end restraint strains (sign and magnitude) as load moves across the bridge. End restraint strains at the south abutment are very small.
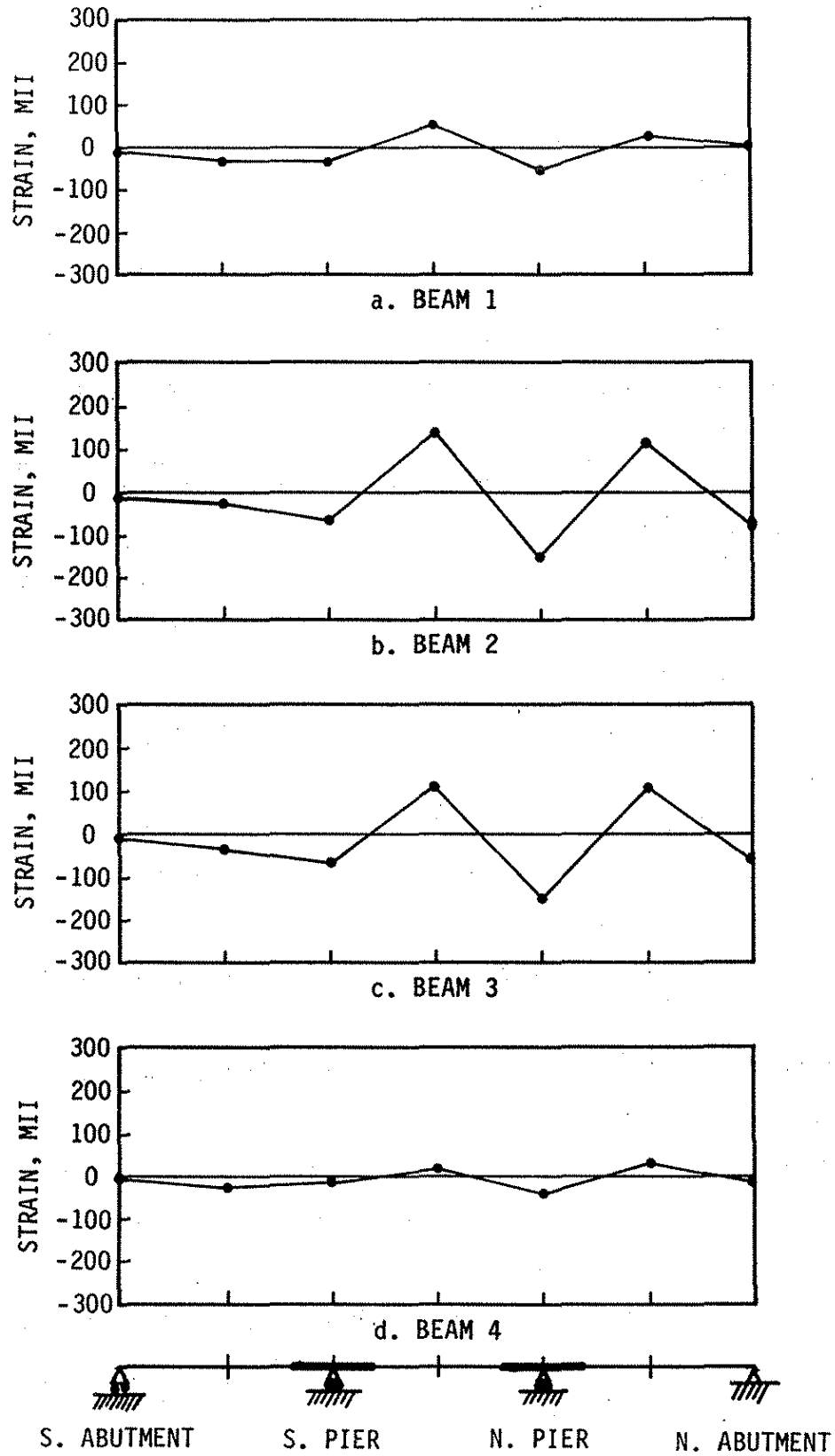
a. BEAM 1

b. BEAM 2

c. BEAM 3

d. BEAM 4

S. ABUTMENT   S. PIER   N. PIER   N. ABUTMENT

Fig. 4.32. LC 37, bottom-flange beam strain distribution.

4.2.3. Tendon Force Changes

Whenever there is a change in deflection of a post-tensioned beam, the forces in eccentric tendons will change. The change in deflection may be caused by application of more post-tensioning or by the application of vertical load. The effect of post-tensioning beams of a continuous-span bridge on beams of the bridge that have previously been post-tensioned was presented in Section 4.1; thus, this section will present the effects of vertical load on post-tensioning forces.

As vertical live loads are applied to a bridge strengthened by post-tensioning, forces will change in the tendons. For a simple-span bridge, the tendon forces will always increase when a vertical load is applied unless the load is applied with extreme eccentricity with respect to the centerline of the bridge, a condition which is impractical. Thus, in practice, the tendon force increases will provide additional post-tensioning when it is most needed.

For continuous bridges, the changes in tendon forces will not necessarily be beneficial. This was initially shown in the laboratory investigation of post-tensioned continuous-span bridges [5,22] and was also found to be the case in this investigation.

Figure 4.33 illustrates the middle-span east exterior beam and east interior beam tendon force changes as truck no. 1 moves across the bridge in the four load lanes. The maximum as well as minimum force changes in this figure have been superimposed in Fig. 4.34 for clarity. A review of these two figures indicates that the maximum increase in the tendon force in the exterior beam is 10.1% while the maximum decrease is -2.5%. For the interior beam, the maximum percentages of increase and decrease are 6.5% and -1.7%, respectively. These figures also verify that the change in tendon force in continuous bridges is a function of both lane and span loading. This is obvious
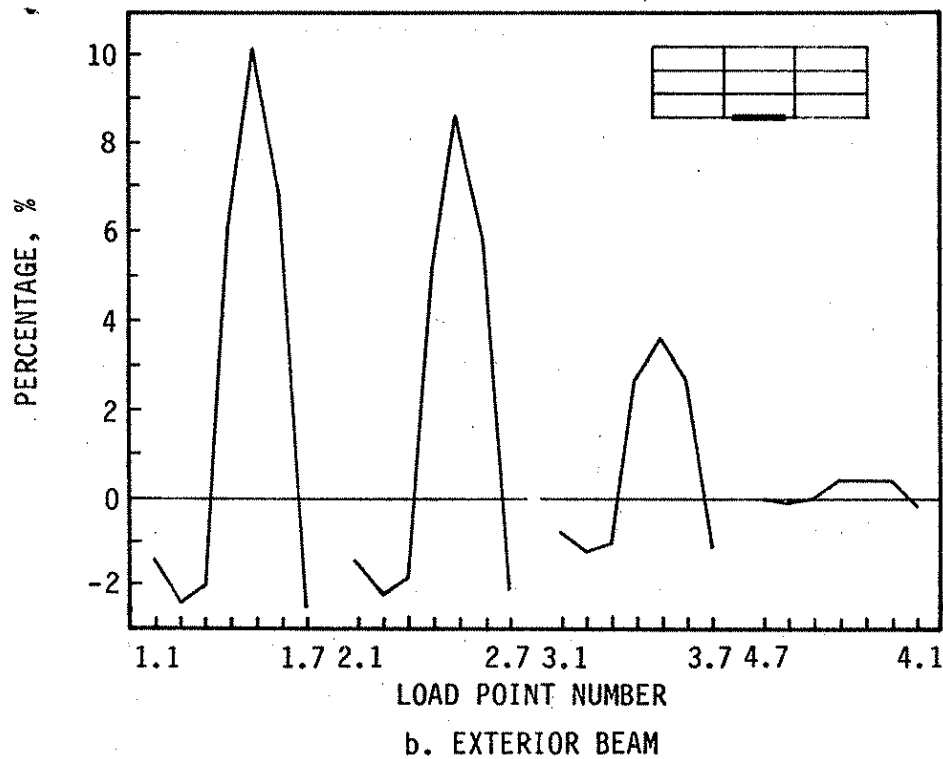
a. INTERIOR BEAM

b. EXTERIOR BEAM
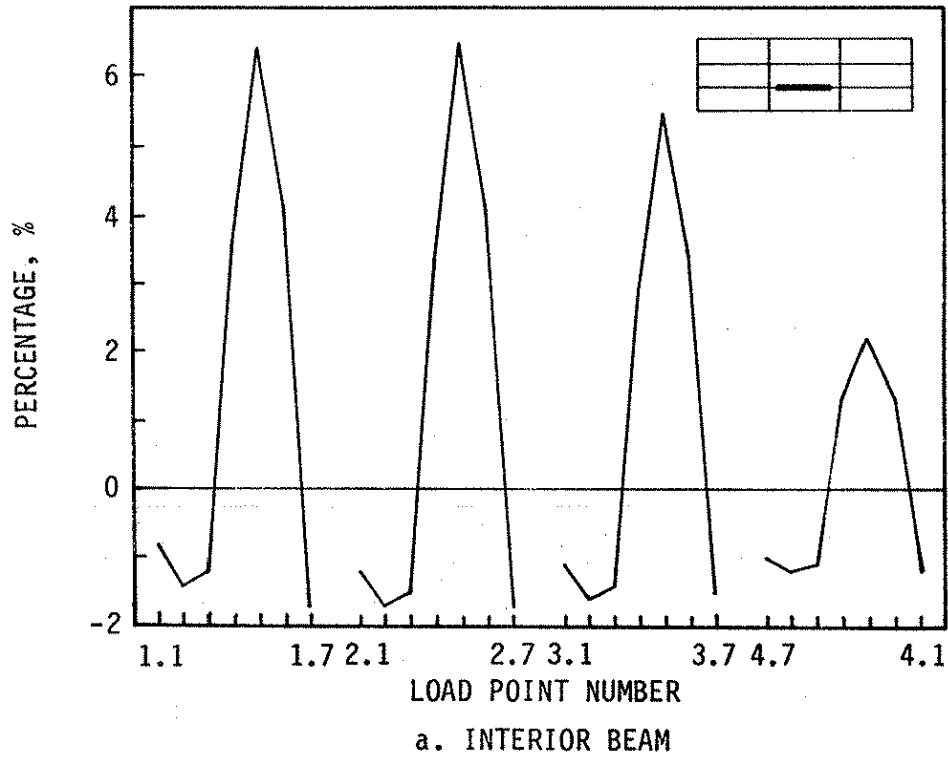
Fig. 4.33. Percent of increase or decrease in the force in middle-span tendons due to vertical loading.
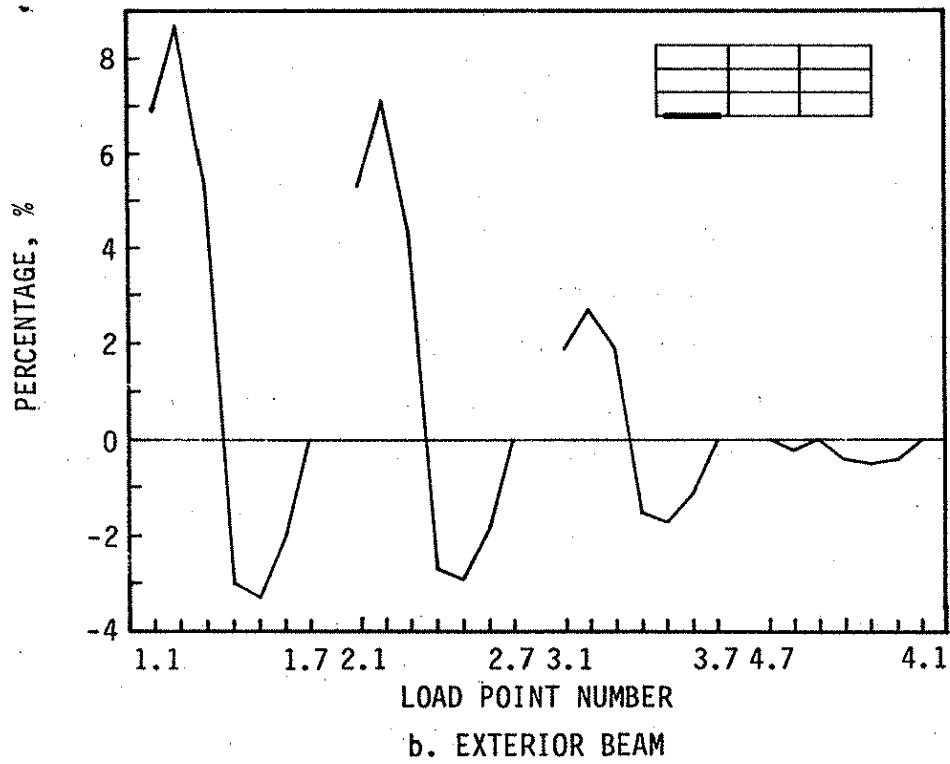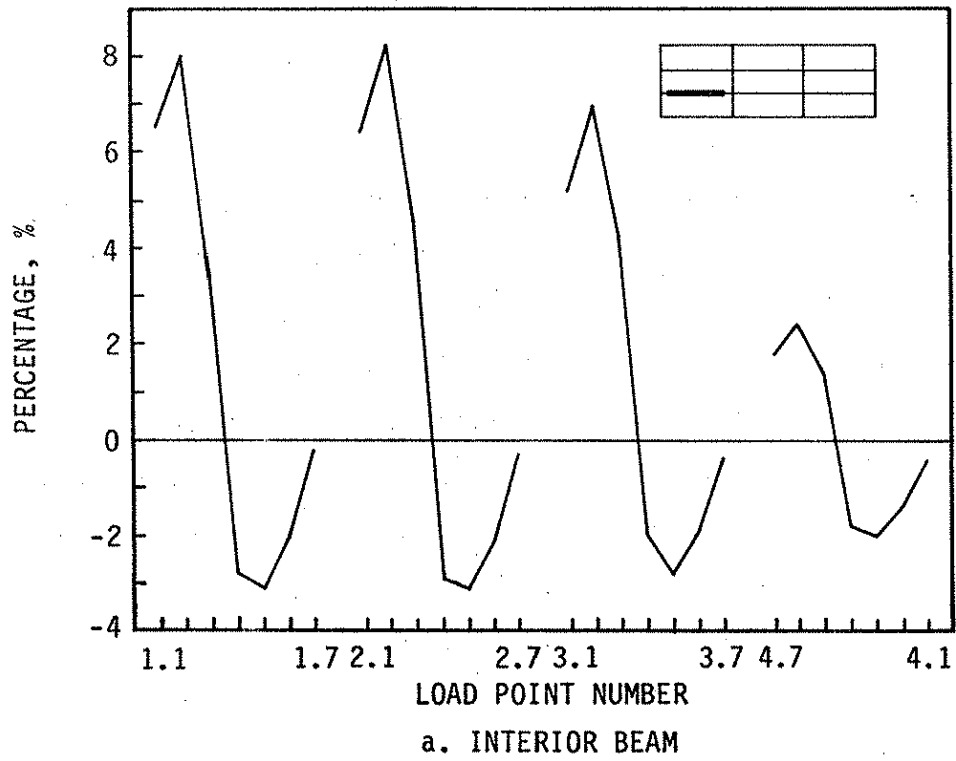
a. INTERIOR BEAM

b. EXTERIOR BEAM

Fig. 4.34. Percent of increase or decrease in the force in south span tendons due to vertical loading.

when one considers the deflection patterns that result from the various positions of the truck loading.

Data similar to that in the previous two figures are illustrated in Figs. 4.35 and 4.36 for the south-span east exterior beam and east interior beam. A review of these figures reveals behavior very similar to that of the tendons in the middle span except that the percentage of increase is smaller (8.7% and 8.2% for the exterior and interior beams, respectively). The percentage of decrease is slightly larger (-3.3% and -3.1% for the exterior and interior beams, respectively). One of the reasons the percentage of change in tendon forces in the middle span is greater than that in the south span is the position of the tendons. In the middle span the tendons are below the bottom flange, while in the end spans the tendons are above the bottom flange. The larger percentage of change in the middle span is even more significant because the post-tensioning forces are considerably larger in the middle span than in the end spans. The percentages of change in tendon forces could be slightly larger in actual practice in that trucks could cross the bridge with one line of wheels directly over one of the beams. None of the lane loadings used in this investigation positioned truck wheels directly over a beam line.

Additional data on the change in post-tensioning force due to vertical loading are presented in Fig. 4.37. Shown in this figure are the actual changes in post-tensioning forces for 9 of the 12 pattern loading cases investigated. Changes measured in both the 1988 (upper valves) and 1989 (lower valves) are listed. Care should be taken in comparing these values directly because the post-tensioning forces were different for the two years (see Fig. 4.6). The increases as well as decreases in tendon forces for the two trucks at the predetermined locations on the bridge are readily apparent in this figure.

Because tendon force changes are both positive and negative and the magnitude of the changes are frequently larger than for simple-span bridges, tendon force changes are an important factor to consider in designing the
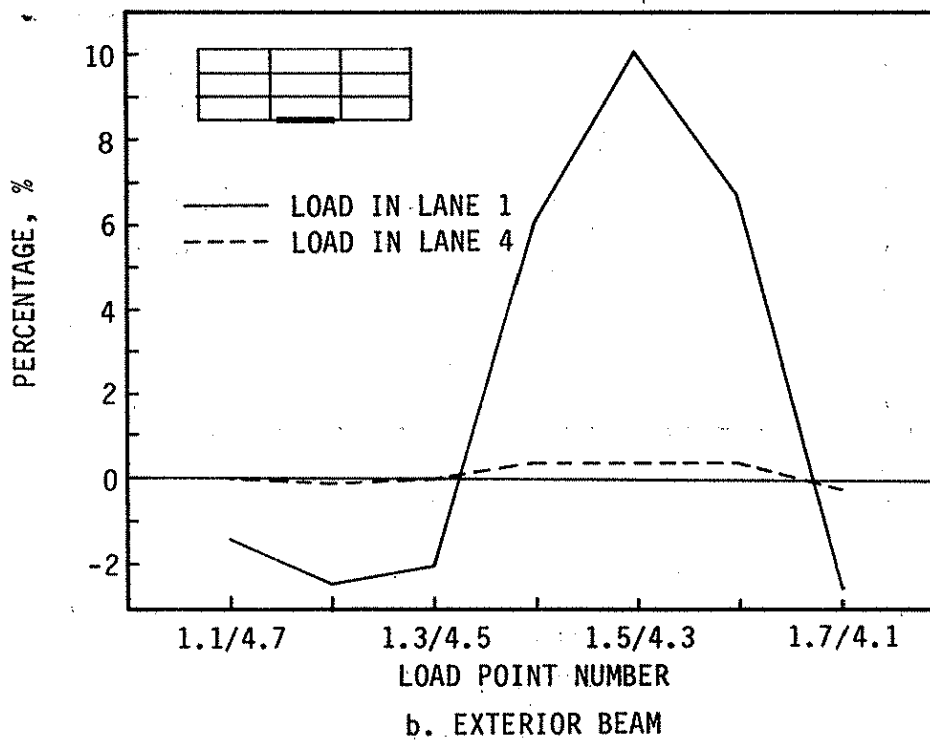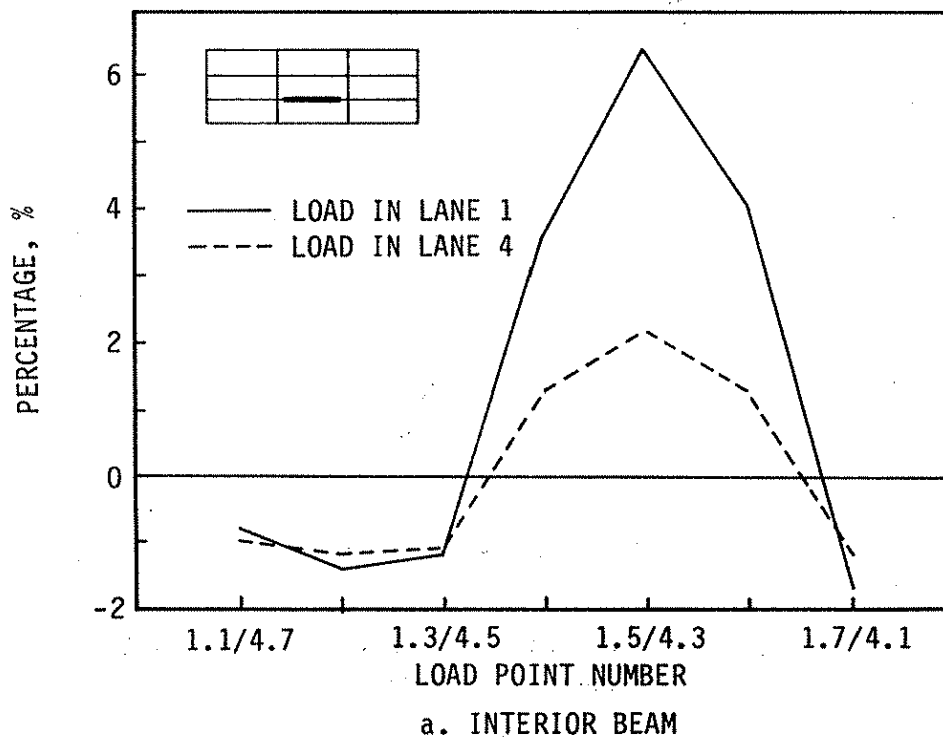
a. INTERIOR BEAM

b. EXTERIOR BEAM

Fig. 4.35. Change in middle-span tendon force due
to vertical loading.

a. INTERIOR BEAM
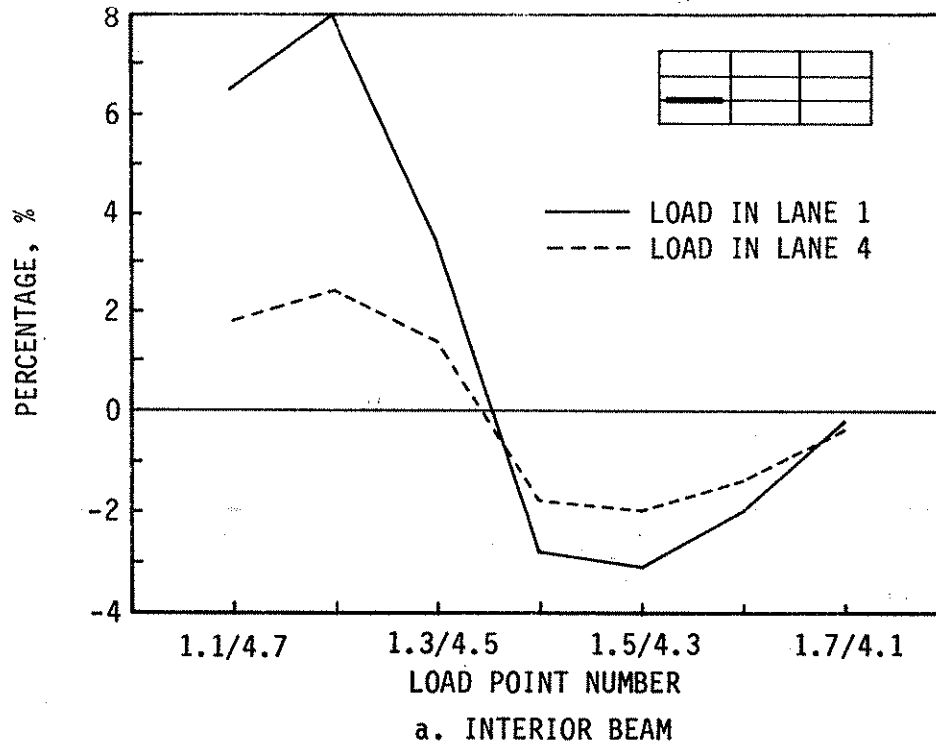

b. EXTERIOR BEAM
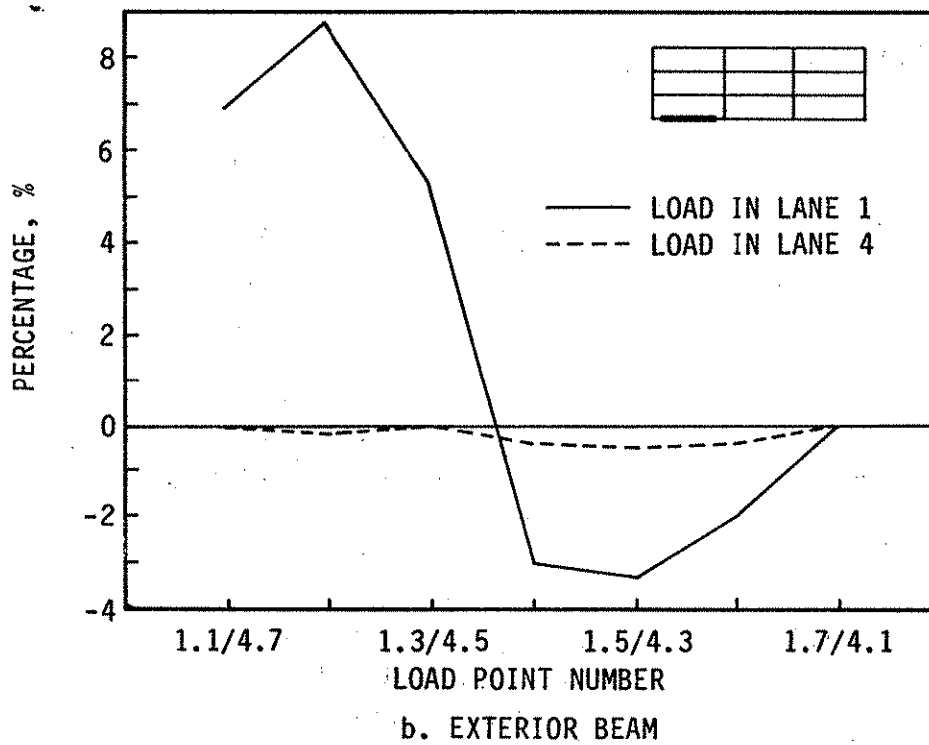
Fig. 4.36. Changes in south span tendon force due
to vertical loading.

a. LANE 1 LOADING

LC 29

	-.2		-.1		0
	0		0		0
	1.0		2.0		-.5
	2.8		4.0		-.4
	5.3		4.4		-1.3
	6.4		9.3		-1.7
	6.6		10.0		-1.8
	7.3		11.2		-2.2

LC 30

	.3		-.5		.3
	.4		-.7		.4
	1.8		-2.9		2.6
	1.5		-4.9		1.5
	8.1		-2.2		6.9
	9.6		-4.6		7.2
	10.2		-6.0		8.3
	11.2		-6.2		9.2

LC 31

	-.3		.5		-.1
	-.3		.2		-.3
	-.5		2.5		1.4
	-2.2		2.7		.6
	-2.3		4.3		4.7
	-2.2		9.7		4.8
	-2.8		9.8		5.4
	-3.0		11.0		6.1

b. LANE 3 LOADING

LC 35

	1.3		3.7		-.8
	1.9		3.4		-.8
	2.6		7.0		-1.0
	7.2		9.6		-.8
	4.6		3.9		-1.3
	6.1		8.6		-1.3
	1.4		3.1		-.9
	1.8		3.6		-1.0

LC 36

	3.1		-3.2		2.4
	3.9		-3.4		2.4
	3.8		-4.4		6.0
	3.6		-9.0		3.9
	6.9		-1.9		6.1
	8.7		-3.7		6.6
	3.3		-3.3		2.7
	3.8		-3.1		3.0

LC 37

	-1.9		3.4		.6
	-1.4		3.8		.8
	-1.0		6.7		4.1
	-5.3		5.3		2.6
	-2.5		3.8		4.2
	-1.9		8.7		4.6
	-1.5		3.1		1.0
	-1.5		3.8		1.2

Legend:
- ←— '88 DATA, kips
- ←— '89 DATA, kips
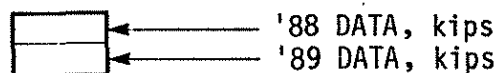
Fig. 4.37. Change in post-tensioning force due to pattern loading (two trucks).

-3.7	10.6	4.3
-2.8	12.0	5.0
-1.2	7.9	3.8
-5.8	6.1	2.9
-2.0	1.6	.9
-1.2	3.6	1.3
-.5	-.1	-.3
-.4	.4	-.2

LC 38

8.9	-6.9	7.3
11.0	-6.6	8.6
4.0	-5.7	6.3
3.4	-10.4	4.6
2.7	-1.2	2.3
3.6	-2.4	2.7
.1	-.5	.3
.4	-.4	.4

LC 39

5.3	10.0	-2.8
7.2	10.6	-1.9
2.6	6.9	-1.6
7.6	10.7	-1.0
1.2	1.3	-.7
1.9	3.6	-.9
-.3	-.3	-.1
-.2	.5	-.1

LC 40

c. LANE 4 LOADING

Fig. 4.37. Continued.

post-tension strengthening of continuous bridges. It may also be necessary to check allowable stresses with maximum tendon force gain and include maximum tendon force loss as well.

4.3. Additional Results

4.3.1. Temperature Variations

As was noted in Section 3.1.1, temperature sensors were mounted at six locations on the bridge (see Fig. 3.3). Originally, temperature data were collected so that corrections could be made in the strain measurements from the gages with the incorrect temperature compensation. However, because a "new zero" was recorded before each loading event and was checked at the end of the event, errors in strain measurements from having incorrect temperature-compensated gages were essentially eliminated.

Temperature data that were collected during the 1988 testing (1 day) and the 1989 testing (2 days) are presented in Appendix A as Figs. A.2 and A.3, respectively. In these figures temperatures at the six previously described locations on the bridge as well as air temperature are plotted vs the time of day. A review of the temperature data reveals several interesting trends as well as several variations that are difficult to explain. More than likely the trends that are difficult to explain are due to the angle of the sun, reflection on gages, velocity and direction of wind, and the like.

4.3.2. Longitudinal Bridge Movement

As was noted in Chapter 3, in both years instrumentation was installed on the bridge to measure longitudinal movement from post-tensioning or truck loading. In 1988 four dial gages (see Fig. 3.2) were positioned and oriented on the bridge so that longitudinal movement could be measured at the two end

abutments and the two interior piers. Crack monitors–one at each support; see Fig. 3.5–were used in 1989 to detect horizontal as well as vertical movements. For clarity, results from the 1988 and 1989 testing programs have been presented separately in the following paragraphs.

During the six stages of post-tensioning in 1988, the maximum horizontal movement that occurred was 0.018 in. north at the south abutment; all other horizontal movements during the six stages were considerably smaller. As a result of the post-tensioning (all beams post-tensioned), the bridge moved 0.023 in. south at the north abutment; horizontal movement at the other three supports was essentially zero (i.e., a few thousandths of an inch). Horizontal movements were also very small when truck loading was applied at numerous positions on the bridge. The maximum horizontal movements (truck at any of the previously described locations) at the four support positions, 1, 2, 3, and 4, were 0.045 in. south, 0.044 in. north, 0.012 in. south, and 0.005 in. north, respectively. Although these movements are extremely small, the presence of the pin at the north end is obvious.

As previously noted, the crack monitors were able to detect horizontal movement at the support points as well as vertical movement. Fortunately, there was no vertical movement (i.e., bridge beams lifting off the supports). The largest longitudinal movement in either 1988 or 1989 occurred when the post-tensioning forces were removed from the bridge in 1989. The maximum movement occurred during un-tensioning at the south abutment; the four beams moved an average of 0.200 inches south during this operation. This value is considerably greater than the movement that occurred a year earlier when the bridge was post-tensioned. However, the fact that the bridge was post-tensioned for a year and subjected daily to dynamic truck loading more than likely "freed" some or all the supports and thus permitted the movement when the loading was removed. When post-tensioning was reapplied to the bridge, very small movements similar to those measured in 1988 were

observed. Truck loading produced very small movements. The maximum movements once again occurred at the south abutment and occurred when the truck was in the south span; the maximum movement recorded was less than one-quarter of an inch (0.236 in.).

As a result of how the instrumentation was positioned and attached to the bridge in both years, the data obtained during the strengthening procedure (and during the truck loading) were a combination of horizontal movement plus beam rotation over the supports. However, as post-tensioning adjacent spans in the bridge produces rotations of opposite sense at the common support, the rotational contribution of the horizontal movement is minimized.

4.3.3. Guardrail Strains

Four strain gages were positioned on the upper channels of the guardrails--one at the centerline of the three spans on the east side of the bridge and one at the centerline of the bridge on the west side (see Fig. 3.2). Unfortunately, two were damaged at the start of the 1988 field testing and none were operational in the 1989 field testing. However, data were obtained in 1988 from the remaining two functioning gages--one on the west side at the centerline of the bridge (location 1) and one on the east side at the centerline of the north span (location 2). Values reported here resulted from truck no. 1 being positioned on the bridge before post-tensioning. At location 1, the largest compressive strain -65 MII (micro-inch per inch) (-1.9 ksi) was measured with the truck at position 4.3 (see Fig. 3.7) while the largest tensile strain was 9 MII (0.3 ksi) with the truck at position 4.5. At location 2, the largest compressive strain -24 MII (-0.7 ksi) and tensile strain 52 MII (1.5 ksi) occurred when the truck was at positions 4.1 and 1.6, respectively. Stresses noted in the previous sentences were obtained by assuming $E_s = 29,000$ ksi. Although limited data have been obtained to date, it is obvious that the guardrail system is contributing to the load resistance of the bridge.

5. SUMMARY AND CONCLUSIONS

5.1. Summary

This report summarizes the research that has been completed in the implementation phase of the investigation of strengthening of continuous, composite bridges by post-tensioning. The work completed during the initial phase of the investigation–the fabrication, strengthening and testing of a three-span, continuous composite bridge model–has been presented in Ref. 5. The research program in this phase included reviewing the literature, selecting, rating, and designing a post-tension strengthening scheme for a typical continuous, composite bridge, installing the strengthening system and testing the bridge with the system in place, monitoring the bridge's behavior for approximately one year, and retesting the bridge.

Because the authors have made several comprehensive literature reviews on post-tension strengthening of bridges [1,2,3,4] and bridge strengthening in general [6] that are readily available to the majority of engineers, this report only reviews post-tension strengthening articles published since July 1987. This literature review is thus supplemental to the previous literature reviews. For a broader review of the literature on post-tension strengthening of bridges the reader should consult the previously noted references in addition to the articles in this report. The literature review reveals that there has been a considerable amount of research completed in the last couple of years on simple-span beams as well as continuous structures. The majority of this research was performed in Maryland, California, and Canada.

With the assistance of the Iowa DOT Office of Bridge Design and several county engineers, the authors selected one of the V12 (1957) series of bridges for experimental strengthening. The bridge selected was a three-span (150 ft × 26 ft) continuous, composite bridge west of Fonda in Pocahontas

County on County Road N28. After selection of the bridge for strengthening, an analysis was made to determine the overstressed regions. By using finite element analysis, a strengthening system was designed for the bridge. Theoretically, the system designed and implemented was successful in reducing critical stresses in steel beams below the allowable inventory level except for a few locations (primarily over piers) at which there still were up to 2 ksi inventory load overstresses. Thus, the bridge was successfully post-tensioned to remove the need for load posting; however, all beam flexural stresses could not be reduced below the allowable inventory load level and stresses in curb reinforcing remain above the allowable operative load level. The bridge was also found to have inadequate shear connection. As a result of the success in using high-strength bolts for shear connection in a previous project [4], they were employed on this bridge. Fifty-two bolts were added to each of the two exterior beams while 58 were added to each of the interior beams (220 total on the bridge).

The primary purpose of strengthening continuous bridges by post-tensioning is to reverse the moments and resulting stresses from service loads. Thus, the strengthening system developed to strengthen this bridge post-tensioned the positive moment regions of all the beams (12 different regions). Overstress problems in the negative moment regions were relieved by the longitudinal distribution of the positive post-tensioning moments. Because only four hydraulic cylinders were available for post-tensioning, it was necessary to post-tension the bridge in six stages.

In 1988, the required shear connectors were added, the strengthening system was installed, and instrumentation (strain gages, temperature sensors, DCDT's, etc.) was positioned. The bridge was then subjected to various loading conditions (one truck at 28 different locations and two trucks in 12 cases of pattern loading) before and after post-tensioning was applied to determine the effectiveness of the strengthening system. Data were collected for each of the

loading schemes previously described as well as after each of the six stages of post-tensioning.

In addition to determining strains and deflections at critical locations on the bridge, changes in post-tensioning forces due to post-tensioning other beams and the application of vertical loading were determined. Depending on the position of vertical loading or the location of beams being post-tensioned in the bridge, these changes can be positive (an increase in tendon force) or negative (a decrease in post-tensioning force) and thus must be carefully considered in design of a post-tension strengthening system.

With the strengthening system in place the bridge was inspected approximately every three months. No noticeable change in its behavior or appearance occurred except for the development of additional deck cracks.

During the summer of 1989, approximately one year after the initial strengthening and testing of the bridge, the bridge was retested. Before the testing, a few modifications (additional strain gages and DCDT's) were made in the instrumentation on the bridge. With the modified instrumentation system in place, the bridge was loaded with one truck at the 28 locations previously used. Except for the small differences caused by the truck in 1989 weighing 8% more than the 1988 truck, there was essentially no difference in the data obtained in the two years or changes in the bridge's behavior. Post-tensioning was then removed from the bridge in six stages. The average change in the post-tensioning force on the bridge was a loss of 2.1%. There was, however, variation from beam to beam; the highest loss was 10.3% while the largest gain was 3.8%. The bridge was re-tensioned and loaded using the same loading program used in 1988.

5.2. Conclusions

The following conclusions emerged as a result of this investigation:

1. Strengthening continuous, composite, concrete-deck bridges by post-tensioning has been found (during more than four years of research) to be a viable, economical strengthening technique. Design of a strengthening system for continuous bridges is, however, more complex than for single-span bridges; thus, care should be taken to account for the numerous variables. Note: In some continuous bridges it may be necessary to add negative moment post-tensioning or superimposed trusses to achieve the desired stress reductions.

2. Field testing verified that longitudinal distribution of post-tensioning applied in the positive moment regions is effective in reducing flexural stresses in both positive and negative moment regions.

3. Changes in the post-tensioning force in tendons on a bridge that has been post-tensioned are a function of the deflection of the beam and thus may be a gain or loss. Because they are a function of beam deflection, they vary depending on the position of applied vertical loading on the bridge or the location of the beam being post-tensioned relative to other beams that have previously been post-tensioned. This change must be carefully taken into account when a post-tension strengthening scheme is designed for a given bridge.

4. End restraint was detected at the north end of the bridge, where the pin support was located. A small degree of end restraint was also found at the south end of the bridge (roller support). Data indicate that the degree of end restraint at the north end of the bridge is a function of the direction the beam rotated at that support.

5. Loss of post-tensioning force over the one-year period was minimal. It did vary (loss or gain) from member to member and thus should be carefully considered in the designing of a post-tension strengthening scheme for a given bridge.

6. Except for the cracks, which have been documented, there was essentially no change in the bridge's appearance or behavior in the period 1988–1989. This was verified by the testing program employed in 1988 and 1989.

7. Although minimal data were obtained as to the contribution of guardrails to the load resistance of a given bridge, significant strains were measured. Thus, depending on size, connection details, and the like, guardrails are resisting a portion of the load applied to the bridge and could be counted in certain situations in the bridge's rating.

8. The SAP IV, quarter-symmetry, finite element model is capable of accurately modeling the behavior of a symmetrically loaded post-tensioned bridge. The effects of symmetrical end restraint guardrails and the like can be included if desired.

9. Post-tensioning did not significantly affect truck load distribution, as essentially the same deflections and strains were measured before and after post-tensioning.

6. RECOMMENDED FURTHER RESEARCH

On the basis of the literature review, field testing, and finite element analysis, it would be logical to continue strengthening research as follows:

1. In the bridge strengthened in this investigation, strain reduction in the negative moment regions was obtained by post-tensioning the positive moment regions. However, as with this bridge, there are certain situations where the reduction may not be as large as desired–that is, it is desired to reduce strains in the negative moment regions a larger amount than is possible by post-tensioning only the positive moment regions. Thus, two alternatives should be investigated:

   - Post-tensioning of the negative moment regions in combination with the post-tensioning of the positive moment regions.
   - Utilization of the superimposed trusses developed in HR-302 with a modified positive moment post-tensioning system.

   Both of these alternatives could be investigated on the same bridge with the most effective system left in place for strengthening.

2. To date there are few data on the effects of dynamic loading on post-tension-strengthened beams or the post-tensioning system itself. Likewise, there are no data on the fatigue strength of the strengthened beams or the post-tensioning system. In a laboratory study, the same specimens could be used to obtain information in all four of these areas.

3. Strengthening of continuous span composite bridges by post-tensioning has been shown to be feasible. There is thus a need for a design procedure for strengthening continuous composite bridges that is similar to the procedures developed for simple-span bridges [3]. A design manual for designing post-tension strengthening

systems for continuous span bridges should be developed. This manual should include procedures for post-tensioning positive moment regions and negative moment regions.

4. To date, all post-tension strengthening research has been tested and implemented on steel beams. The post-tension strengthening procedures developed should be tested on reinforced concrete and prestressed concrete beams. (Note: There have been NCHRP investigations on the repair (in some instances strengthening) of damaged, prestressed concrete beams.) Creep of the concrete and attachment of the post-tensioning brackets are just two of the areas that need investigation. A preliminary study to determine the current state of the art and feasibility of the procedure is appropriate.

7. ACKNOWLEDGMENTS

8. REFERENCES

1. Klaiber, F. W., K. F. Dunker, and W. W. Sanders, Jr. "Feasibility Study of Strengthening Existing Single Span Steel Beam Concrete Deck Bridges." Final Report. ERI Project 1460, ISU-ERI-Ames-81251. Ames: Engineering Research Institute, Iowa State University, Ames, Iowa, 1981.

2. Dunker, K. F., F. W. Klaiber, B. L. Beck, and W. W. Sanders, Jr. "Strengthening of Existing Single-Span Steel-Beam and Concrete Deck Bridges." Final Report–Part II. ERI Project 1536, ISU-ERI-Ames-85231. Ames: Engineering Research Institute, Iowa State University, Ames, Iowa, 1985.

3. Dunker, K. F., F. W. Klaiber, and W. W. Sanders, Jr. "Design Manual for Strengthening Single-Span Composite Bridges by Post-Tensioning." Final Report–Part III. ERI Project 1536, ISU-ERI-Ames-85229. Ames: Engineering Research Institute, Iowa State University, Ames, Iowa, 1985.

4. Klaiber, F. W., D. J. Dedic, K. F. Dunker, and W. W. Sanders, Jr. "Strengthening of Existing Single Span Steel Beam and Concrete Deck Bridges." Final Report–Part I. ERI Project 1536, ISU-ERI-Ames-83185. Ames: Engineering Research Institute, Iowa State University, Ames, Iowa, 1983.

5. Dunker, K. F., F. W. Klaiber, F. K. Daoud, W. E. Wiley, and W. W. Sanders, Jr. "Strengthening of Existing Continuous Composite Bridges." Final Report. ERI Project 1846, ISU-ERI-Ames-88007. Ames: Engineering Research Institute, Iowa State University, Ames, Iowa, 1987.

6. Klaiber, F. W., K. F. Dunker, T. J. Wipf, and W. W. Sanders, Jr. "Methods of Strengthening Existing Highway Bridges." National Cooperative Highway Research Program Report 293, Transportation Research Board, 1987, pp. 114.

7. Troitsky, M. S., Z. A. Zielinski, and A. Nouraeyan. "Pre-Tensioned and Post-Tensioned Composite Girders." *Journal of Structural Engineering*, ASCE, 115, No. 12, December, 1989, pp. 3142-3153.

8. Troitsky, M. S., Z. A. Zielinski, and M. S. Pimprikar. "Optimum Design of Prestressed Steel Girders." *Proceedings of the Canadian Society for Civil Engineering Annual Conference.* Toronto, Ontario, May 12-16, 1986, 4, pp. 1-19.

9. Troitsky, M. S., Z. A. Zielinski, and M. S. Pimprikar. "Experimental Evaluation of Prestressed Steel Plate Girder Bridges." *Experimental*

Assessment of Performance of Bridges, Proceedings. New York: American Society of Civil Engineers, 1986.

10. Wiley, W. E. *Post-Tensioning of Composite T-Beams Subjected to Negative Moment.* M. S. Thesis, Iowa State University, Ames, Iowa, 1988.

11. Troitsky, M. S., Z. A. Zielinski, M. S. Pimprikar, and H. B. Poorooshasb. "Prestressed Steel Cable Bridge Trusses." *Proceedings of the International Symposium on Structural Steel Design and Construction.* Singapore, July 3-4, 1985, pp. 466-487.

12. Ayyub, B. M., Y. G. Sohn, and H. Saadatmanesh. "Static Strength of Prestressed Composite Steel Girders." Final Report. National Science Foundation Award No. ECE-8413204. Department of Civil Engineering, University of Maryland, College Park, Maryland, May, 1988.

13. Saadatmanesh, H., P. Albrecht, and B. M. Ayyub. "Experimental Study of Prestressed Composite Beams." *Journal of Structural Engineering,* ASCE, 115, No. 9, September, 1989, pp. 2348-2363.

14. Saadatmanesh, H., P. Albrecht, and B. M. Ayyub. "Analytical Study of Prestressed Composite Beams." *Journal of Structural Engineering,* ASCE, 115, No. 9, September, 1989, pp. 2364-2381.

15. Pritchard, B. P. "Strengthening of the M62 Rakewood Viaduct." Presentation at the Symposium on Strengthening and Repair of Bridges, Leamington, England, June 23, 1988.

16. Farnan, T. W. "Strengthening Methods for Increases in Live Loads for Short Span Bridges." Presentation at the Western Bridge Engineers' Seminar, Coeur d'Alene, Idaho, October 2-4, 1989.

17. Seible, F., M. J. N. Priestley, and G. C. Pardoen. "Strengthening Techniques for RC Bridge Structures." Presentation at the Western Bridge Engineers' Seminar, Coeur d'Alene, Idaho, October 2-4, 1989.

18. Mellon, F. L. and G. D. Mancarti. "Strengthening Steel Girder Bridges for Live Loads." *Memo to Designers 9-7.* Sacramento: California Department of Transportation, September, 1989, pp. 1-6.

19. Eshani, M. R. and H. Saadatmanesh. "Behavior of Externally Prestressed Concrete Girders." *Structural Design, Analysis and Testing.* New York: American Society of Civil Engineers, 1989, pp. 218-222.

20. Albrecht, P. and W. Li. "Fatigue Strength of Prestressed Composite Beams." Final Report. National Science Foundation Award No. ECE-8513684. Department of Civil Engineering, University of Maryland, College Park, Maryland, June, 1989.

21. American Association of State Highway and Transportation Officials. *Standard Specifications for Highway Bridges*, 13th Edition. Washington: American Association of State Highway and Transportation Officials, 1983.

22. Daoud, F. K. *Experimental Strengthening of a Three-Span Composite Model Bridge by Post-Tensioning.* M. S. Thesis, Iowa State University, Ames, Iowa, 1987.

23. American Association of State Highway and Transportation Officials. *Manual of Maintenance Inspection of Bridges 1978.* Washington: American Association of State Highway and Transportation Officials, 1979.

24. Bathe, K. J., E. L. Wilson, and F. E. Peterson. *SAP IV, A Structural Analysis Program for Static and Dynamic Responses of Linear Systems.* Berkeley: College of Engineering, University of California, 1974.

25. Lotus Development Corporation. *1-2-3 Reference Manual.* Cambridge: Lotus Development Corporation, 1985.

26. Planck, S. M. *Post-Compression and Superimposed Trusses Utilized in Bridge Rehabilitation.* M. S. Thesis, Iowa State University, Ames, Iowa, 1989.

27. Klaiber, F. W., T. J. Wipf, K. F. Dunker, R. B. Abu-Kishk, and S. M. Planck. "Alternate Methods of Bridge Strengthening." Final Report. ERI Project 1961. ISU-ERI-Ames-89262. Ames: Engineering Research Institute, Iowa State University, Ames, Iowa, 1989.

28. Troitsky, M. S., Z. A. Zielinski, and N. F. Rabbani. "Prestressed-Steel Continuous-Span Girders." *Journal of Structural Engineering*, ASCE, 115, No. 6, June, 1989, pp. 1357-1370.
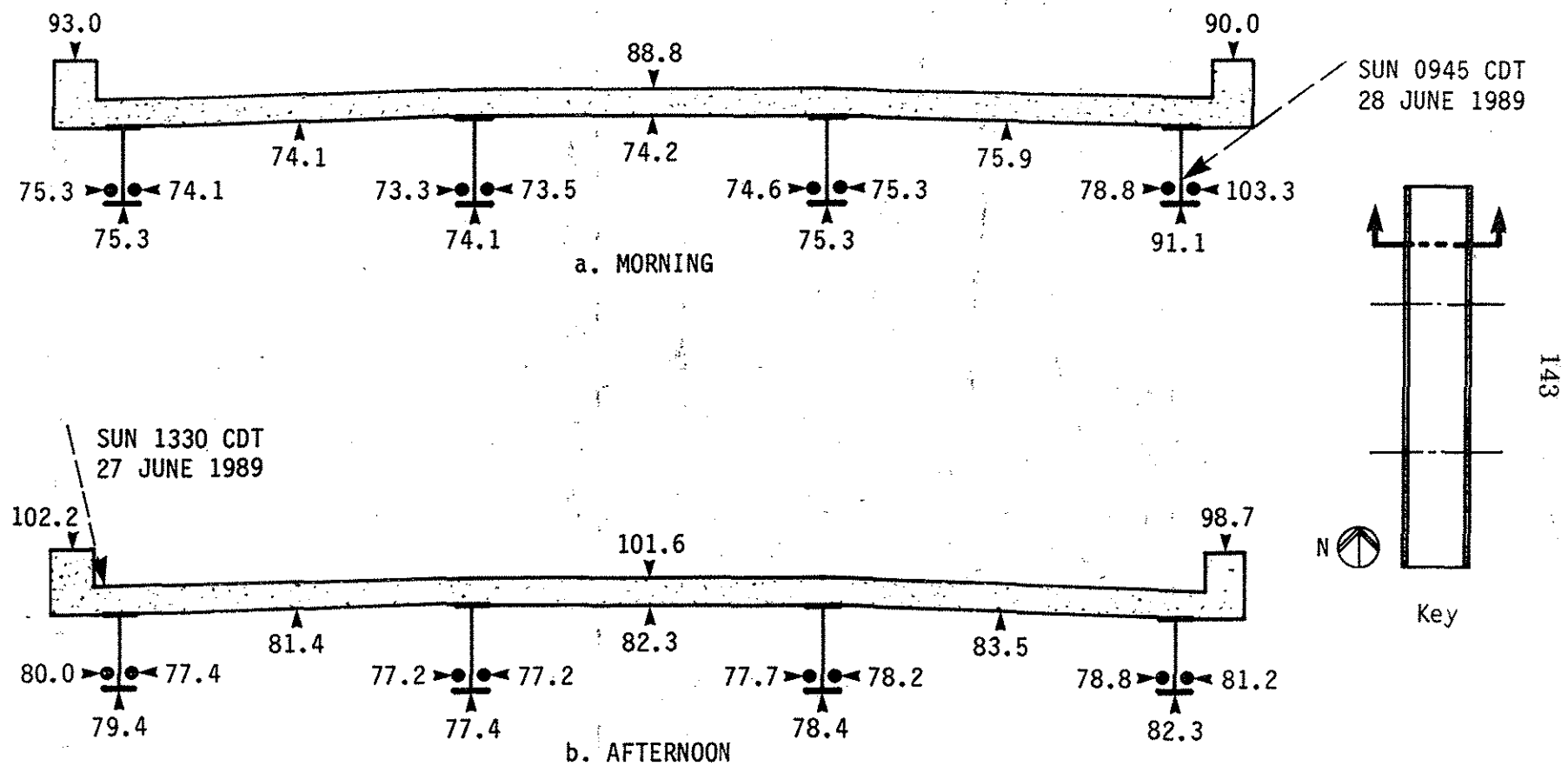
APPENDIX A

Bridge Temperature Variations

93.0   88.8   90.0

SUN 0945 CDT
28 JUNE 1989

74.1   74.2   75.9

75.3 ►●|●◄ 74.1   73.3 ►●|●◄ 73.5   74.6 ►●|●◄ 75.3   78.8 ►●|●◄ 103.3

75.3   74.1   75.3   91.1

a. MORNING

SUN 1330 CDT
27 JUNE 1989

102.2   101.6   98.7

81.4   82.3   83.5

80.0 ►●|●◄ 77.4   77.2 ►●|●◄ 77.2   77.7 ►●|●◄ 78.2   78.8 ►●|●◄ 81.2

79.4   77.4   78.4   82.3

b. AFTERNOON

N

Key

143

Fig. A.1. Thermocouple surface temperature measurements, north span - 1989.
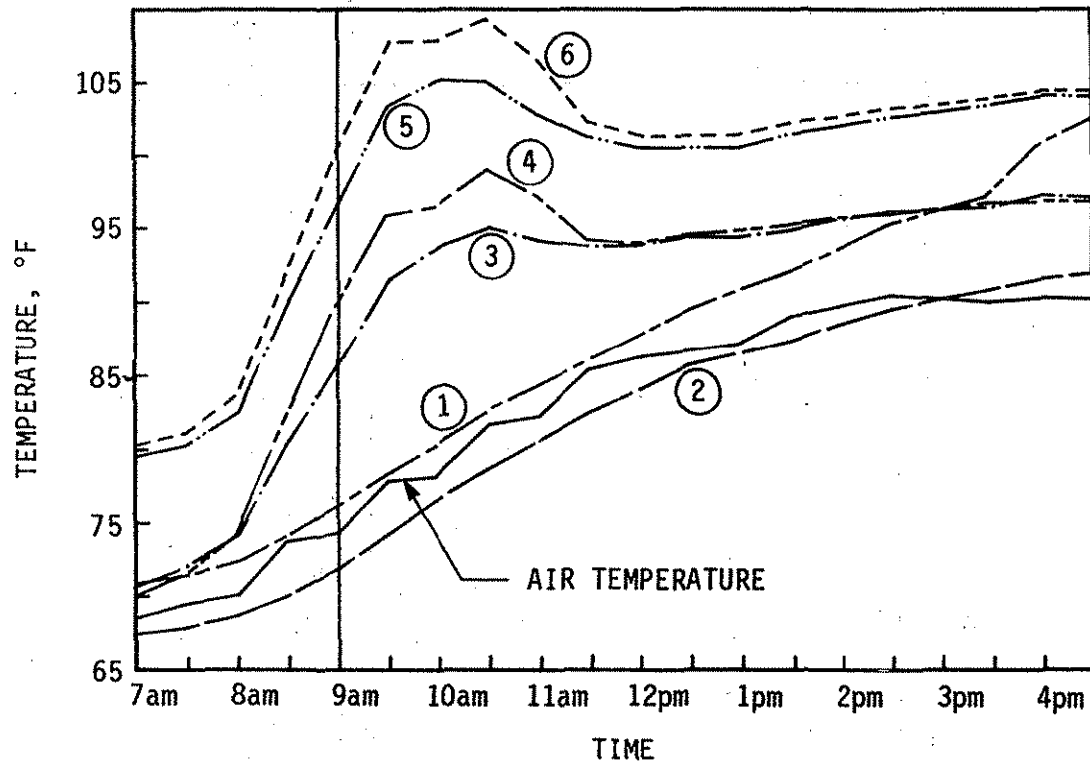
Fig. A.2. Bridge temperatures - 1988.
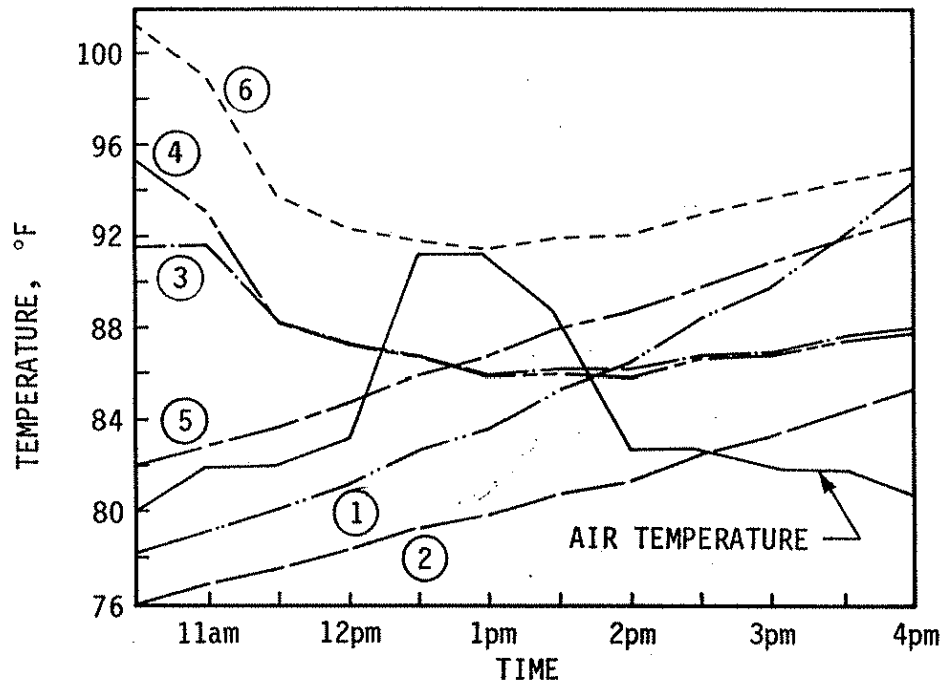
a. DAY 1: 6/27/89
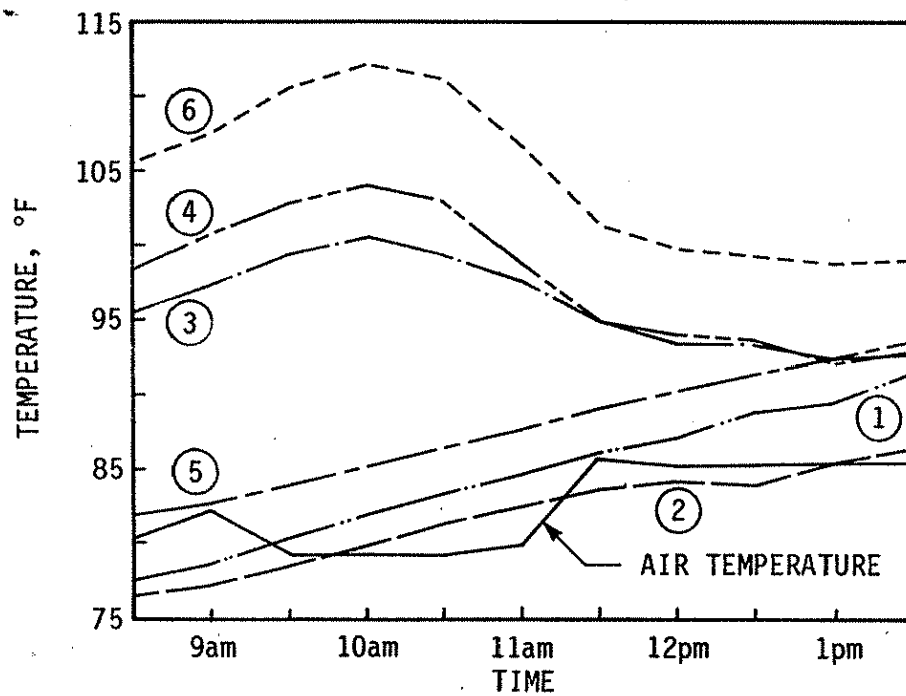
b. DAY 2: 6/28/89

Fig. A.3. Bridge temperatures - 1989.
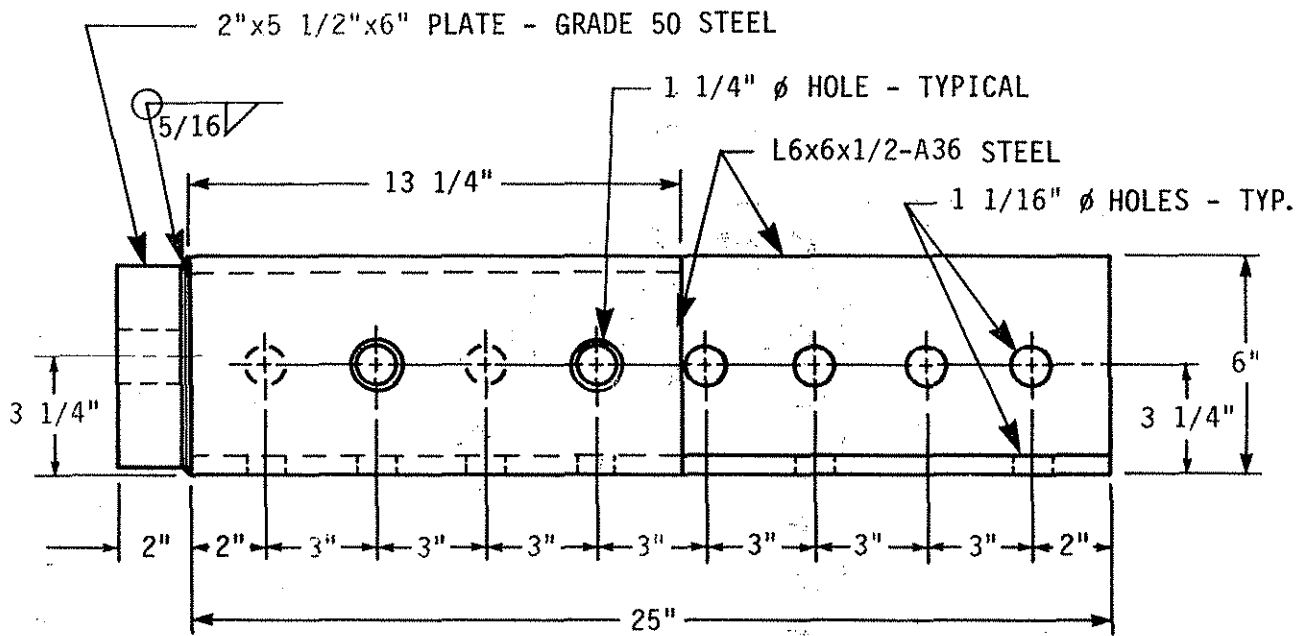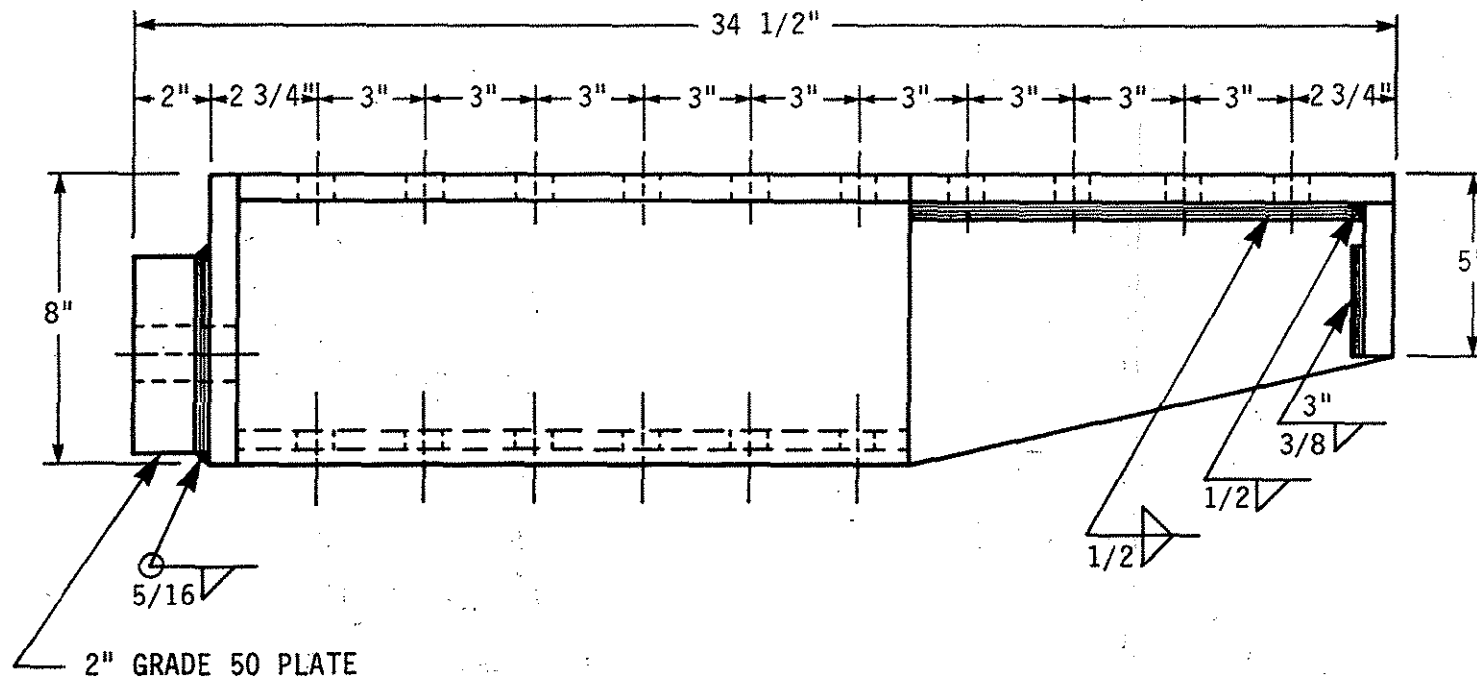
APPENDIX B

Post-Tensioning Bracket Details

2"x5 1/2"x6" PLATE - GRADE 50 STEEL

5/16

1 1/4" ∅ HOLE - TYPICAL

L6x6x1/2-A36 STEEL

1 1/16" ∅ HOLES - TYP.

13 1/4"

6"

3 1/4"

3 1/4"

2" | 2" | 3" | 3" | 3" | 3" | 3" | 3" | 3" | 2"

25"

a. SIDE VIEW

7/16

1/4" MIN. BEARING
PLATE ON ANGLES

1 1/2" ∅

7/16

6"

3 1/4"

3 1/4"

5/8" RADIUS - ROUND TO FIT
BEAM FILLET OR 1/2" BEVEL

2 1/2"

BRIDGE BEAM
POSITION

3 1/4"

b. END VIEW
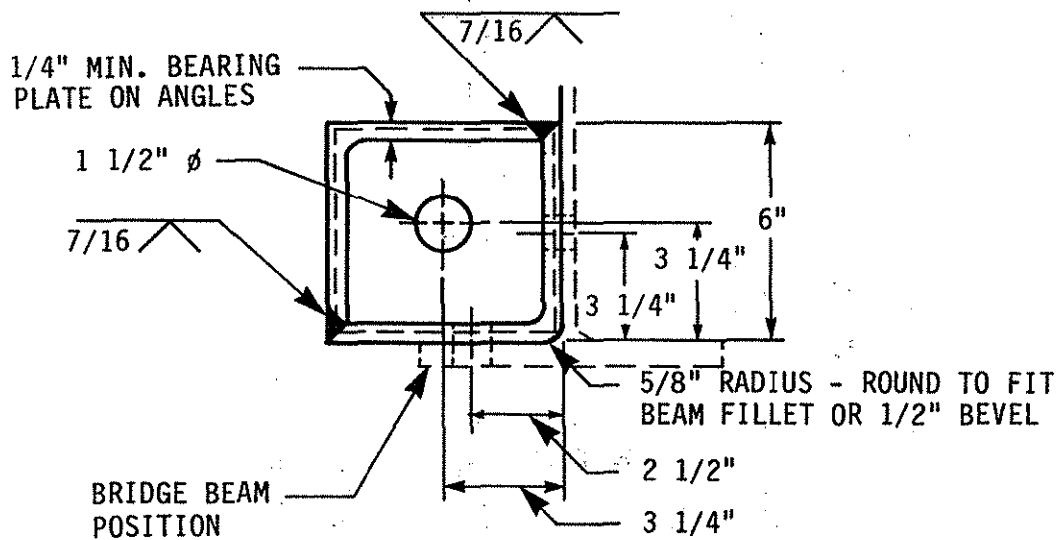
Fig. B.1. Post-tensioning bracket A.

a. SIDE VIEW

Fig. B.2. Post-tensioning bracket B.

34 1/2"

2" 19 1/4" 13 1/4"

2"

4 1/8"

13" 3/4"

4 1/8"

2"

1 1/16" ⌀ TYPICAL

1 1/4" ⌀ TYPICAL

5/16

5/16

5/16

1/2

1/2

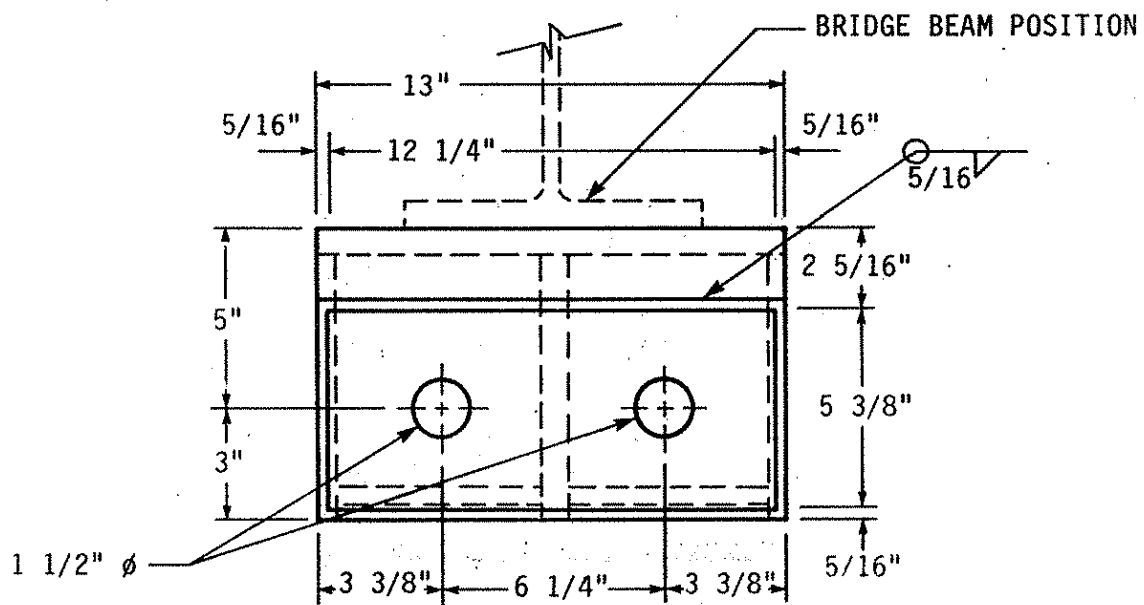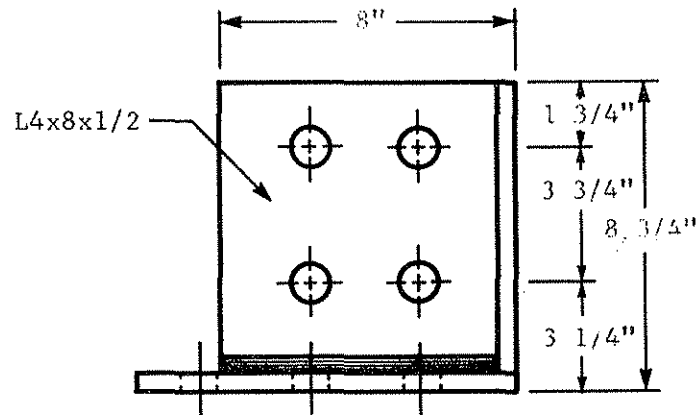ALTERNATE PLATE SHAPE

b. BOTTOM VIEW
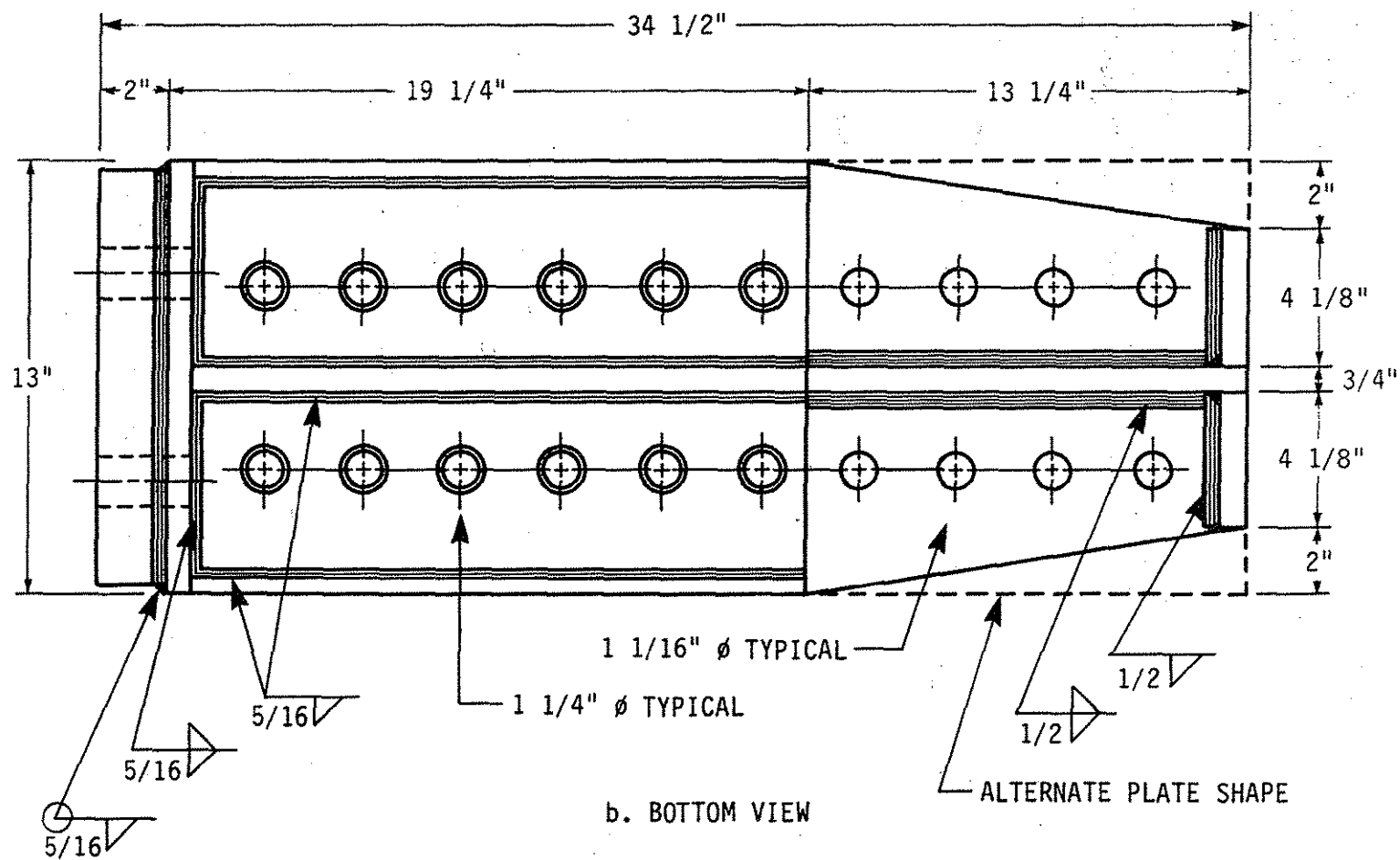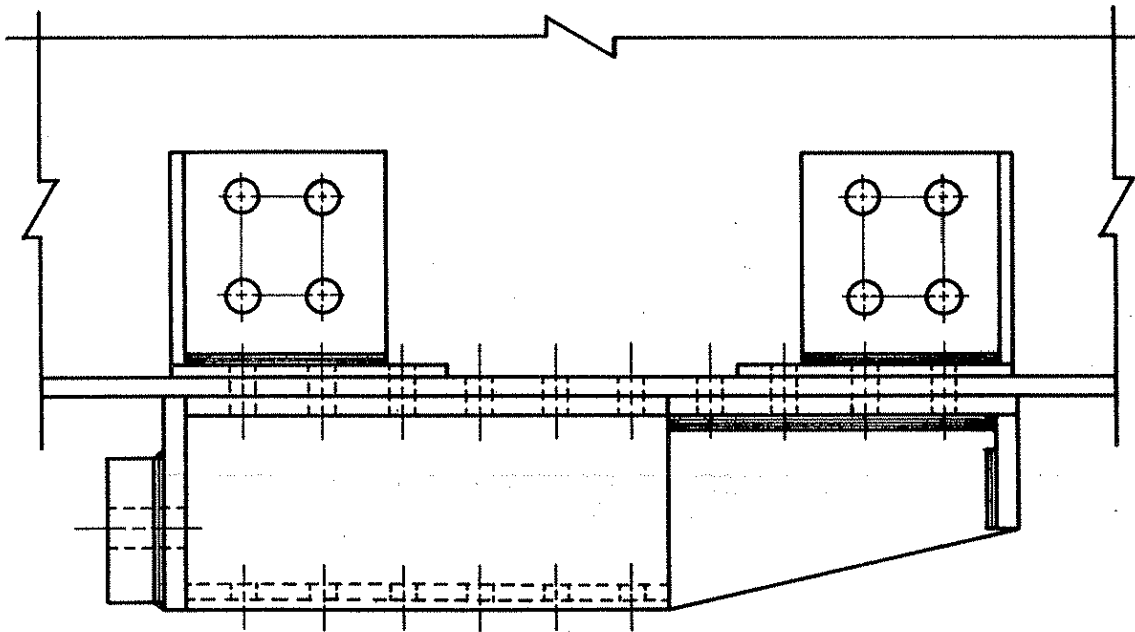
Fig. B.2. Continued.

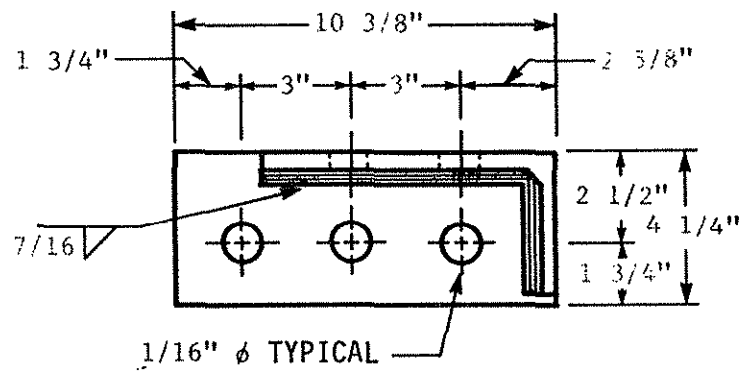c. BRACKET B PLUS STIFFENERS IN PLACE

d. FRONT VIEW

Fig. B.2. Continued.

a. SIDE VIEW

b. TOP VIEW

Fig. B.3. Bracket B beam stiffener.
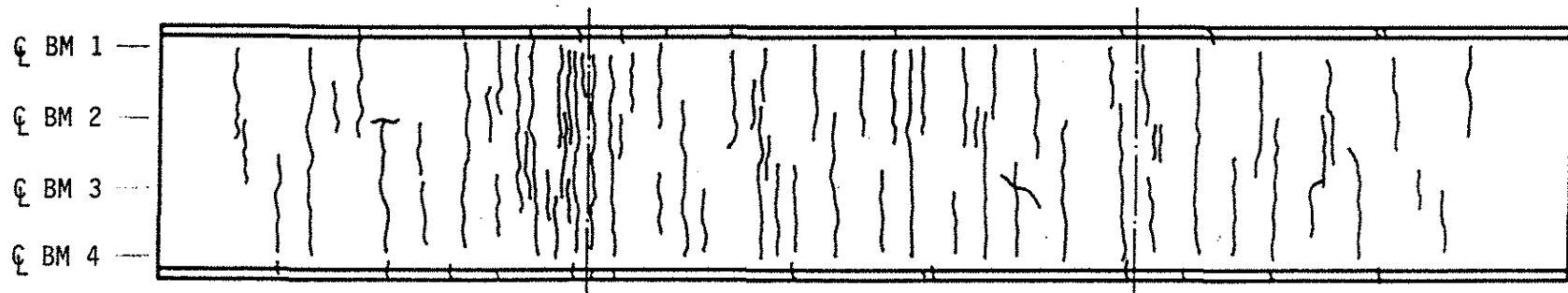
APPENDIX C

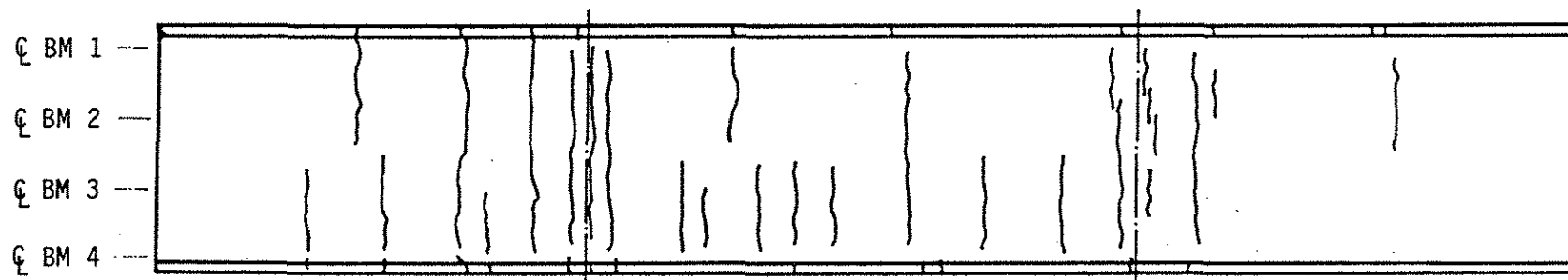## Deck Crack Patterns, Fonda Bridge
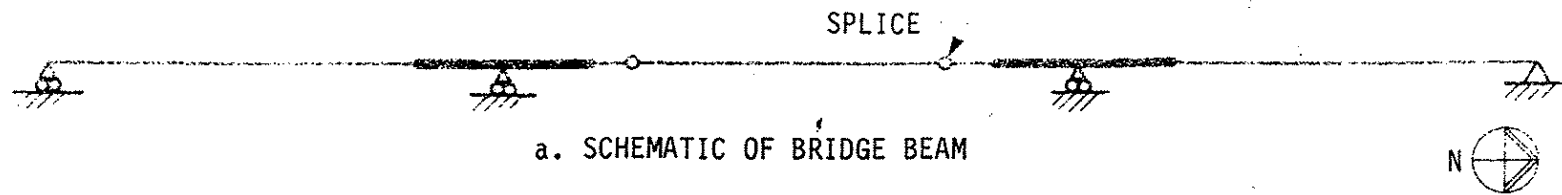
SPLICE

a. SCHEMATIC OF BRIDGE BEAM

N

b. PATTERN BEFORE POST-TENSIONING, 8/10/88

c. PATTERN BEFORE RELEASE OF POST-TENSIONING, 6/27/89

Fig. C.1.   Deck crack patterns before and after
post-tensioning, Fonda bridge.

APPENDIX D

Deck Crack Patterns, Single-Span Bridges

Bridge 1: Terril, Iowa

Bridge 2: Paton, Iowa

APPENDIX D: SINGLE SPAN BRIDGES

After observing the extent of the deck cracking in the Fonda bridge, the authors documented the deck crack patterns in the two single-span bridges strengthened under previous research projects [2,4].

Bridge no. 1, located in Dickinson County north of Terril, Iowa, is a nominal 50-ft-span right-angle bridge. At the time of the original strengthening in 1982, the deck was generally in good condition, with some cracking. The pattern shown in Fig. D.1a was constructed both from an author's handwritten notes for the locations of cracks about one year after post-tensioning and from the present crack pattern.

The recently documented crack pattern in Fig. D.1b shows more extensive cracking and a considerable number of deck patches. Although the cracking has increased, it has not increased at the same rate as the cracking in the Fonda bridge deck.

Two bridges similar to bridge no. 1 and apparently constructed at the same time are located within a few miles to the north of bridge no. 1. The deck crack pattern for the bridge nearest to bridge no. 1 is documented in Fig. D.2. For the bridge that was not post-tensioned, the crack pattern is about as extensive as the 1983 pattern for bridge no. 1. There is slightly more deck patching near the abutments but less in the center of the deck.

On the basis of photographs, the approximate 1983 crack pattern, and the crack pattern for the bridge north of bridge no. 1, it appears that the post-tensioning has caused a moderate amount of additional deck cracking. Comparison of Figs. D.1b and D.2 also suggests that post-tensioning has caused an extensive amount of curb cracking. Because curb stresses were unacceptably high in tension, curbs were neglected in the computation of stresses for bridge no. 1. (See the example in Ref. 3.)

After the authors post-tensioned Bridge no. 2 north of Paton, Iowa, the Iowa DOT resurfaced the deck and removed much of the curb the following summer, in 1983. The Iowa DOT left the post-tensioning in place, and this resulted in some post-tensioning loss as noted in Ref. 2. In 1984, the authors removed and replaced the post-tensioning on the resurfaced bridge.

The recent deck crack pattern in Fig. D.3 shows little evidence of deck cracking caused by post-tensioning. Most of the cracking is at the abutments, where bridge no. 1 and the bridge north of it are heavily patched. The deck cracking near the abutments thus is unlikely to be caused by post-tensioning.

The curb crack patterns in Fig. D.3 show that the new sections of curb have cracked considerably less than the old sections. The old sections of curb have weathered considerably since the deck resurfacing and may need repair in the near future.

Observation of the existing deck and curb cracking patterns of the post-tensioned and unstrengthened single-span bridges suggests that post-tensioning causes moderate cracking of the bridge deck. If the deck is resurfaced using the Iowa high-density concrete overlay process, it apparently is not subject to significant cracking caused by post-tensioning. Either old or new curbs are subjected to significant cracking caused by post-tensioning.
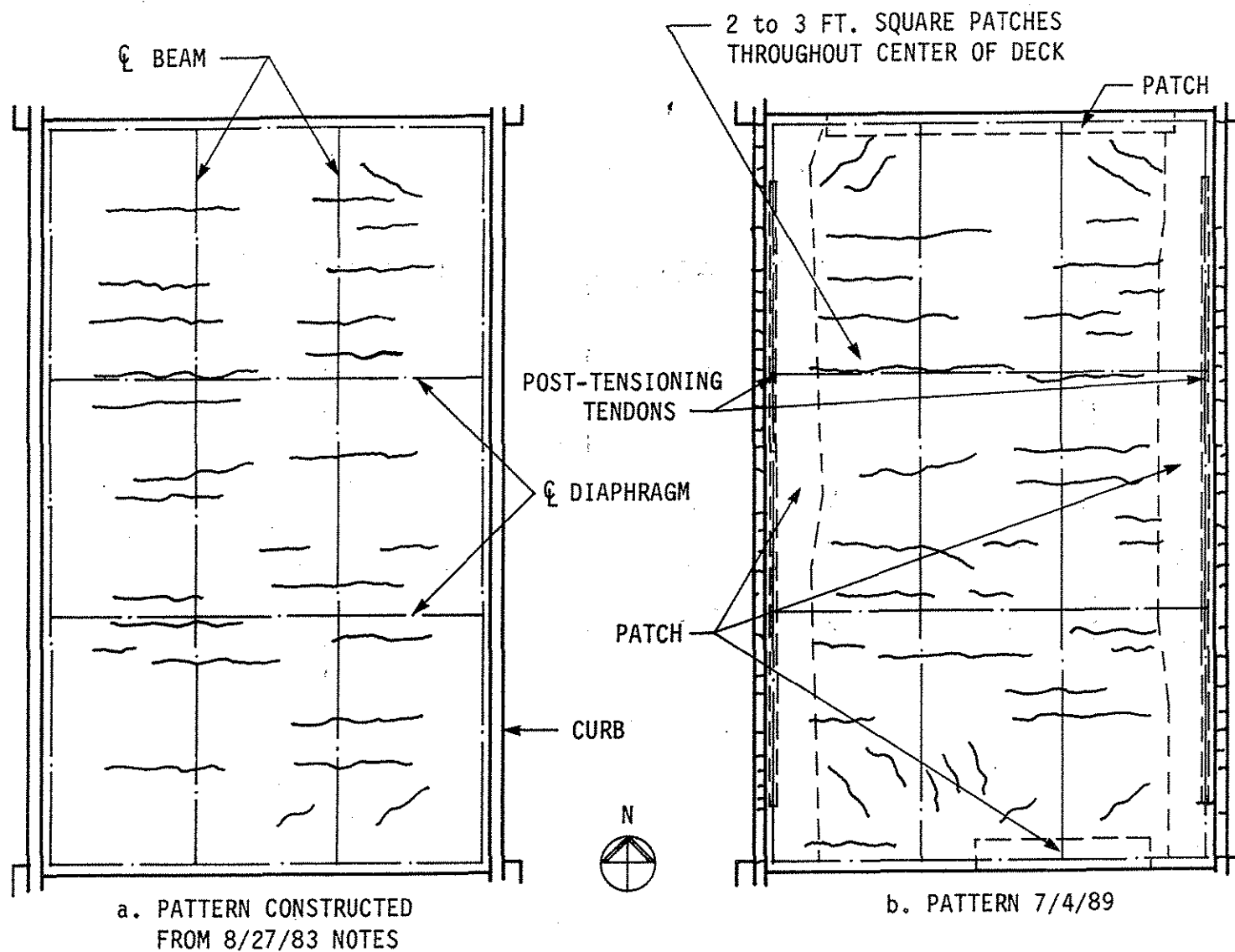
Fig. D.1   Deck crack patterns, bridge no. 1, Terril, Iowa.

PATCH

ONE 2 TO 3 FT.
SQUARE PATCH IN
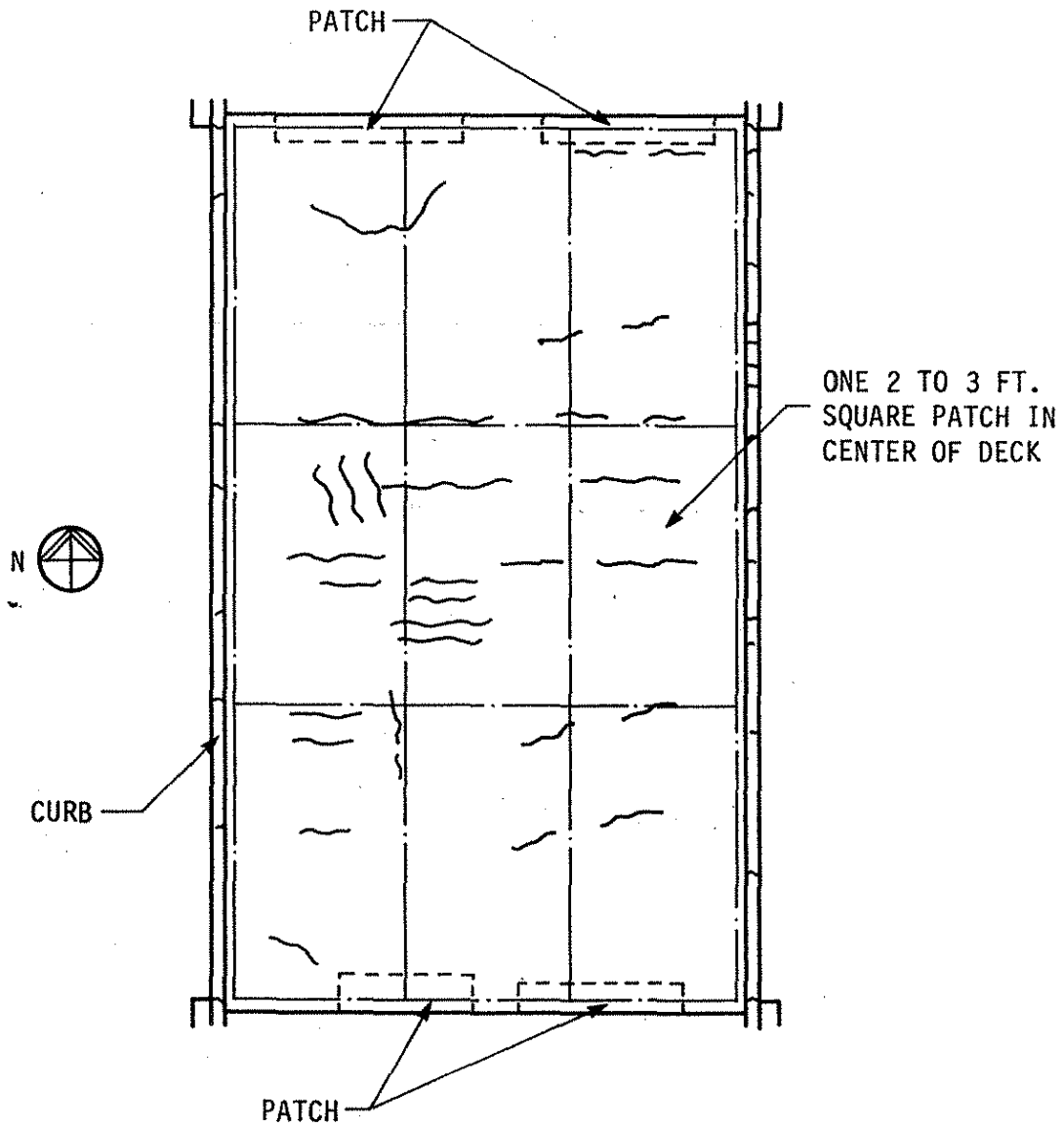CENTER OF DECK

N

CURB

PATCH

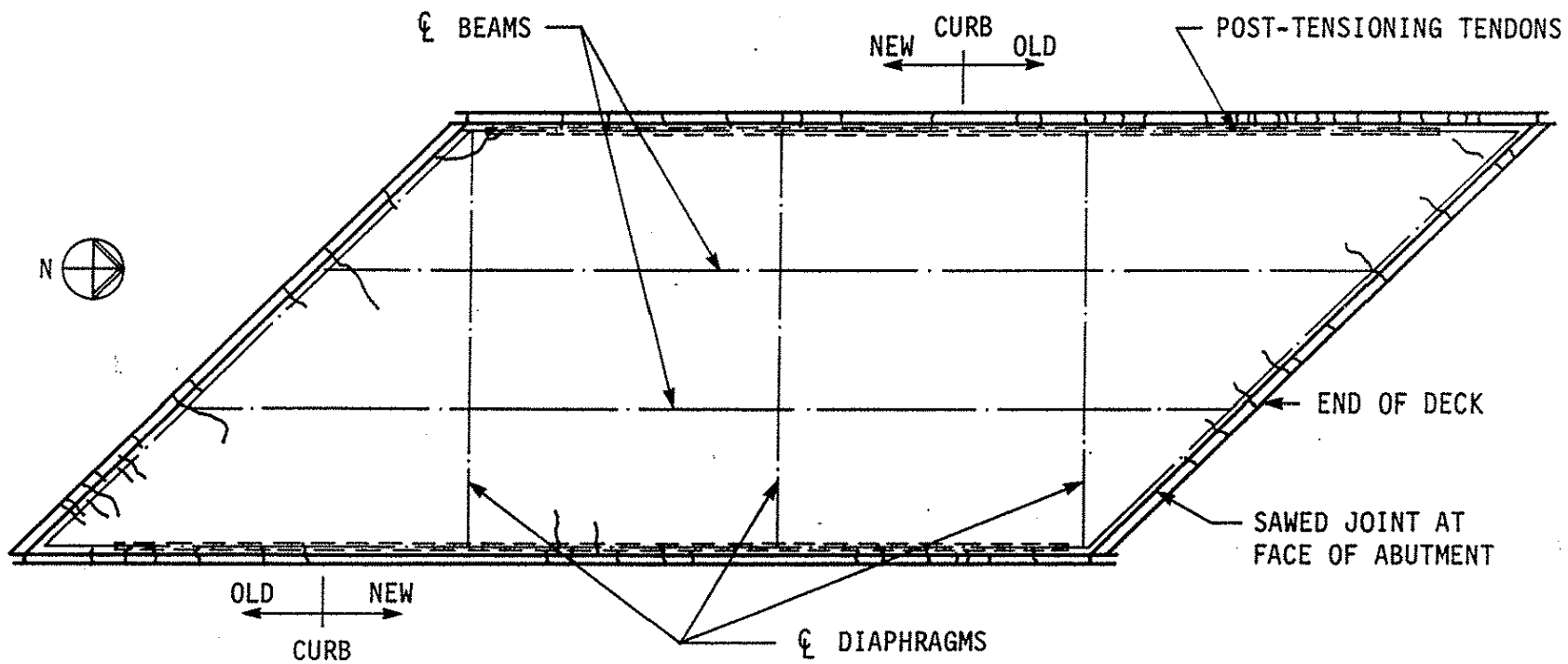Fig. D.2. Deck crack pattern, bridge 0.7 miles
north of bridge no. 1, 7/4/89.

Fig. D.3.   Deck crack patterns, bridge no. 2, Paton, Iowa 7/4/89.